Technical Report SL-93-3
April 1993

US Army Corps
of Engineers
Waterways Experiment
Station

Design and Development of a Miniature Column-Based Interface (MCBI) Stress Gage

by Denis D. Rickman
Structures Laboratory

Prepared for Defense Nuclear Agency

Technical Report SL-93-3
April 1993

Design and Development of a Miniature Column-Based Interface (MCBI) Stress Gage

by Denis D. Rickman
Structures Laboratory

U.S. Army Corps of Engineers
Waterways Experiment Station
3909 Halls Ferry Road
Vicksburg, MS 39180-6199

Final report

Approved for public release; distribution is unlimited

Prepared for Defense Nuclear Agency
Washington, DC 20305-1000

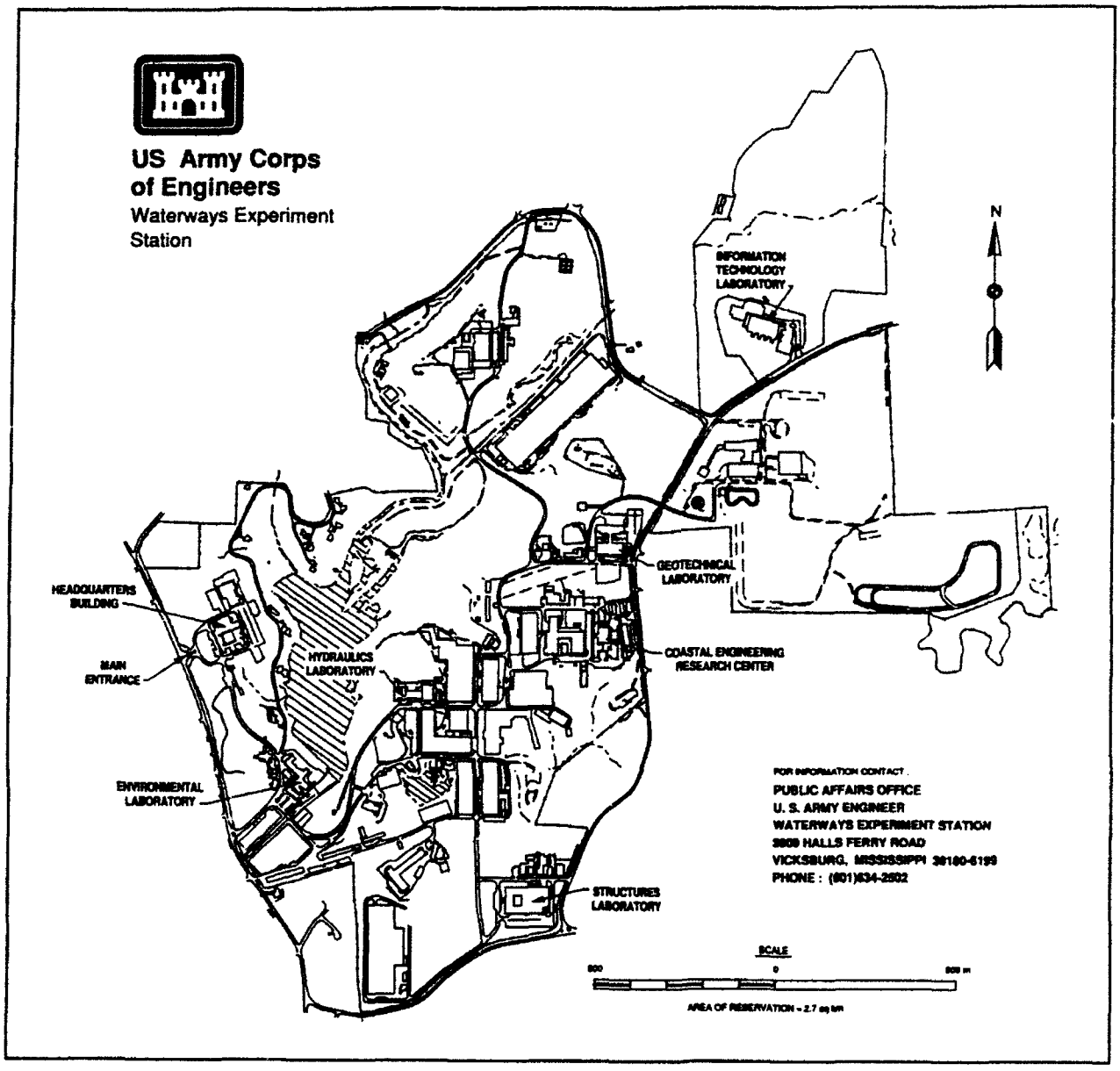

Waterways Experiment Station Cataloging-in-Publication Data

Rickman, Denis D.
Design and development of a miniature column-based interface (MCBI) stress gage / by Denis D. Rickman ; prepared for Defense Nuclear Agency.
144 p. : ill. ; 28 cm. — (Technical report ; SL-93-3)
ncludes bibliographical references.
1. Underground construction — Testing — Instruments. 2. Soil-structure interaction — Testing — Instruments. 3. Stress waves — Measurement — Instruments. 4. Blast effect — Testing — Instruments. I. United States. Defense Nuclear Agency. II. U.S. Army Engineer Waterways Experiment Station. III. Title. IV. Series: Technical report (U.S. Army Engineer Waterways Experiment Station); SL-93-3.
TA7 W34 no.SL-93-3

TABLE OF CONTENTS

LIST OF TABLES

LIST OF ILLUSTRATIONS

PREFACE

The effort to design and develop a Miniature Column-Based Interface (MCBI) stress gage was undertaken as part of the Defense Nuclear Agency (DNA) - sponsored Test Instrumentation Development (TID) Program. Mr. Mark Flohr was the DNA technical monitor for the TID Program. Funding for this effort was provided under DNA Military Interdepartmental Purchase Request No. 88-503.

The research reported here was conducted at the U.S. Army Engineer Waterways Experiment Station (WES), Vicksburg, Mississippi.

The work was under the overall direction of Mr. Charles R. Welch. Mr. D. D. Rickman was the Project Scientist and performed research as a Master's thesis submitted to Mississippi State University. Dynamic testing of the MCBI gage was supervised by Messrs. F. W. Skinner and S. K. Lobred of EED.

Instrumentation support was provided by the WES Instrumentation Services Division (ISD) under the overall supervision of Mr. F. P. Leake. Gage calibration was directed by Mr. E. L. Sadler, and static and dynamic laboratory testing were conducted by Messrs. H. P. Parks and J. W. Johnson.

During this investigation, Mr. L. K. Davis was Chief, EED, and Mr. Bryant Mather was Director, SL. At the time of preparation of this report, the Director of WES was Dr. Robert W. Whalin. The Commander was COL Leonard G. Hassell, EN.

CONVERSION FACTORS, U.S. CUSTOMARY UNITS OF MEASUREMENT
TO METRIC (SI)

Multiply	By	To Obtain
inches	25.40	millimetres
feet	0.3048	metres
pounds (mass)	0.4536	kilograms
pounds (force) per square inch (psi)	0.006895	megapascals
pounds per cubic foot	16.02	kilograms per cubic metre
g (standard free-fall)	9.807	metres per second squared
degree (angle)	0.01745	radians

SECTION 1

INTRODUCTION

1.1 BACKGROUND

The Waterways Experiment Station (WES) conducts numerous tests funded by the Defense Nuclear Agency (DNA) and other sponsors requiring the measurement of static and dynamic normal stresses induced on buried structures by explosion-induced loadings. The tests are designed to simulate and evaluate the effects of nuclear or conventional weapons against various structures of military interest. A typical method for acquiring these measurements is through the use of flush-mounted, normal interface stress gages. These gages are placed at points of interest in the subject structure's outer surface so that the sensing area of the gage is positioned at the soil-structure interface. In this orientation, the gage measures the applied stress at the interface.

During recent years, the levels of shock (acceleration) and interface stress applied to buried test structures have increased dramatically. Stresses in excess of 10,000 psi (69 MPa) and accelerations greater than 100,000 g's may be reached. The proven interface stress gages currently in use are not capable of accurately measuring stresses in excess of 5,000 psi (34.5 MPa). In addition, many normal interface stress gages are overly sensitive to acceleration and/or structure-transmitted stress effects which produce unwanted gage output, thus distorting the recorded stress wave form.

Interface stress measurements may also be complicated by the intense pattern of steel reinforcing bars (rebar) found in many concrete test structures. Since it is desirable to leave the rebar pattern as undisturbed as possible when placing interface gages, the gages should be small enough to fit within the rebar patterns of most structures.

The DNA has sponsored an on-going Test Instrumentation Development (TID) program at WES in an effort to improve capabilities in many areas of blast and shock measurement. During the early 1980's, DNA funded WES to develop a Column-Based Interface (CBI) stress gage as part of the TID effort. The CBI gage was designed to measure interface stresses up to 50,000 psi (34.5 MPa), and initial tests of the CBI gage were promising. Unfortunately, the CBI gage proved to be very sensitive to lateral stresses and accelerations. In addition, the CBI gage had an overall diameter of 5 inches, which made it very difficult to fit into small-scale structural models.

Because of the continuing need for a reliable, high-range, laterally-isolated, interface stress gage, DNA funded WES to design an improved column-based interface stress gage. As a result of this effort, WES designed and developed the Miniature Column-Based Interface (MCBI) stress gage.

1.2 OBJECTIVE

The objective of this study was to develop a reliable, normal interface stress gage capable of measuring significantly higher stresses than previous gages of this type. The new gage was to possess low sensitivity to applied accelerations and lateral stresses, while being small enough to fit into most reinforced concrete test structures.

1.3 SCOPE

This report describes the design and evaluation of the MCBI gage. A theoretical basis and design equations are presented for the strain-gaged load column and lateral isolation systems incorporated in the MCBI gage. The gage evaluation process is presented in the form of laboratory and field test results, along with a comprehensive list of MCBI gage electrical, physical, dynamic, and environmental characteristics.

SECTION 2

DESIGN REQUIREMENTS AND CALCULATIONS

2.1 DESIGN REQUIREMENTS

A number of design requirements governed the development of a new, high-range, interface stress gage. First, an operating range was needed that would greatly exceed that of existing interface stress gages, and, if possible, allow measurement of all interface stresses expected to be applied from anticipated explosion test situations. The most frequently used interface stress gage is the Kulite VM-750 (Reference 1). The VM-750, however, has a maximum measurement range of only 5,000 psi, while the highest range of interest may be on the order of 30,000 psi. Thus, the ideal maximum operating range for a high-range, interface stress gage is somewhat greater than 30,000 psi. In addition, since the applied stress loadings may have rise-times on the order of a few 10's of microseconds, the gage should have a natural frequency greater than 100 kHz.

The gage output's sensitivity to acceleration and lateral stress effects was another important consideration. In many cases, the acceleration acting on interface stress gages is sufficient to deform the sensing elements, causing an unwanted gage output. In addition, lateral stresses transmitted through the test structure walls may be transferred to interface stress gages, once again resulting in sensing element deformation and unwanted gage output. Output from these sources may cause significant measurement distortion in severe shock environments, and should be minimized.

Finally, the diameter of the gage and its mounting system must be considered. The mount diameter should be less than three inches, both to facilitate placement in steel reinforced structures, and to minimize the depth of gage recesses when attached to curved structure surfaces. The gage's active sensing area should be large enough to provide a

stress sample which will not be effected by soil inhomogeneities. Test experience has shown that the sensing area should be at least 0.196 sq in., as indicated in References 2 and 3.

2.2 GAGE DESIGN

Several lessons were learned from the design and development of the old CBI gage. First, it was very evident that a strain-gaged column should be used as the stress-sensing element, due both to its inherently linear output from an applied normal stress, and the ability of columns to withstand high levels of stress without permanent deformation. The strain-gaged load column used in the CBI gage, however, was not well isolated from lateral stress and acceleration effects. This was due largely to the fact that the column was actually an integral part of a larger piece of steel which formed the bottom of the CBI gage body. Thus, the column was very sensitive to loading by lateral forces. Based upon these observations, a separate, strain-gaged steel column was selected as the stress-sensing element for the MCBI gage.

The MCBI is designed to measure pressures at soil/structure interfaces up to a maximum of 35,000 psi (a complete set of machine drawings for the MCBI gage are at Appendix A). The stress-sensing column is contained within a steel housing, which provides a protective cover for the strain gages and their associated wiring. The wiring is secured inside the housing by means of a steel retaining plug (Figure 1). During assembly, the column (which has an "o"-ring near its top end) is inserted into the housing. Once assembled, the top of the sensing column is flush with the top of the housing, and the "o"-ring maintains an airtight seal between the top of the column and the housing. The retainer plug is then screwed into the back of the housing to prevent the sensing column from being displaced by applied loads.

The three-piece, steel gage mount (Figure 2) allows the MCBI gage to be installed in concrete structures after the concrete is poured, and reduces gage sensitivity to lateral accelerations and stresses. The mount consists of a main body, an isolation ring which fits into the main body and supports the MCBI gage when mounted, and an isolation cap

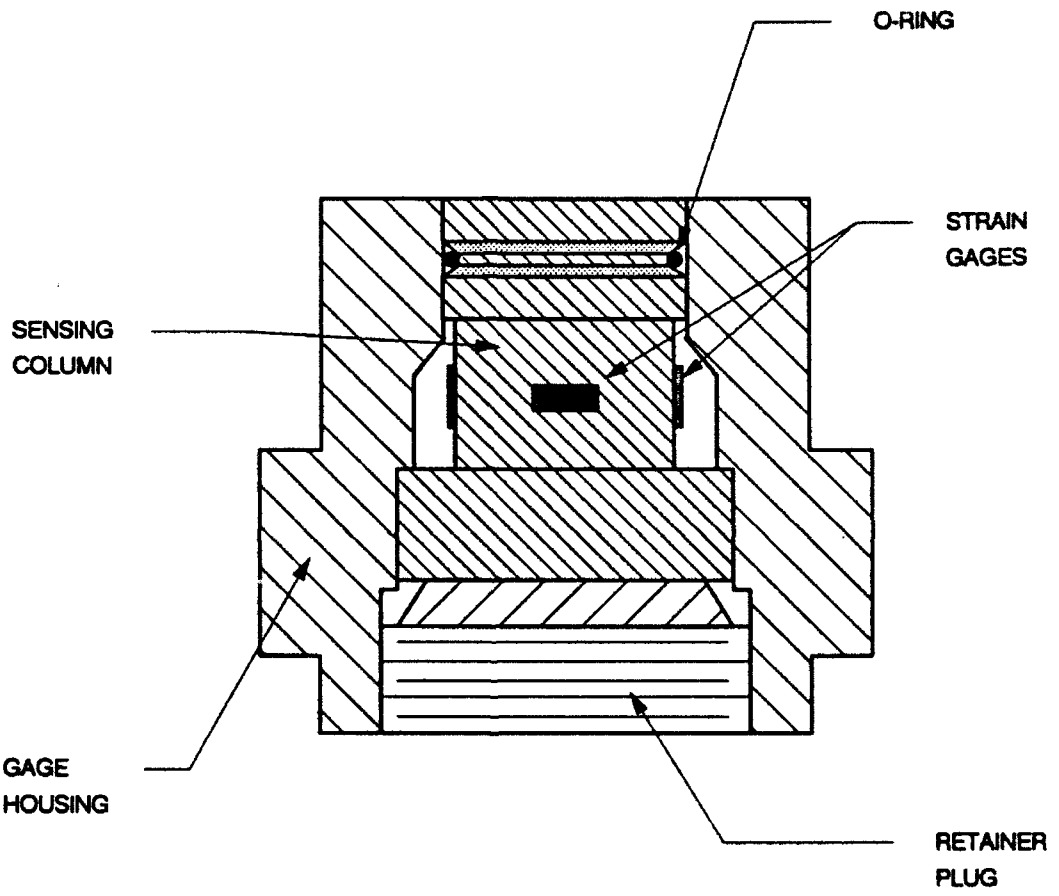

Figure 1. Cross-section of assembled MCBI gage

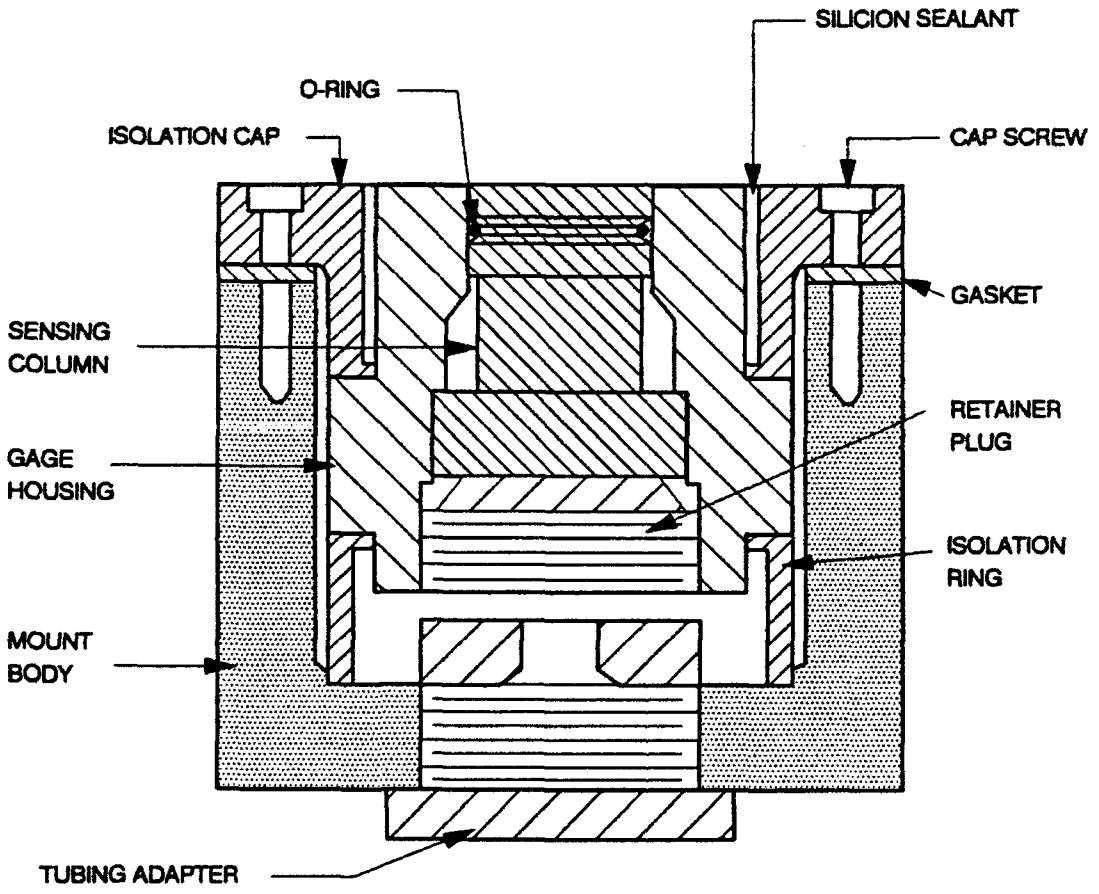

Figure 2. Cross-section of assembled MCBI gage and mount

which is bolted to the top of the main body and holds the MCBI gage in place. A fully assembled MCBI gage and mount are shown in Figure 3.

2.2.1 MCBI Gage.

The gage body consists of a sensing column, housing, and retaining plug, all composed of 4340 alloy steel. The gage face, which is on the side of the upper portion of the sensing column, is 0.750 in. in diameter. This diameter is maintained in the upper 0.450 in. of the column, except for a groove to accommodate an "o"-ring (Parker Part No. 2-113) centered 0.225 in. from the top of the column. The column diameter decreases to 0.700 in. over the next 0.500 in. of the column's length. The originallv rounded sides of this section are milled to provide four flat surfaces; two horizontal gage flats 0.390 in. by 0.500 in. located 180 degrees apart, and two vertical gage flats 0.200 in. by 0.500 in. located 180 degrees from each other and 90 degrees from the horizontal gage flats. Below this section, the diameter increases to 1.100 in. A 0.125-in. diameter cable exit hole is drilled through this section at a 45-degree angle slcping toward the column's center. The hole is located at the base of one of the horizontal gage flats.

The MCBI gage housing is a right circular cylinder that has been bored out to accommodate the sensing column. The upper 0.450 in. inside the housing must be polished to at least a No. 32 finish to provide a smooth surface for the "o"-ring of the sensing column. The bottom end of the housing is tapped for the 1-1/4 - 16 UN thread of the retainer plug. The outer diameter of the housing is 1.498 in., except for a flange which protrudes 0.150 in. from the top of the housing. The upper and lower flange surfaces are polished to at least a 32 machine finish, since these surfaces are involved in an "o"-ring seal during calibration of the MCBI gage.

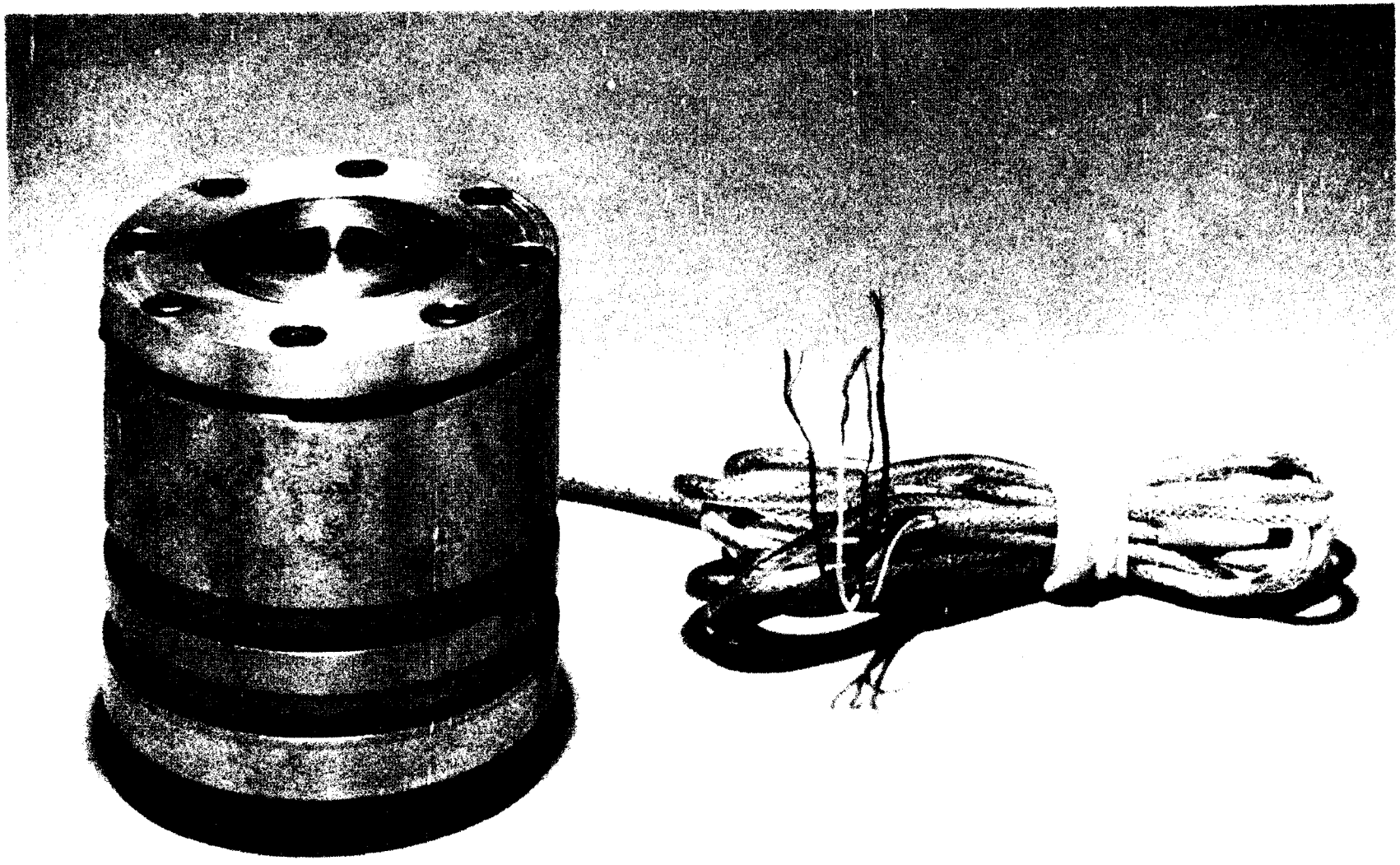

Figure 3. Fully assembled MCBI gage and mount

The retainer plug is approximately 5/8 in. long, and has a 1-1/4 - 16 UN thread cut into its external surface for a length of 1/2-inch. The remainder of the plug is tapered to an end diameter of 0.905 in. A notch is cut into the plug at the end opposite the taper, and a 1/2-inch diameter hole is bored through the center of the plug.

2.2.2 Sensing Elements.

Four Kulite S/UDP-350-160 semiconductor strain gages (Reference 4) are bonded to the gage flats of the sensing column with epoxy. Strain gages are positioned horizontally on the larger gage flats for Poisson compensation, and vertically on the smaller gage flats for primary sensing (Figures 4 and 5). The strain gages are electrically connected to form a full Wheatstone bridge circuit, as shown in Figure 6. An excitation current of 10 mA is typically used, which corresponds to a bridge excitation of approximately 5 volts. Bridge excitation should not exceed 20 volts.

2.2.3 Gage Mount.

The gage mount consists of a main body, an isolation ring, and an isolation cap, all constructed of 4340 alloy steel. The main body is a right circular cylinder which is bored out to accept the MCBI gage. Eight holes are drilled at equal spacings around the top of the main body and tapped for 8-32 UNC cap screws. Two 1/8-in. diameter grooves are cut around the outer circumference of the main body to improve its bonding to concrete and grout. A hole is drilled through the bottom of the main body and along its center line. This hole is tapped for a 1-1/4 in. - 16 UN thread and will accommodate a commonly used tubing adapter.

The isolation cap and ring hold the MCBI gage in place and provide lateral stress isolation. Eight holes are drilled at equal spacings through the top of the cap and counter-sunk for 8-32 socket head cap screws. An isolation section extends downward from the bottom of the

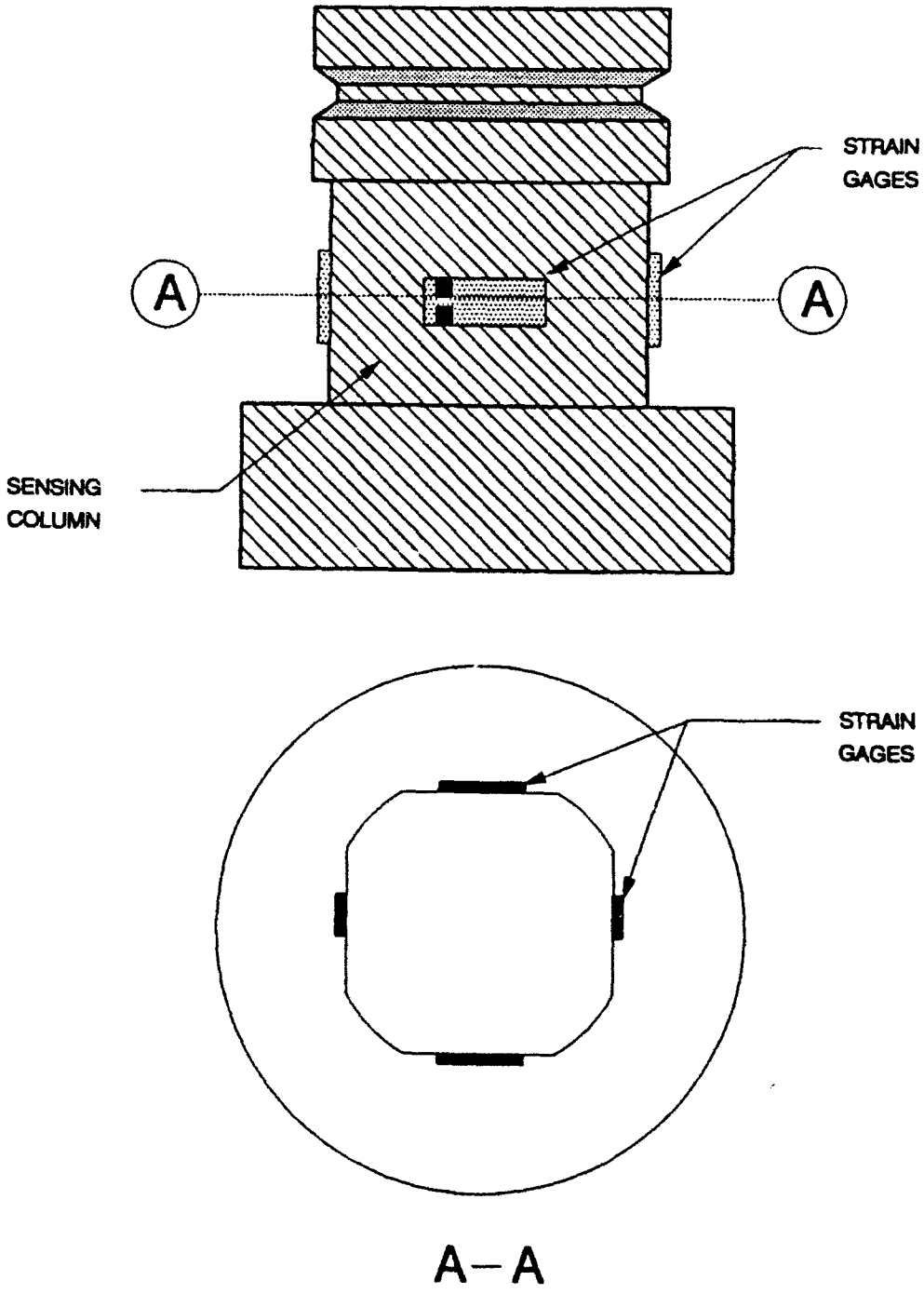

Figure 4. Location of strain gages on sensing column

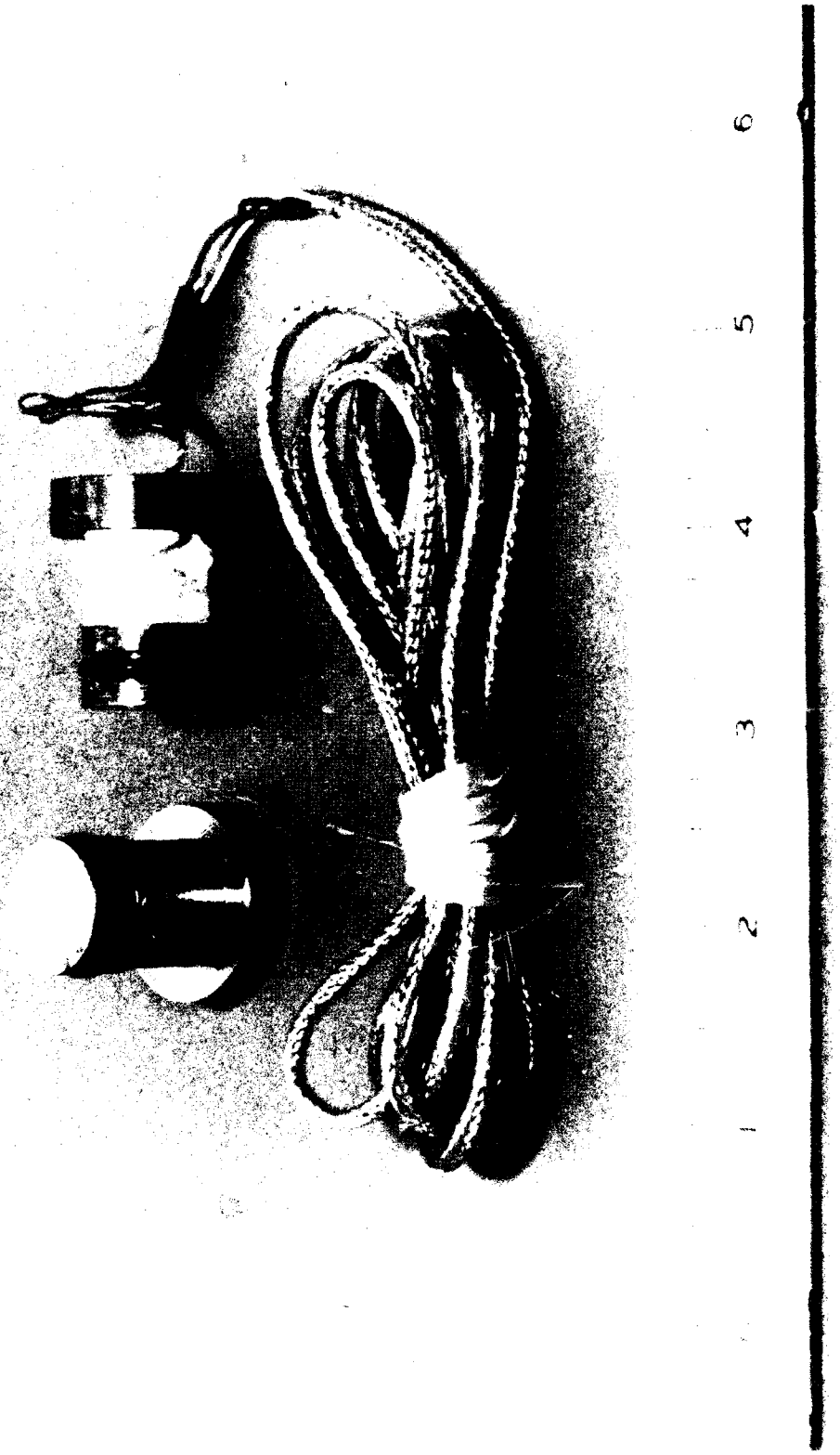

Figure 5. Sensing column before (left) and after strain gaging

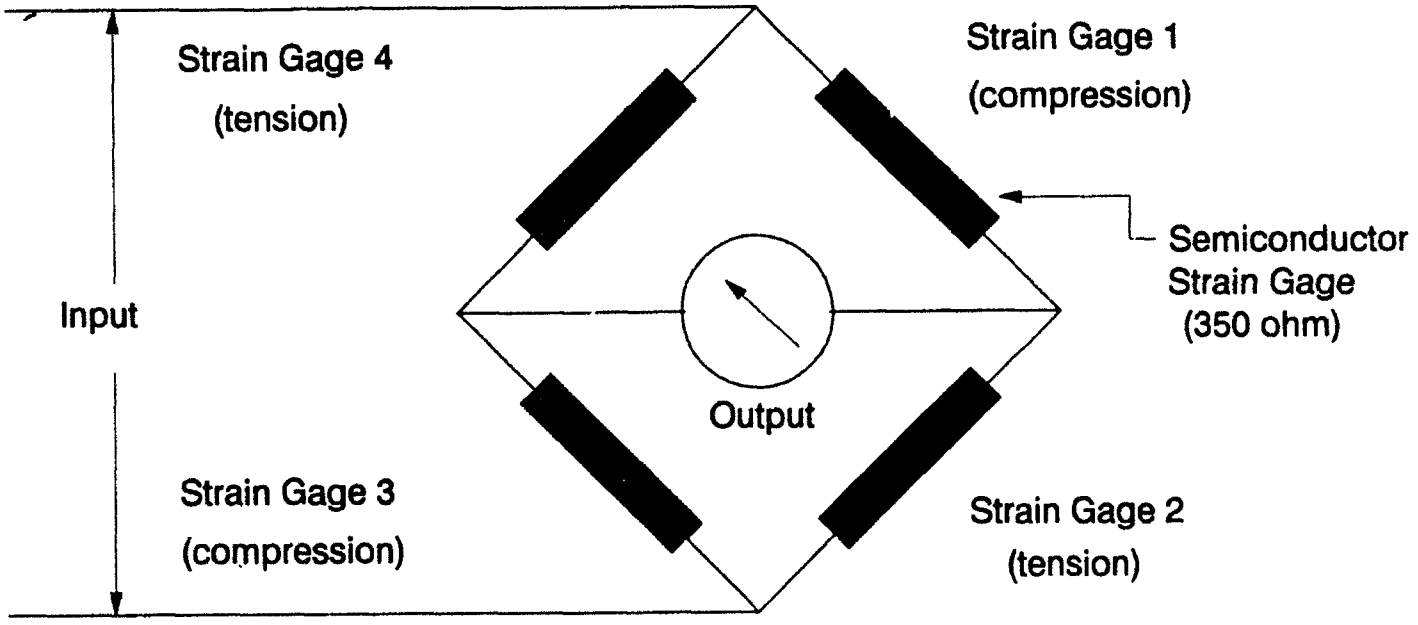

Figure 6. Wheatstone bridge circuit diagram for the MCBI gage

Figure 6. Wheatstone bridge circuit diagram for the MCBI gage

cap in the form of a thin annulus. A small lip at the bottom of the isolation section provides a lateral separation between the gage mount and the top of the MCBI gage. The lateral isolation ring supports the MCBI gage from beneath and also incorporates a lip in order to separate the bottom of the gage from the gage mount.

2.3 DESIGN CALCULATIONS

Design calculations were undertaken for all critical components of the MCBI gage and its mount. The results of those calculations are presented in the following discussion.

2.3.1 MCBI Gage.

Assuming the active area of the sensing column's gage face to have a diameter of 0.750 in. (1.905 cm), the total load on the column for the maximum design pressure, P, of 35,000 psi (241 MPa), will be:

$$F = \pi (d^2/4) P = 15,463 \text{ lb}$$

The smallest cross-sectional area, A, of the column to carry this load is 0.587 in. in diameter. Thus, the greatest axial stress developed is:

$$F/A = 57,138 \text{ psi}$$

A possible failure mode for the column is shear in the section of the gage face which overhangs the "o"-ring groove. The overhang has a thickness, T, of 0.150 inches. The shearing force is applied to the area of a ring with inner radius, R_1 of 0.285 in., and outer radius, R_2 of 0.375 in. The applied force is the design pressure, P, multiplied by the area of the ring:

$$F = P \pi (R_2^2 - R_1^2) = 6,531 \text{ lb}$$

The area resisting this shearing force is:

$$A = 2 \pi TR_1 = 0.269 \text{ in.}^2$$

Thus, the calculated shearing stress is:

$$F/A = 24,279 \text{ psi}$$

Now consider shear beneath the column. The force acting on the column was earlier computed to be:

$$F = 6,531 \text{ lb}$$

The area resisting this shearing force is:

$$A = 2 \pi TR_1$$

where T is the thickness of the column base, 0.300 in., and R is the lower column radius, 0.350 in. Therefore, the area resisting the shearing force is:

$$A = 0.660 \text{ in.}^2,$$

and the maximum shearing stress is 9,895 psi. Based on these calculations, unheat-treated 4340 alloy steel, with a yield strength of 70 ksi, was chosen as the construction material for all components of the MCBI gage.

2.3.2 Gage Mount

The mount components most likely to fail under loading of the MCBI gage to the maximum design pressure, P (35,000 psi), are the lateral isolation cap and ring. Assuming that the top surface of the gage has a radius, R, of 0.750 in., the resulting force is:

$$F = \pi PR^2 = 61,850 \text{ lb}$$

The force is applied to a ring with inside radius, R_1, of 0.800 in. and outside radius, R_2, of 0.900 in. Thus, the area resisting the force is:

$$A = \pi (R_2^2 - R_1^2) = 0.534 \text{ in.}$$

The calculated stress is:

$$F/A = 115{,}824 \text{ psi}$$

Based on these calculations, unheat-treated 4340 steel was selected as the construction material for the MCBI gage mount. Because the yield strength of unheat-treated 4340 steel is only 70 ksi, however, the lateral isolation ring should be heat-treated after machining to provide a yield strength of 200 ksi.

During heat treatment, 4340 steel is normalized at 1600°F, reheated to 1475°F, then oil-quenched and tempered (Reference 5). Tempering at 750°F results in an approximate Rockwell C hardness of 42 and gives the ring a yield strength (200 ksi) significantly greater than that anticipated under maximum loading conditions.

2.3.3 Natural Frequency.

An equation for the natural frequency, f_n, of a column is given by Graff (Reference 6) as:

$$f_n = (K^2/2\ \pi\ L^2)(EI/\rho A)^{1/2}$$

where L is the length of the column; E is Young's modulus for the material; I is the moment of inertia; A is the cross-sectional area of the column; ρ is the density of the column material; and K is a constant for a specified column end condition. Approximating the conditions of the column as being free on one end and clamped on the other, then $K = 3.930$. Substituting these values into Graff's equation:

$$I = \pi\ R^4/4$$

$$A = \pi\ R^2$$

$$L = 1.25 \text{ in.}$$

$$R = 0.350 \text{ in.}$$

$$E = 29 \times 10^6 \text{ psi for steel}$$

$$\rho = 15.22 \text{ lb - sec}^2/\text{ft}^4$$

The resulting natural frequency is:

$$f_n = 110 \text{ kHz}$$

The other mode of vibration, with stress waves reflecting back and forth along the length of the column, is given by:

$$f_{nb} = C/2L$$

where C, the sound speed in steel, is 16,600 ft/sec. The resulting natural frequency is:

$$f = 142 \text{ kHz}$$

Thus, the lowest natural frequency of the column is 110 kHz.

SECTION 3

LABORATORY TESTING

3.1 INITIAL TESTS

After assembly at WES, the first two prototype MCBI gages, designated R1 and R2, were checked to assure electrical continuity and ample resistance to ground (i.e., greater than 20 MΩ). The MCBI gages were then checked to determine sensitivity or full-scale output using a small pressure chamber (Figure 7) built for this purpose. The gages were loaded in 2,000-psi increments from 0 to 20,000 psi using a high-pressure hydraulic pump. Comparison pressure-output curves for Gages R1 and R2 are shown in Figure 8. The two curves were very similar, and the average gage sensitivity was 0.073 mV/V/psi (Note: all MCBI gage physical, electrical, and dynamic characteristics are compiled in Table 1).

After this initial high-pressure test, both gages were dismantled in order to determine if the MCBI gage interior "o"-rings had prevented hydraulic fluid from reaching the strain gages and electrical connections on the column. No sign of leakage was found in either gage, and each was still fully functional, indicating that the current design was adequate to prevent pressure-related damage during dynamic loadings.

The first four MCBI gages, designated R1-R4, were loaded from 0 to 20,000 psi numerous times in the high-pressure chamber in order to develop calibration standards for the gages (see Table 1). Calibration curves for MCBI Gages R1-R4 are shown in Figures 9 and 10. MCBI gage calibration equivalent values were between 38,000 and 45,000 kΩ-psi. Typical gage output versus applied pressure was very linear, with an R2 linearity factor of 0.999 (where a figure of 1.000 is a straight line). Hysteresis averaged 0.5 percent of full scale output.

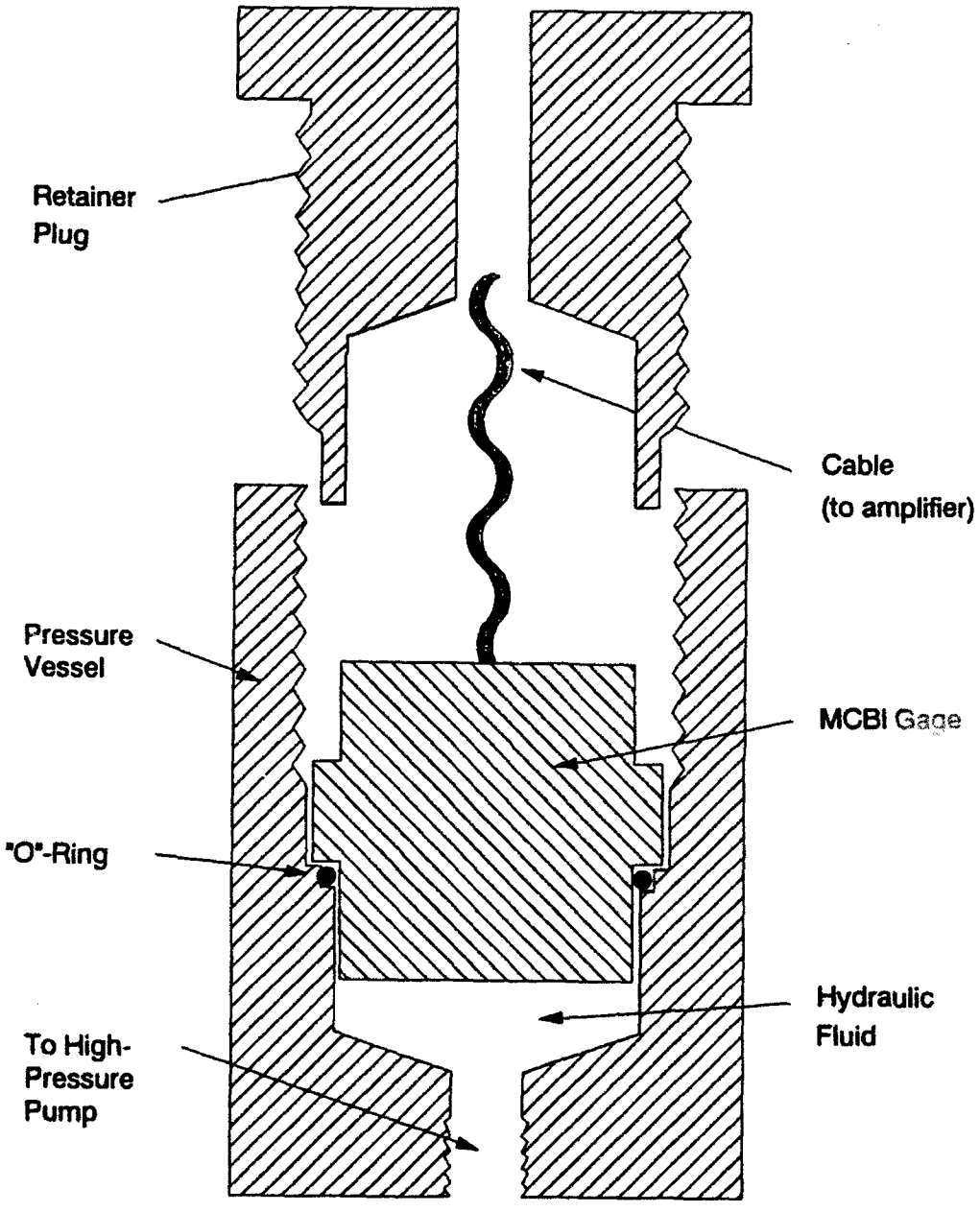

Figure 7. MCBI gage calibration vessel

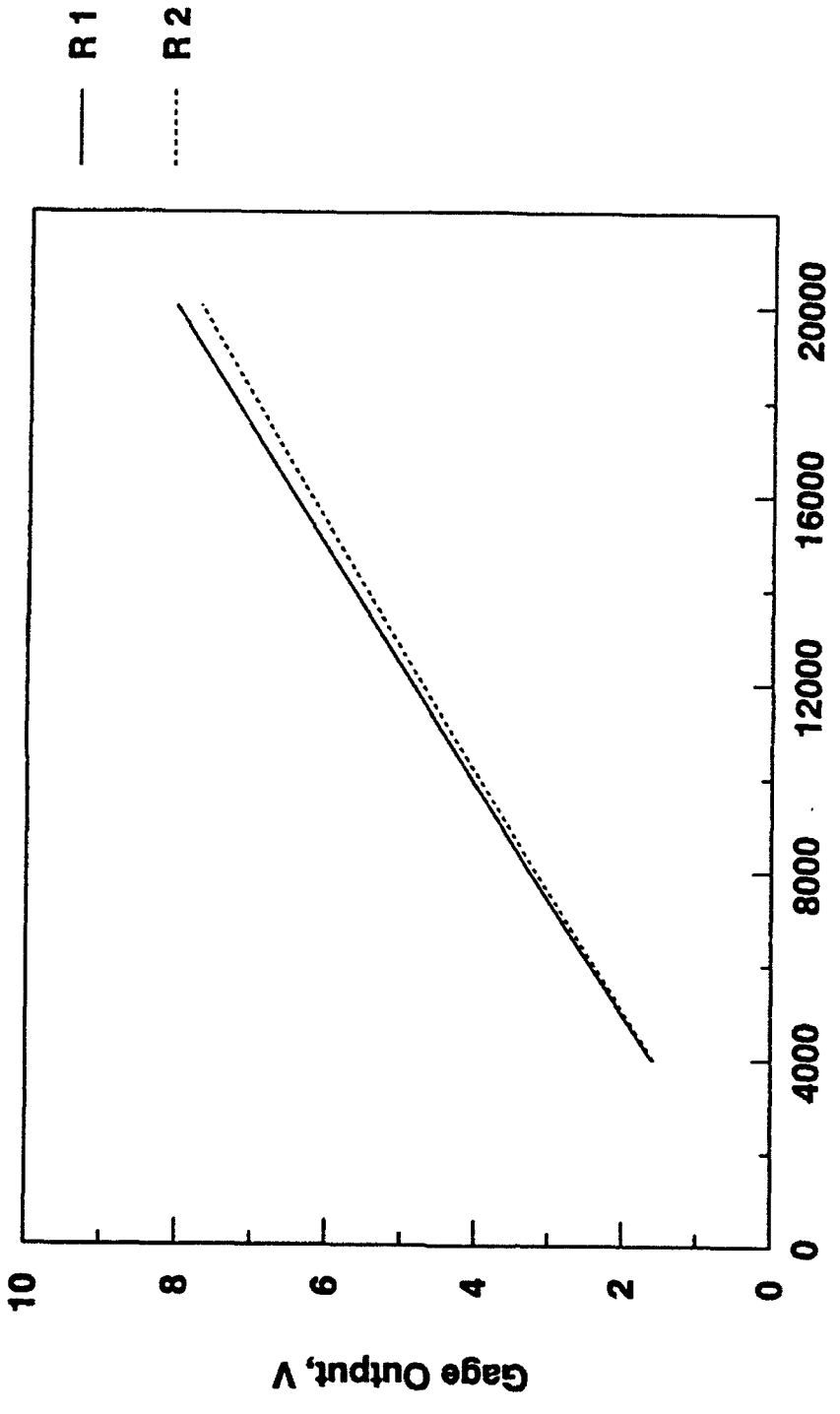

Figure 8. Pressure/output curves for MCBI prototype gages R1 and R2

TABLE 1

MCBI GAGE CHARACTERISTICS

Range:	35,000 psi
Sensitivity:	0.073 mV/V/psi
R2 Linearity: (R2 = 1 for straight line)	0.9997, typical
Acceleration Sensitivity	
Normal:	0.139 psi/g
Transverse:	0.018 psi/g
Sensing Surface:	0.750 in., diameter
Maximum Width (gage only):	1.800 in.
Maximum Width (gage and mount):	2.800 in.
Length (gage):	1.750 in.
Length (gage and mount):	2.500 in.
Lowest Natural Frequency:	110 kHz
Frequency Response:	DC to 30 + kHz
Hystreseis:	0.5 percent of full scale, typical

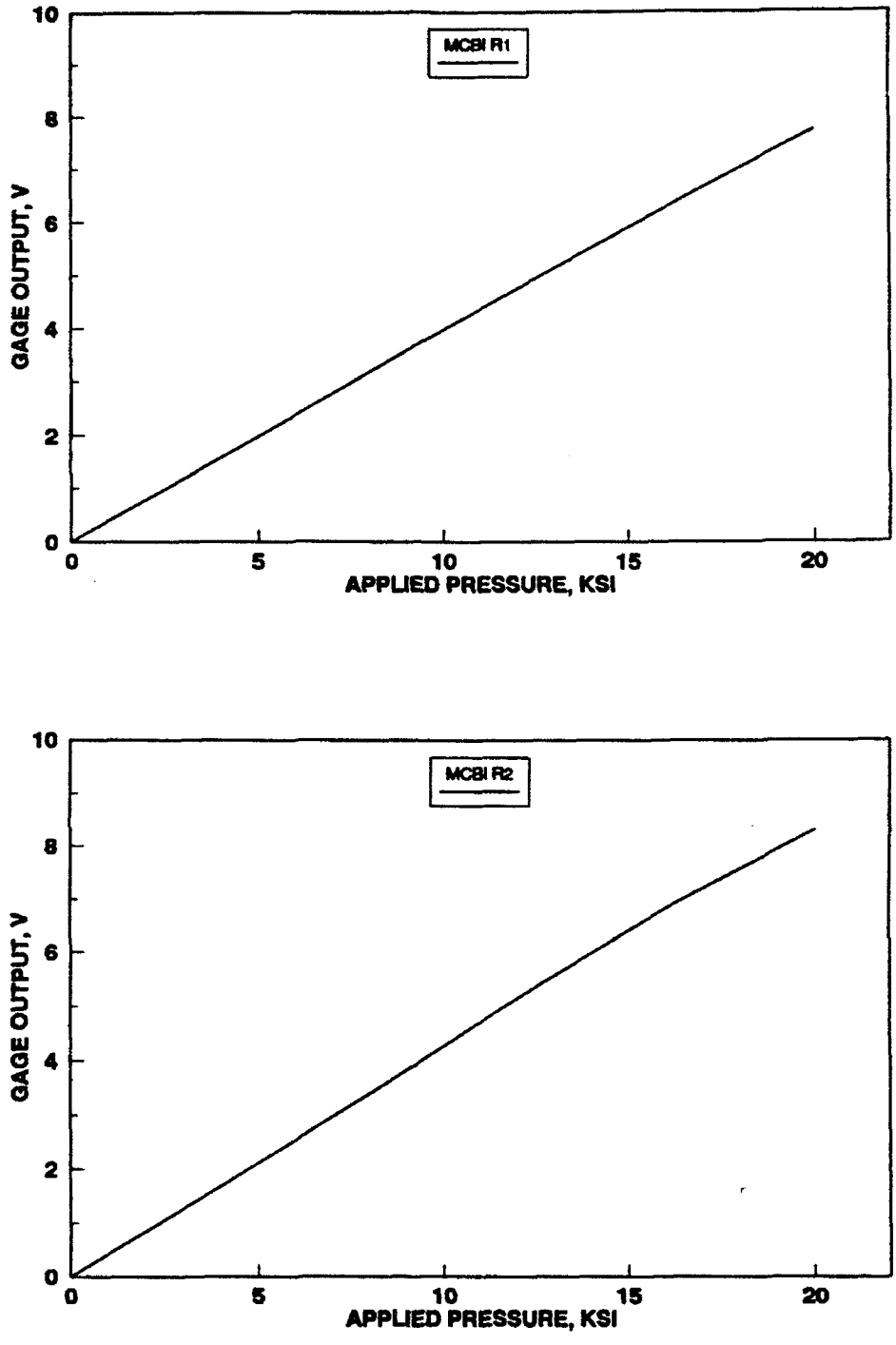

Figure 9. Calibration record for MCBI gages R1 (top) and R2

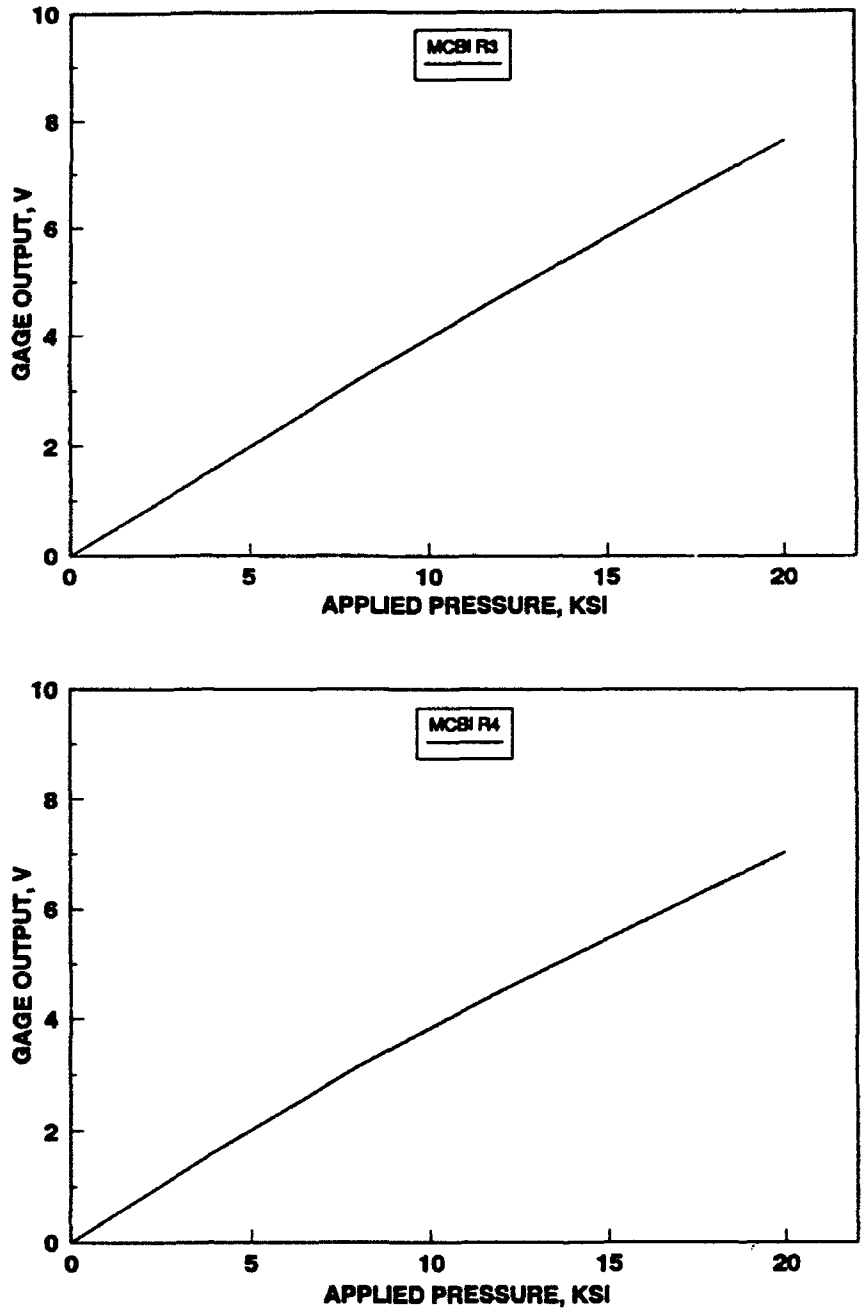

Figure 10. Calibration record for MCBI gages R3 (top) and R4

3.2 ACCELERATION SENSITIVITY

MCBI gages were thoroughly tested for electrical output caused by acceleration effects. The gages were placed within their standard mounting hardware. An accelerometer (Endevco Model 2264) was also fastened to the mounting hardware to measure the acceleration experienced by the MCBI gage (Figure 11). Accelerations were applied to the MCBI gages through the use of a drop-testing device, as shown in Figure 12. The gages were clamped onto a heavy steel carriage, and dropped from a height of three feet, developing accelerations of 2,500 to 3,000 g's upon impact with the bottom of the drop-testing device.

Numerous drop-tests were performed with the MCBI gage positioned horizontally -- the typical orientation for interface pressure measurements. The gages were rotated within their mounts after each drop test in order to determine if gage orientation within the mount affected acceleration sensitivity. Representative plots of MCBI gage output versus applied acceleration are shown in Figures 13-16, while the results of the drop tests are presented in Table 2. Gage orientation within the mount made little difference on the lateral acceleration sensitivity, which averaged 0.018 psi/g. This compares favorably with the Kulite VM-750 interface gage, which exhibited a lateral acceleration sensitivity of 0.019 psi/g during previous testing at WES (Reference 7).

Drop tests were also performed to determine MCBI gage sensitivity to normal accelerations. The testing scheme was identical to that used for the lateral sensitivity tests, except that the gage mount was turned to face downward. Plots of gage output versus acceleration are shown in Figures 17 and 18, and the results are included in Table 2. Normal acceleration sensitivity averaged 0.139 psi/g. Although the MCBI gage sensitivity to normal acceleration appears high, the drop tests represent an extremely severe case, since, in most applications, the gages are typically cast into massive concrete structures which greatly decrease the acceleration imparted to the gages.

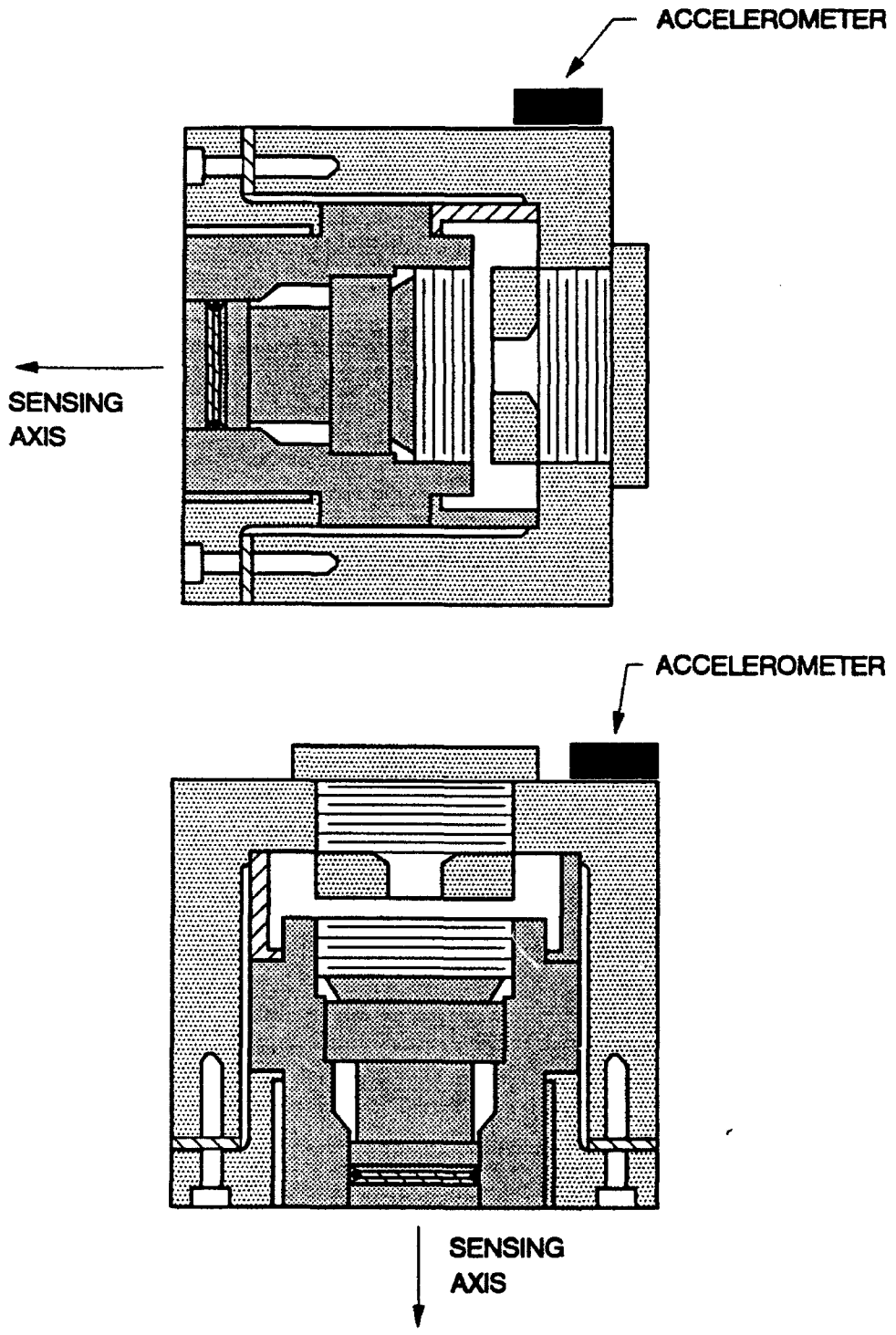

Figure 11. Accelerometer locations on MCBI gage mount during lateral (top) and normal (bottom) acceleration-sensitivity tests

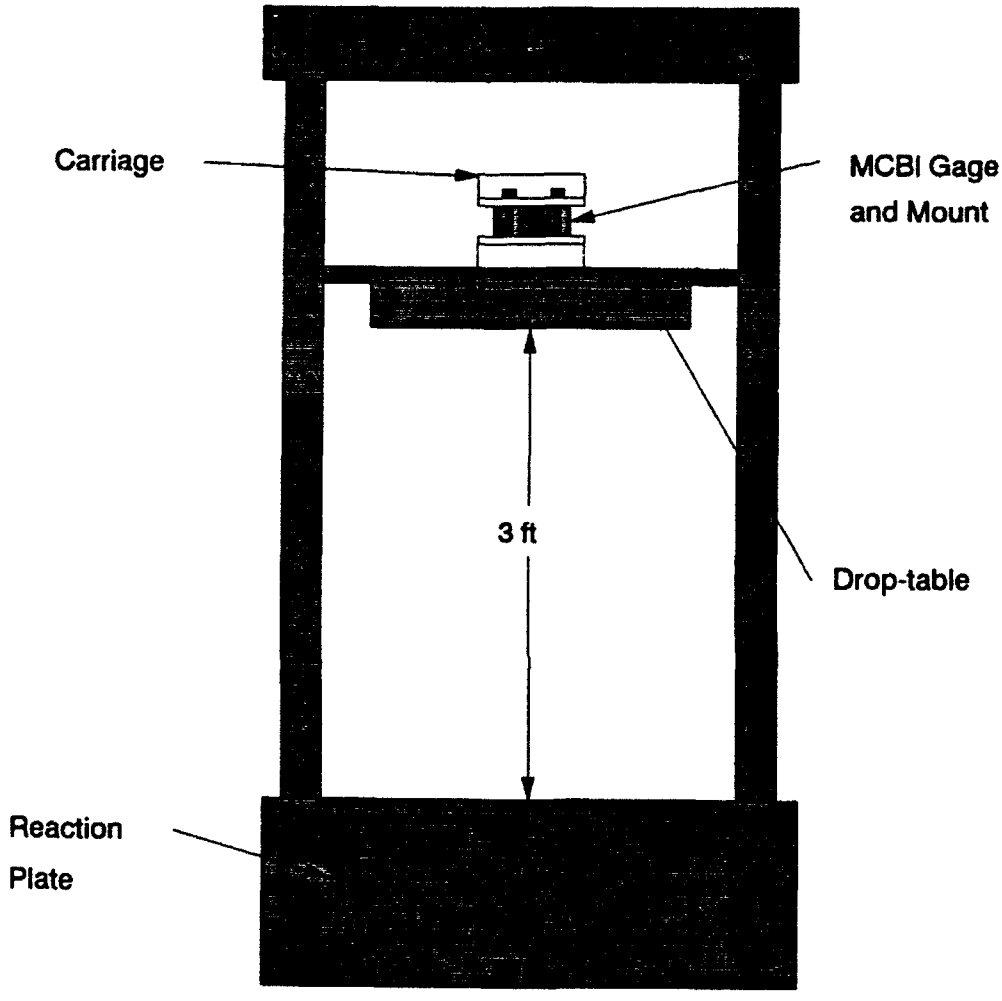

Figure 12. Drop-testing device used in MCBI acceleration-sensitivity tests

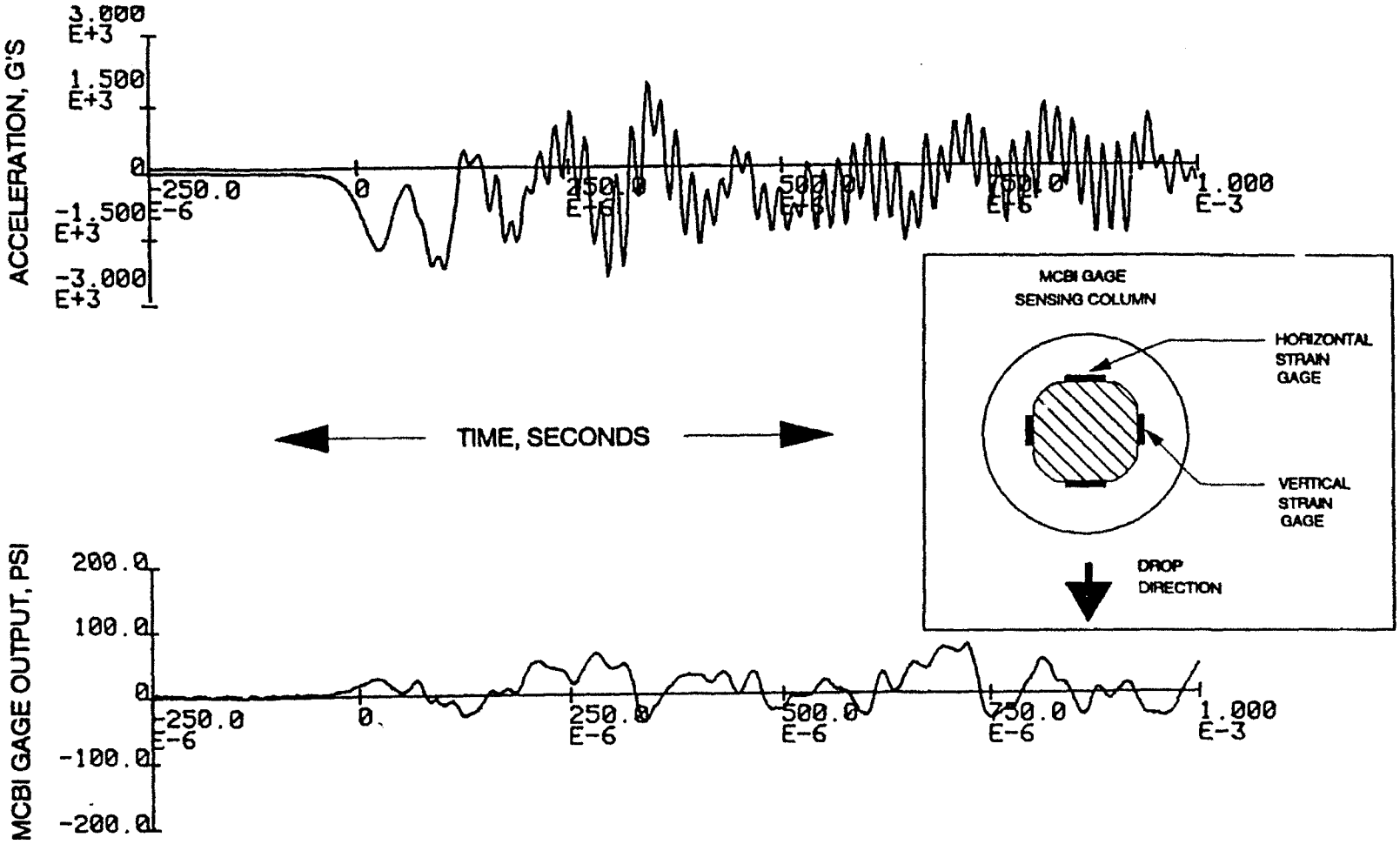

Figure 13. Comparison of MCBI gage output (bottom curve) versus applied lateral acceleration. The MCBI gage is positioned so that the transverse strain gages are vertically oriented

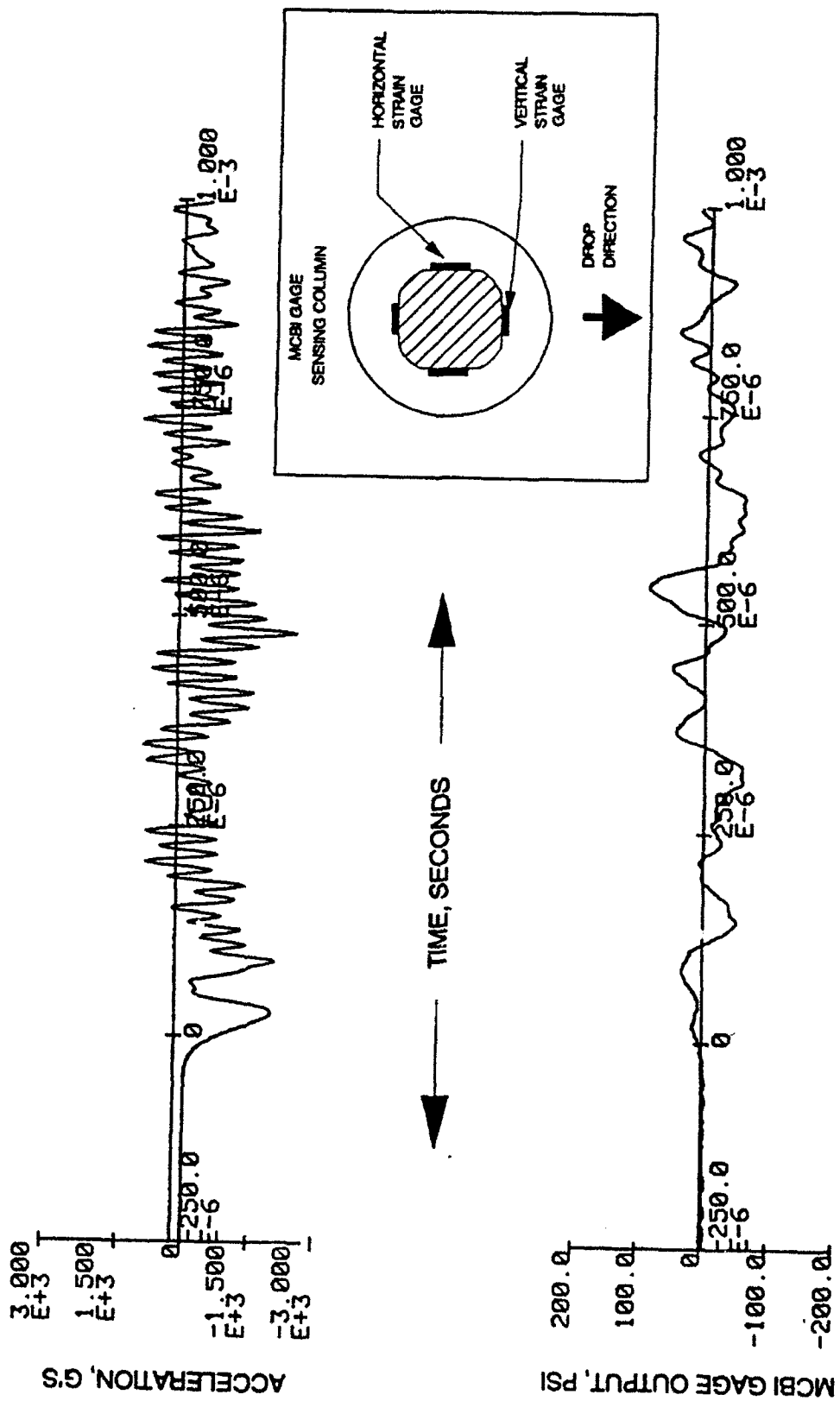

Figure 14. Comparison of MCBI gage output (bottom curve) versus applied lateral acceleration. The MCBI gage is positioned so that the transverse strain gages are horizontally oriented

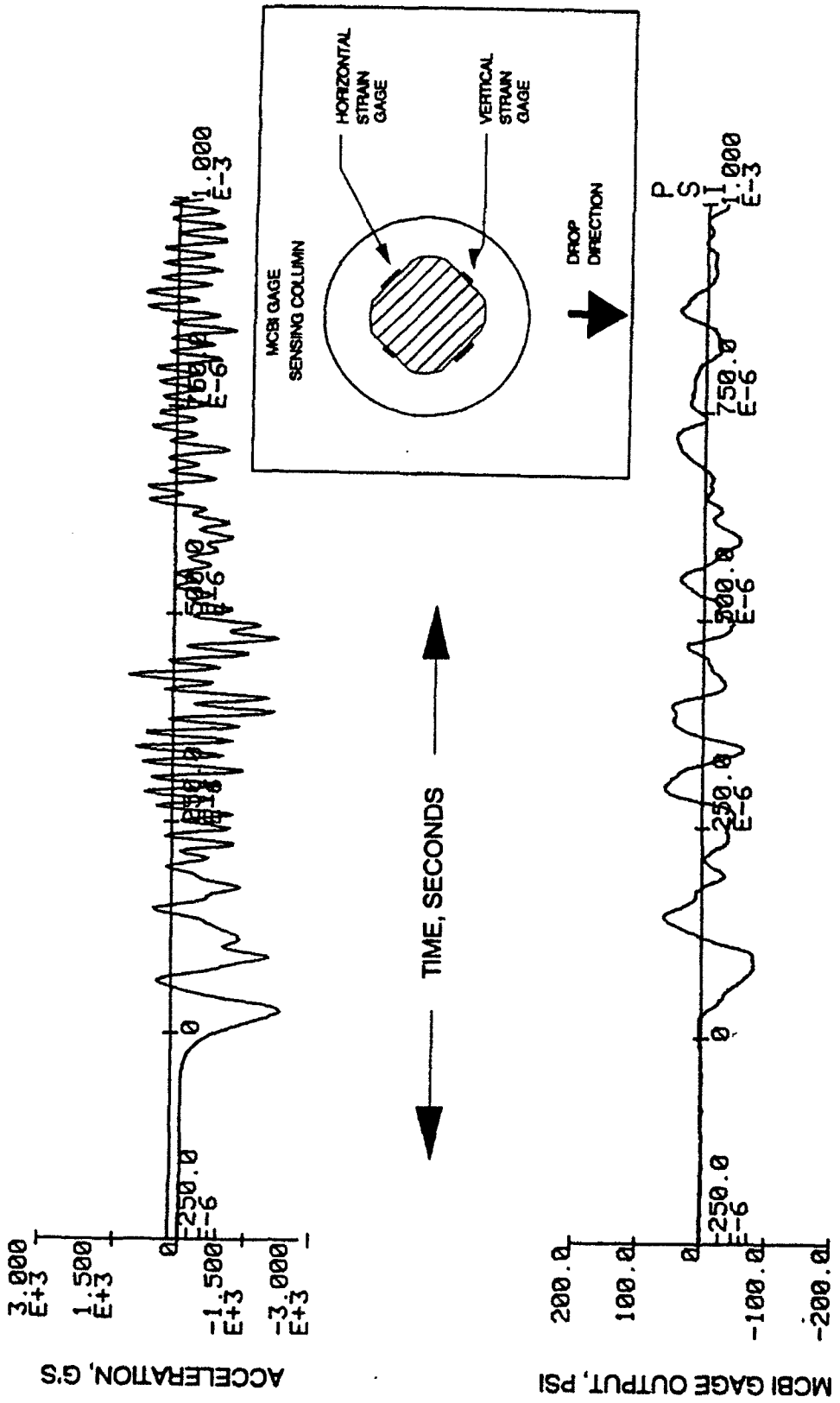

Figure 15. Comparison of MCBI gage output (bottom curve) versus applied lateral acceleration. The MCBI gage is positioned so that the transverse strain gages are 45 degrees from the vertical

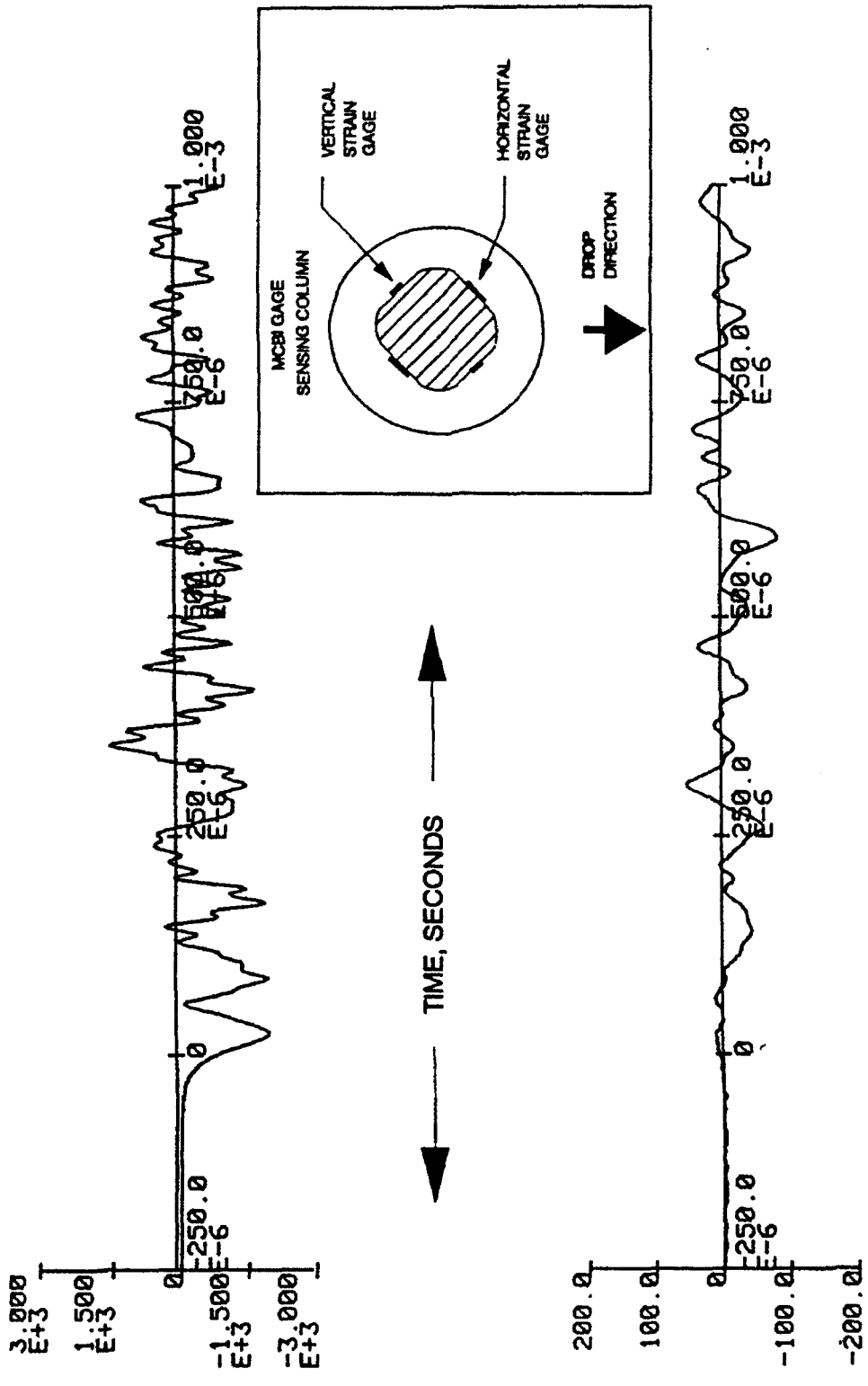

Figure 16. Comparison of MCBI gage output (bottom curve) versus applied lateral acceleration. The MCBI gage is positioned so that the transverse strain gages are 45 degrees from the vertical

TABLE 2

MCBI GAGE ACCELERATION SENSITIVITY
TEST RESULTS

Test No.	MCBI Gage Orientation	Applied Acceleration (g's)	MCBI Output psi	Acceleration Sensitivity psi/g
1	Horizontal	2,000	32.6	0.0163
2	Horizontal	1,923	32.9	0.0171
3	Horizontal	2,533	75.0	0.0296
4	Horizontal	1,956	12.8	0.0078
5	Vertical	1,913	263.1	0.138
6	Vertical	2,760	352.2	0.128

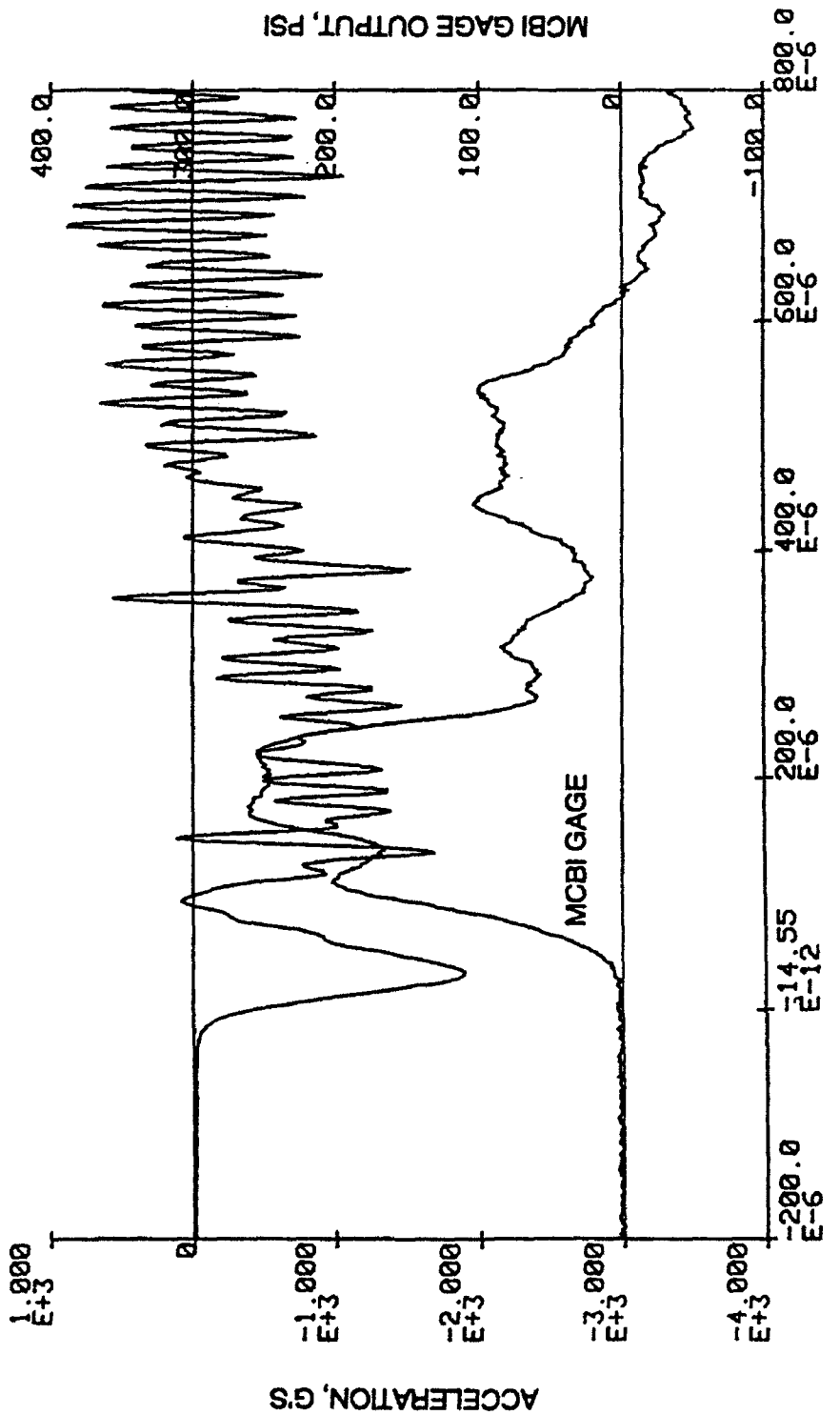

Figure 17. Comparison of MCBI gage output (bottom curve) versus applied normal acceleration, Test 1

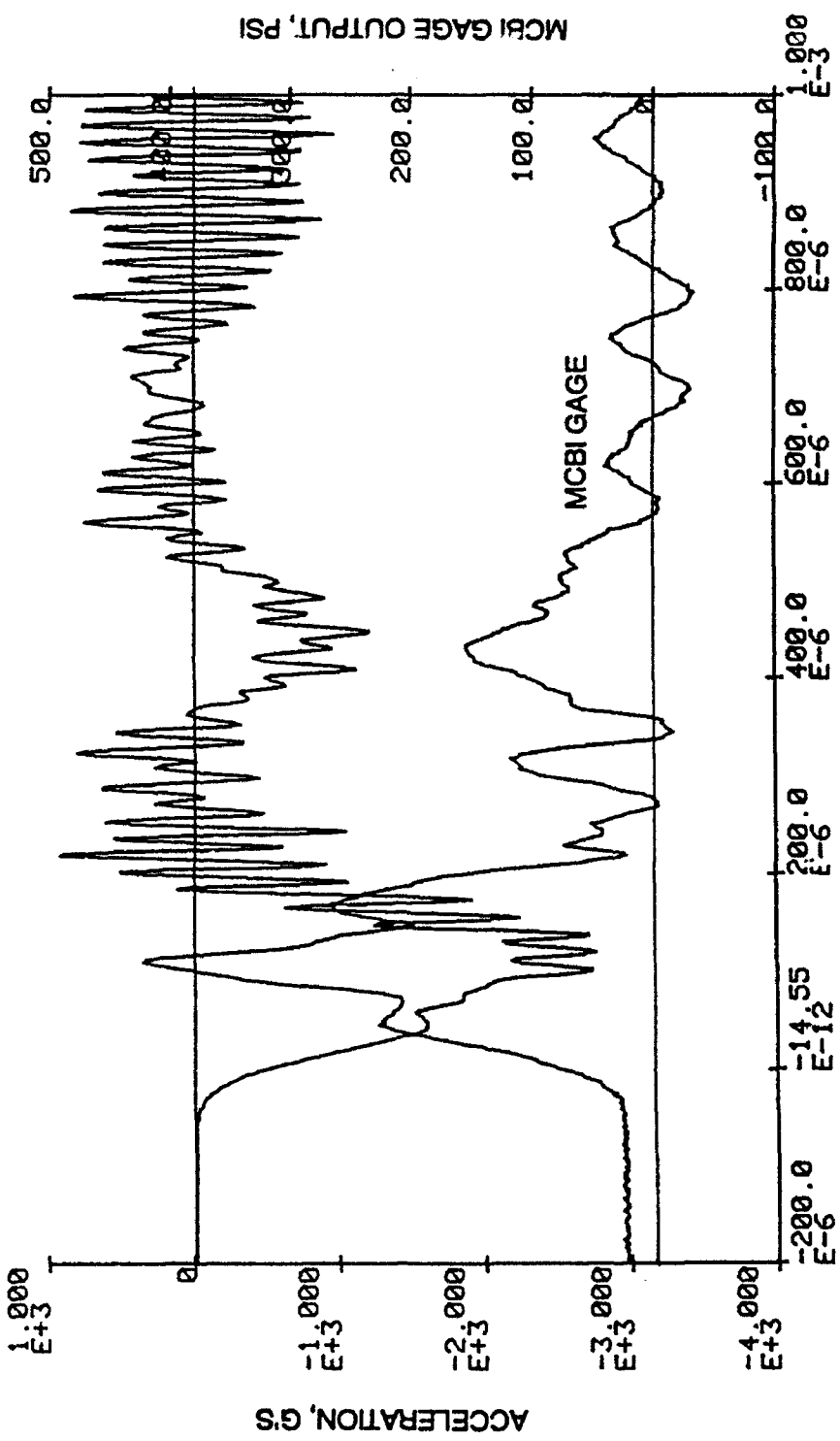

Figure 18. Comparison of MCBI gage output (bottom curve) versus applied normal acceleration, Test 2

3.3 LATERAL STRESS SENSITIVITY

In order to assess MCBI gage sensitivity to lateral stress, it was necessary to subject it to uniaxial stress applied in a direction normal to the gage's sensing axis. To facilitate this, a gage was placed in its mounting hardware and cast in a high-strength grout cylinder with the gage oriented so that the gage face was tangent to the outer curvature of the cylinder (Figure 19). A standard concrete testing machine was then used to load the cylinder.

Loads were applied from 0 to 5,000 psi in 1,000-psi increments with the MCBI gage positioned in each of four different orientations within the gage mount. The MCBI gage used on these tests was connected to a signal conditioner/amplifier unit that produced a full-scale output of 10 V. This full-scale output was equivalent to an applied normal stress of 5,000 psi. Figure 20 presents the results of the loading tests as gage electrical output versus applied stress. Gage output did not exceed the "drift" of ± 0.015 V associated with the signal conditioner/amplifier unit used on the test. This result shows that lateral stresses should not contribute significantly to MCBI gage output.

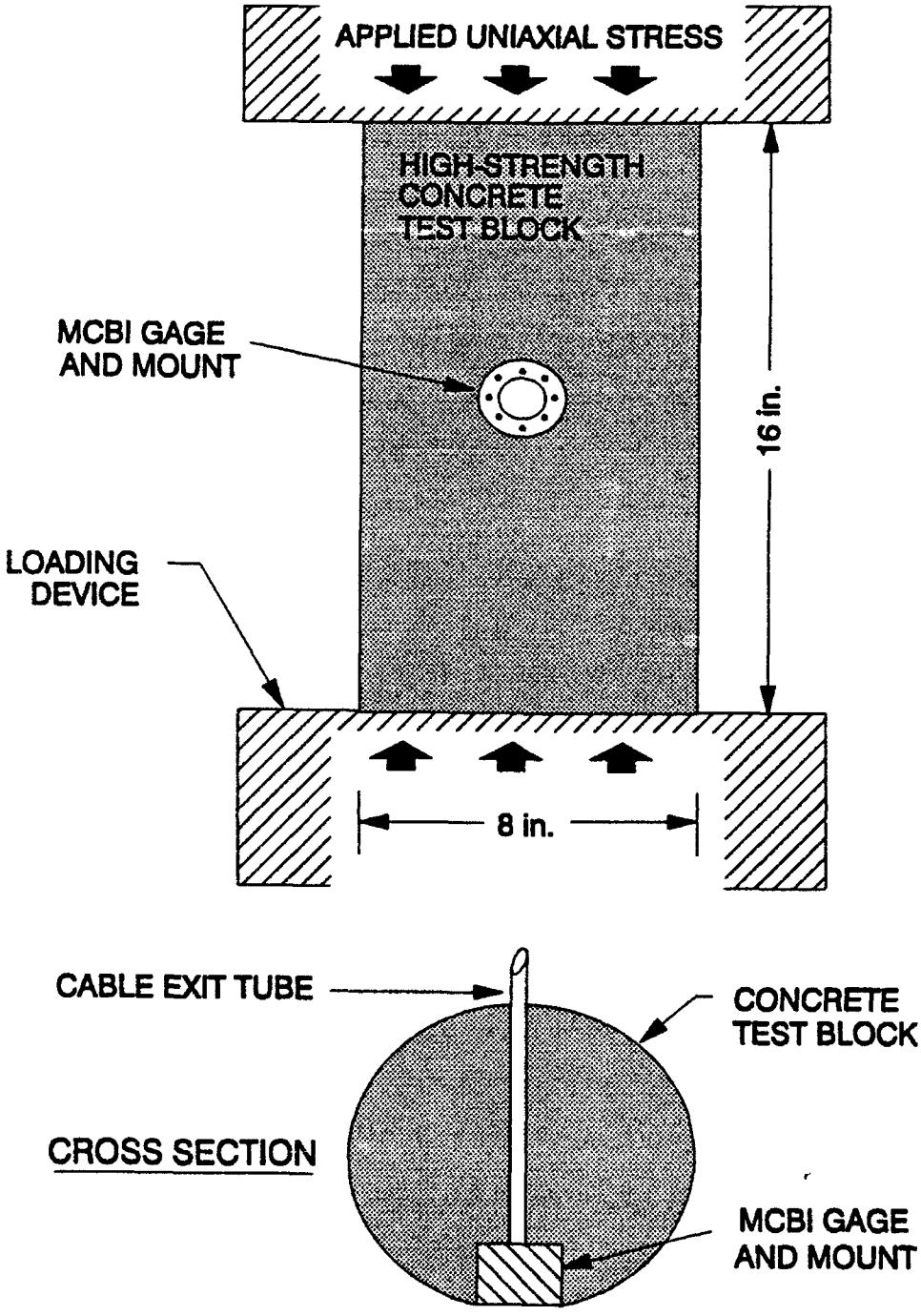

Figure 19. Configuration for the MCBI gage lateral stress sensitivity tests

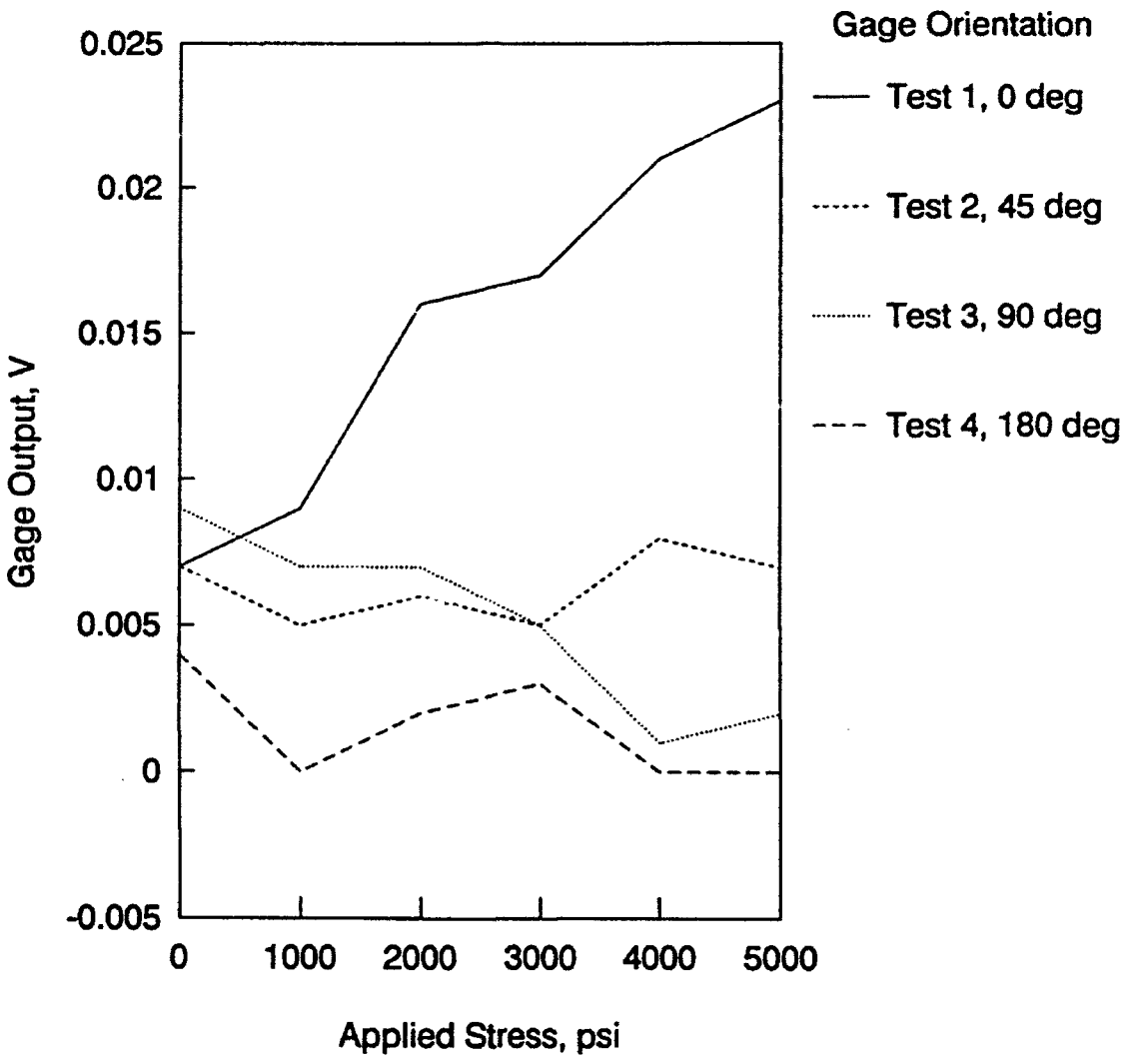

Figure 20. Lateral stress sensitivity test results. Test 1 was conducted with a longitudinal strain gage facing toward the applied stress; other orientations are relative to that of Test 1

SECTION 4

DYNAMIC TESTING

4.1 INITIAL TESTS

The first calibrated MCBI gages became available for dynamic testing in Fall 1986. Gages were placed on selected high explosive tests when empty recording channels were available. Gage R1 was placed for an airblast measurement on the U.S. Air Force Ballistic Missile Office-funded CHT-3 Airblast Calibration Test (Reference 7) near Yuma, AZ. The testbed configuration included bar, airblast, and soil stress gages. The design airblast simulation pressure was 5.5 ksi. Using the MCBI gage to measure airblast served two purposes; first, to determine whether the gage was capable of surviving severe shock loading, and second, to assess the gage's airblast measurement capability.

The MCBI gage survived the test in operable condition, and produced what appeared to be a reasonably good airblast measurement (Figure 21). The only other airblast measurements obtained during the test were fr[illegible] the two bar gages. The MCBI and bar gage records are compared in Figure 22. The MCBI gage measured a peak pressure approximately double that indicated by bar gage BG-1. Bar gage BG-2 measured a peak pressure value similar to that of the MCBI gage, but at approximately 80 μsec later in time. These differences may be due to the higher frequency response of the MCBI gage, which would allow a more faithful measurement of the early-time airblast, or may be due to differences in the airblast environment at the different gage positions.

A comparison of the impulse wave forms at 1.5 msec after shock arrival (the point at which reflections appear on the bar gage records) indicates that the impulse derived from the MCBI record is approximately 6.0 psi-sec, as opposed to 8.5 and 10 psi-sec for the bar gages

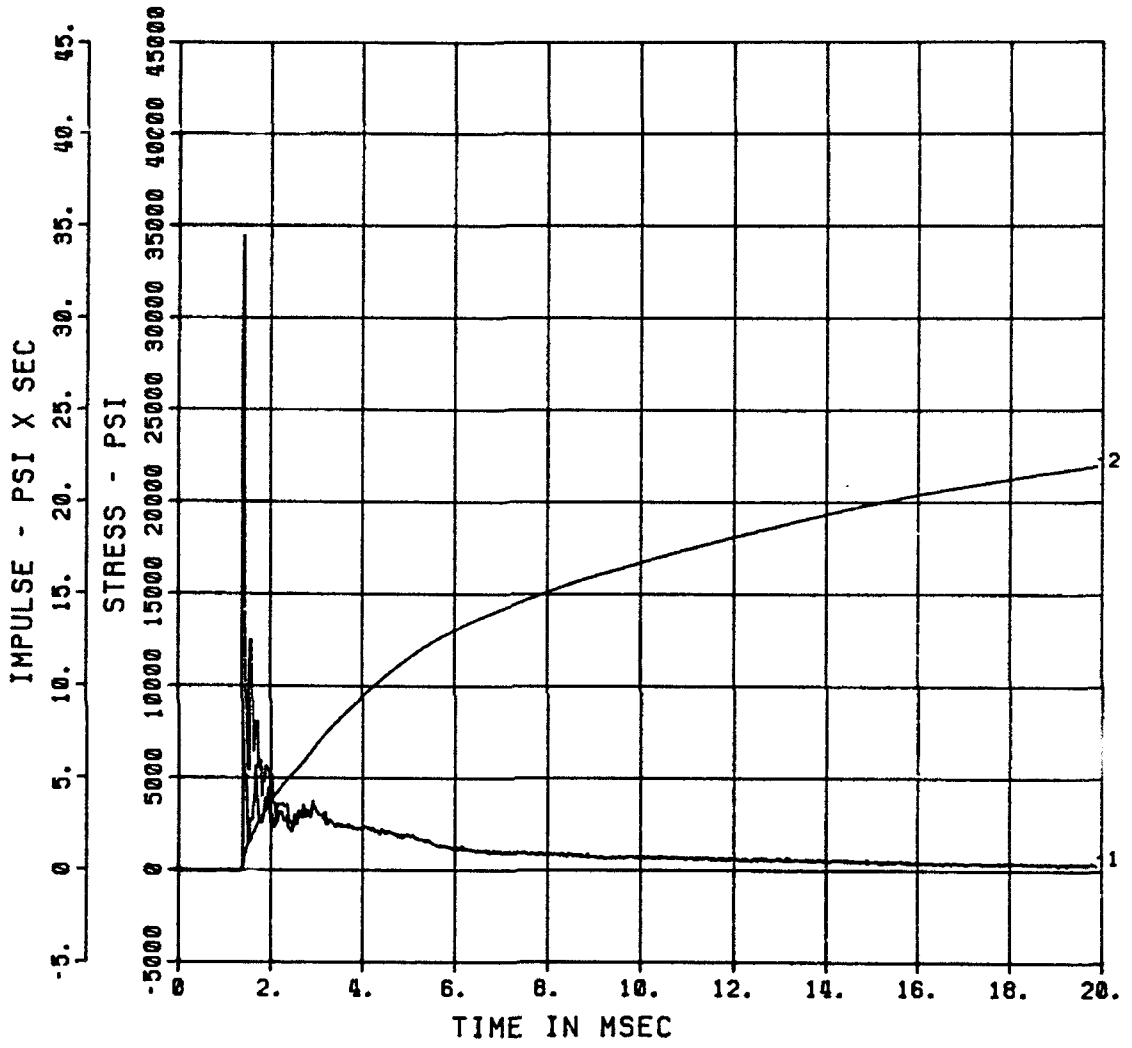

Figure 21. Airblast measurement produced by MCBI gage R1 on the CHT-3 Calibration Test

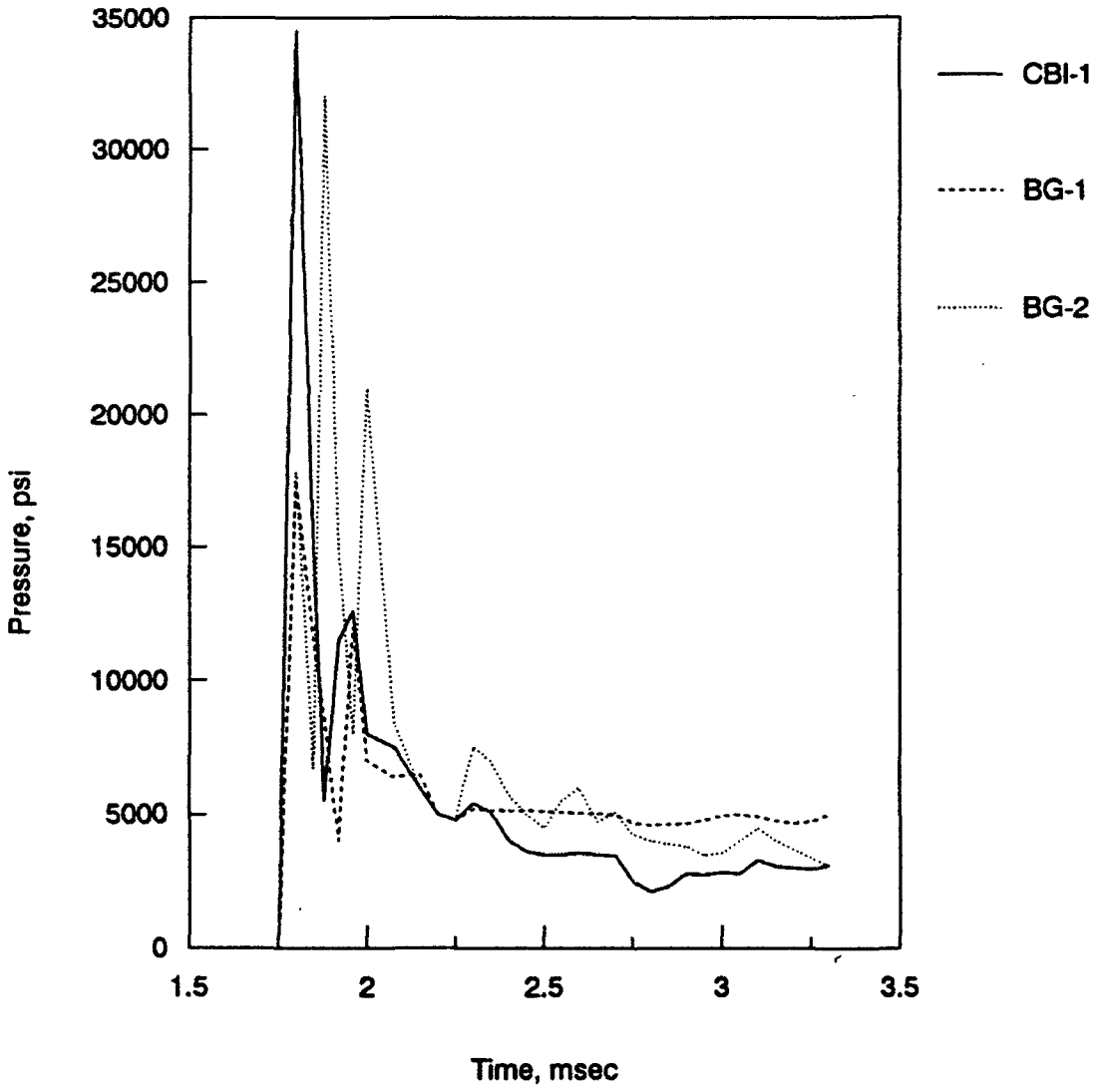

Figure 22. Comparison of airblast wave forms produced by MCBI and bar gages on the CHT-3 Calibration Test

(Figure 23). Recent testing experience indicates that bar gages typically overregister peak airblast pressure (and, consequently, impulse) beginning a few hundred microseconds after shock arrival. Thus, the bar gage measurements serve as an "upper bound" of the actual airblast environment. Further testing is necessary to more accurately determine the MCBI gage's performance as an airblast gage.

Two MCBI gages were used to measure interface stress during a classified explosive test in late 1986. Also included on the test were several Kulite VM-750 interface stress gages. Both MCBI gages produced stress records similar to those of the Kulite gages, although the total recording time was very short due to early shearing of the main trunkline cable bundle. Because the test results are classified, none of the data was included in this report.

4.2 DYNAMIC GAGE VALIDATION TESTS

Two high explosive tests were conducted at the WES Big Black Test Site (BBTS), near Vicksburg, MS, to evaluate MCBI gage performance in a dynamic stress environment. The tests used identical High-Explosive Simulation Technique (HEST) charges as the explosive sources. The HEST charges were designed (using the HESTAF design code) to simulate a peak overpressure of 10,000 psi from a weapon with a 2.7-kT yield, as shown is Figure 24. Figure 25 illustrates the charge design. In order to obtain the desired explosive loading density of 3.16 lb/ft^3, 50 lb of Iremite-60 explosive strands were arranged in two layers of pre-grooved styrofoam spacing material. This spacing was maintained over an area 6 ft long by 6 ft wide.

4.2.1 MCBI Test 1.

The objective of the first validation test was to make a direct comparison between interface stress measurements produced by similarly located MCBI and Kulite VM-750 gages. To facilitate this, two sets of mounting hardware for each gage type were cast in a cylindrical concrete test block. The gage mounts were positioned to form two measurement

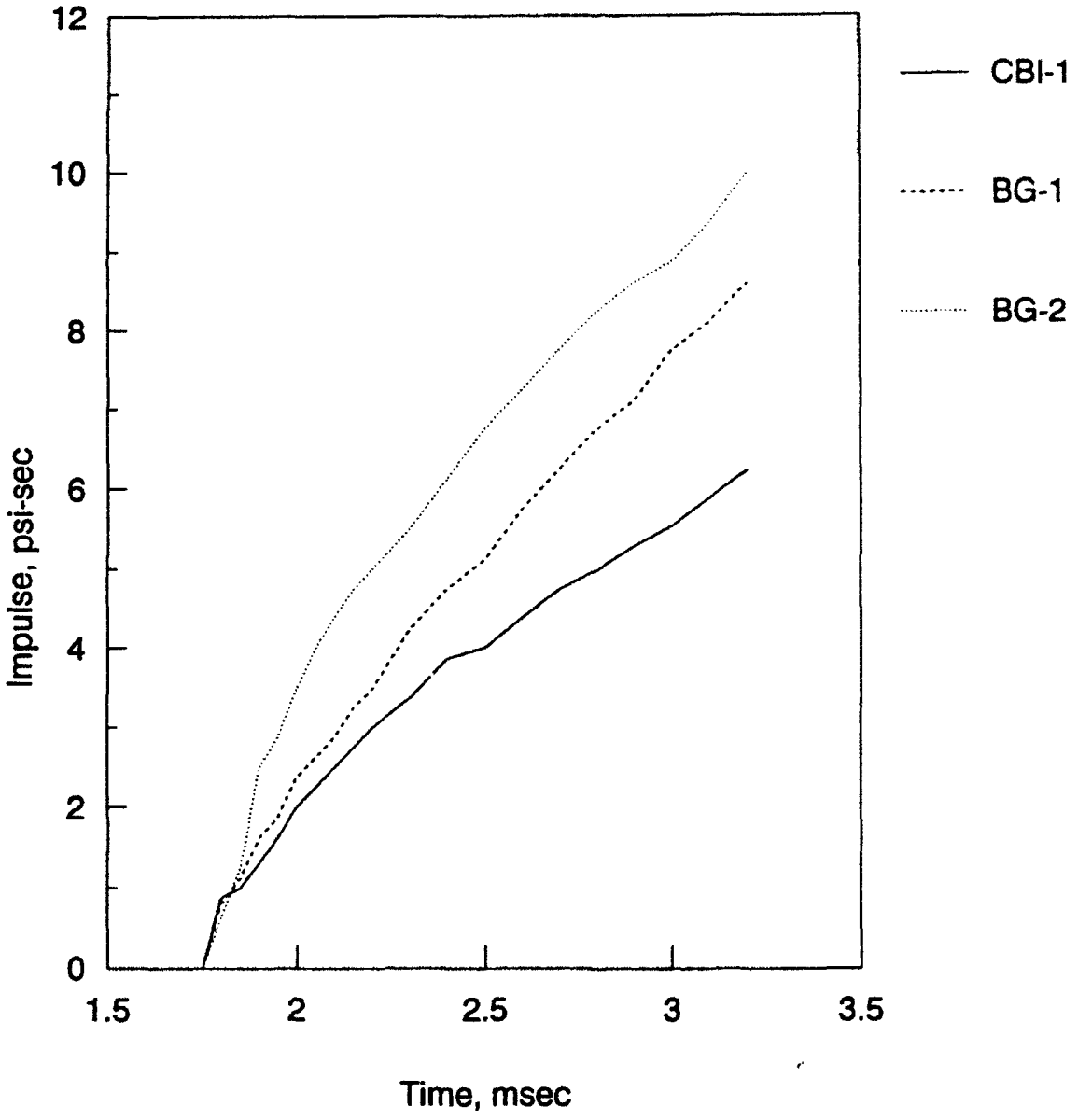

Figure 23. Comparison of impulse wave forms produced by MCBI and bar gages on the CHT-3 Calibration Test

```
PROGRAM HESTAF AS OF 6 AUG. 1987.  RUN AT 1417 HRS.  4 APR. 1988
USING BRODE MODEL DATED 24 OCT. 1984.

     TITLE IS:
 HEST BED DESIGN

 L DEN =      3.164 lb/ft E+3
 PEAKP =   5984.546 psi
 GAMMA =      1.200
DENSITY
 BURDN =    130.000 lb
 T BED =    130.000 lb
OVERBURDEN
 HEIGHT=      4.500 ft
CAVITY
 LENGTH=      6.000 ft
 WIDTH =      6.000 ft
 DEPTH =      0.420 ft
VENTING
  TIME =     36.807 msec
  PRES =     -1.150 psi
  IMPU =     11.565 psi
  VOLU =   2433.159 ft E+3

  FUDGE=      0.500
WEAPON
 YIELD =      2.700 kt
 PPRES = 10000.000 psi
 HOB   =      0.000 ft
 RANGE =     96.441 ft
```

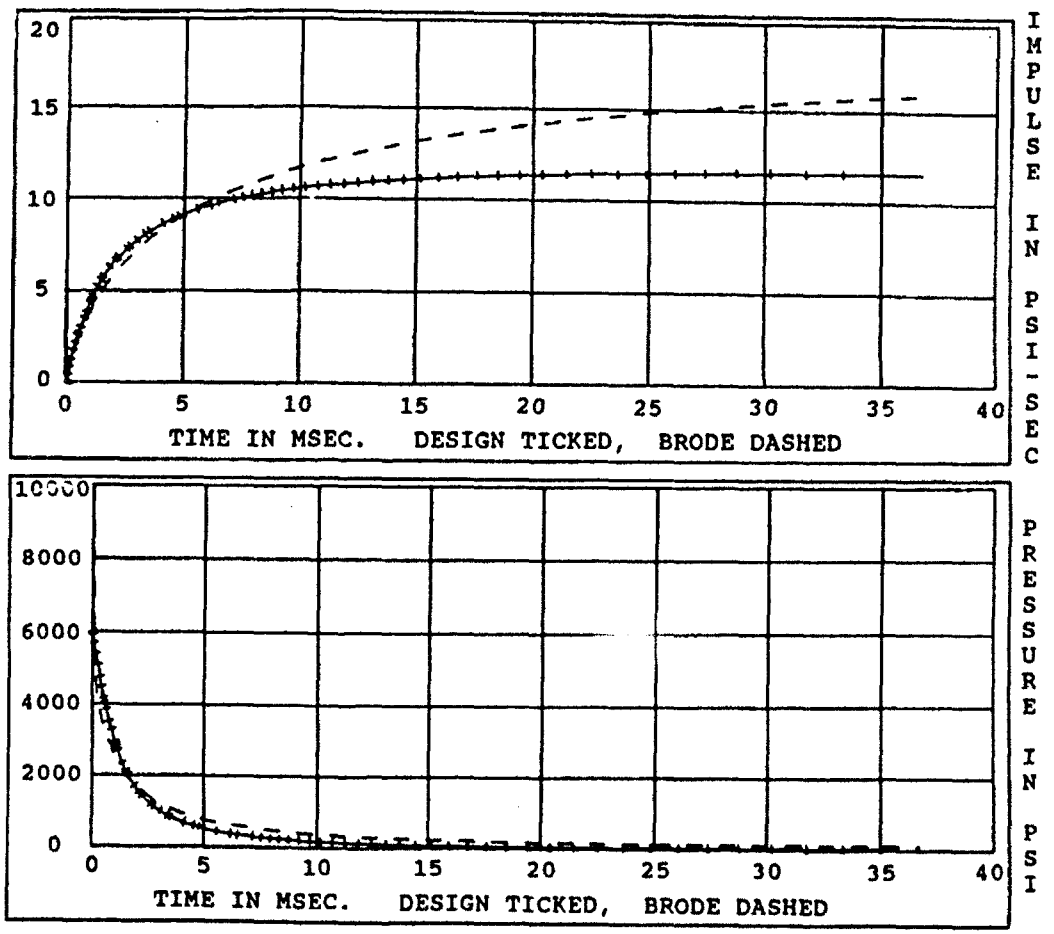

Figure 24. HEST charge design parameters, and calculated pressure and impulse curves produced by the HESTAF design code

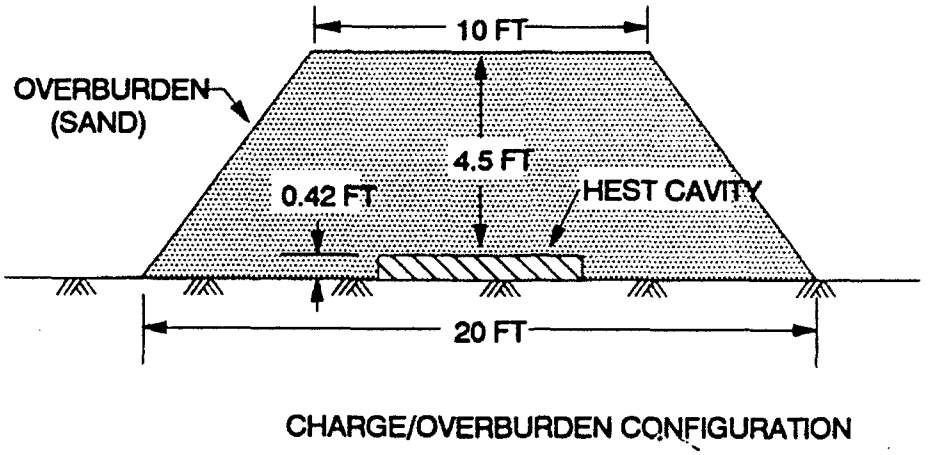

CHARGE/OVERBURDEN CONFIGURATION

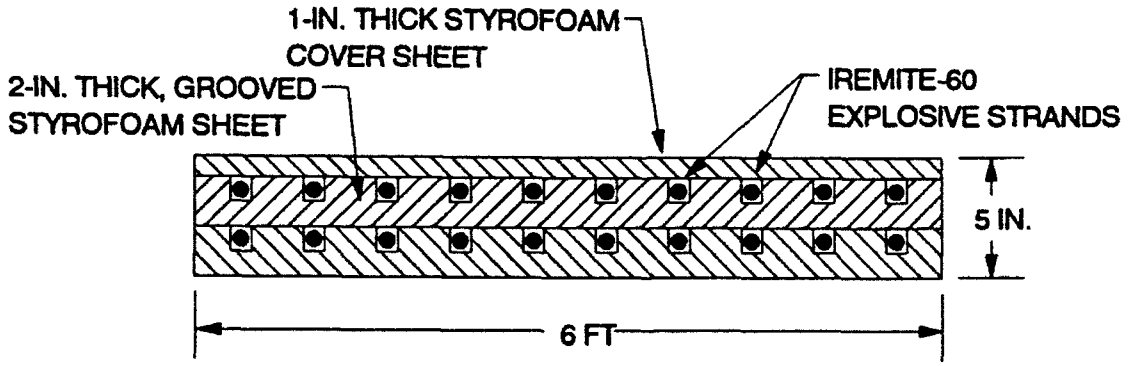

HEST CAVITY CROSS-SECTION

Figure 25. HEST charge design for the MCBI gage validation test

pairs, each consisting of one MCBI and one VM-750 gage. The test block was then cured 28 days before being placed in the testbed.

The testbed configuration for the MCBI Test 1 is shown in Figures 26 and 27. A 6-ft long by 6-ft wide excavation was first made in native BBTS soil. The concrete test block was then set at such a level in the testbed excavation that the interface gages were positioned 2 ft below surface grade. This depth was selected to ensure that the VM-750 gages would not be subjected to interface stresses in excess of 5,000 psi. The excavation was then filled with flume sand which was placed and compacted 6-in. lifts. A total of six Kulite high-range soil stress (HRSE) gages (Figure 27), four vertically (Gages SEV-1, -4) and two horizontally (SEH-1, -2) oriented, were placed in the backfill at a depth of 2 ft below surface grade to measure free-field soil stresses near the interface gages. The SE gages were installed in WES "paddle"-type gage mounts (Figure 28).

MCBI Test 1 was conducted during June 1988. Appendix B contains all wave forms obtained from the test. Interface gages MCBI-1 and VM-1, which were co-located MCBI and VM-750 gages, produced similar stress wave forms, as shown in Figures 29 and 30. Peak interface stresses measured by the MCBI and VM-750 gages were 1,920 and 1,970 psi respectively. Both the MCBI-1 and VM-1 stress wave forms exhibited rather large amplitude spikes prior to stress wave arrival. These were probably due to accelerations of the gages. The spikes did not significantly affect the MCBI-1 impulse, but a severe spike at approximately 1.9 msec did cause a negative 0.10 psi-sec impulse offset on the VM-1 impulse wave form.

The most significant difference between the stress wave forms was the rate of decay of the initial stress pulse. One-half msec after initial peak stress, the stress measured by MCBI-1 was 750 psi, while that measured by VM-1 was 350 psi. This discrepancy essentially disappeared after an additional one-half msec had elapsed, although not before resulting in an impulse offset of 0.35 psi-sec between the MCBI-1 and VM-1 measurements. At 20 msec after 0-time (Figure 30), the MCBI-1 impulse was approximately 0.8 psi-sec higher than the VM-1 impulse.

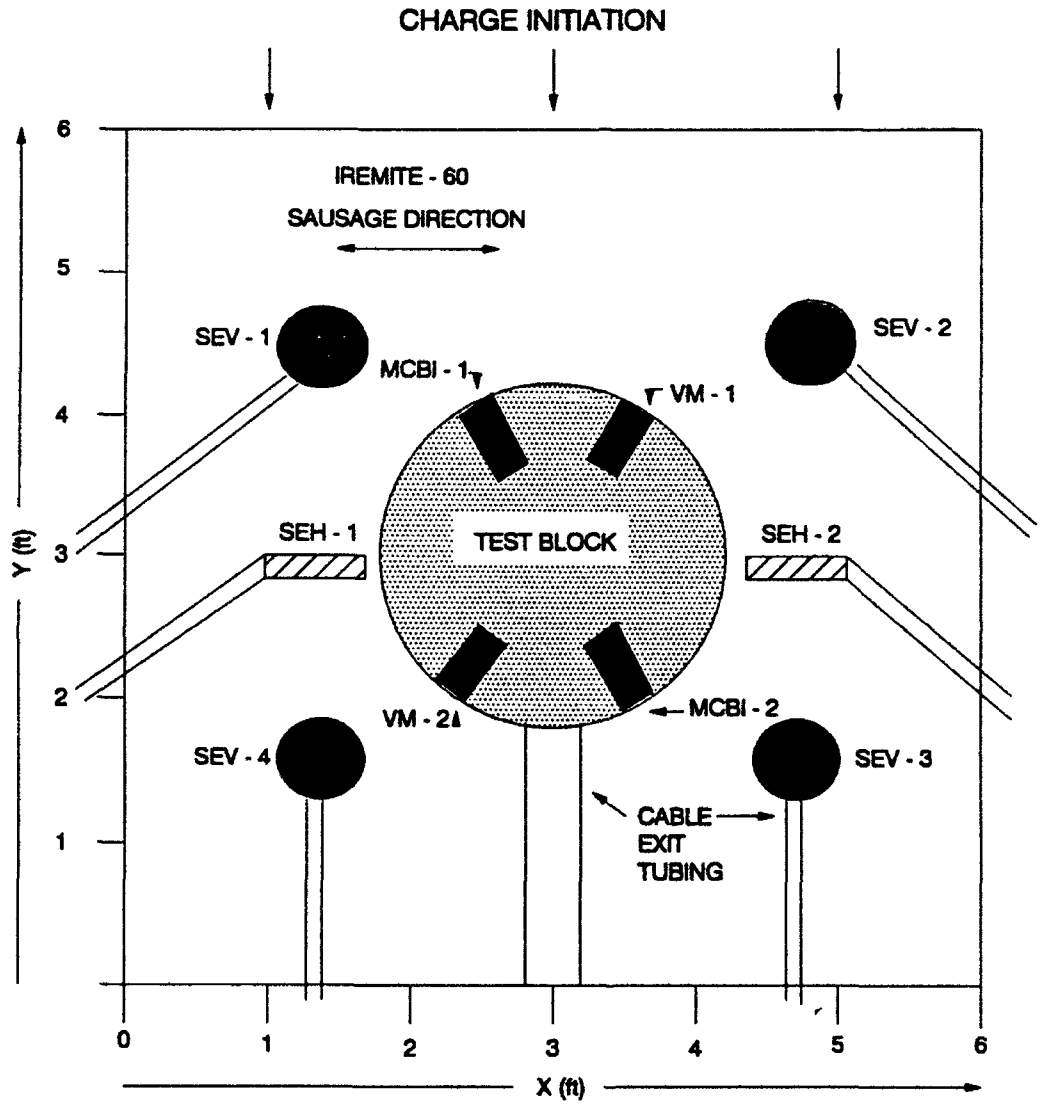

Figure 26. Plan view of the testbed for MCBI Gage Validation Test 1

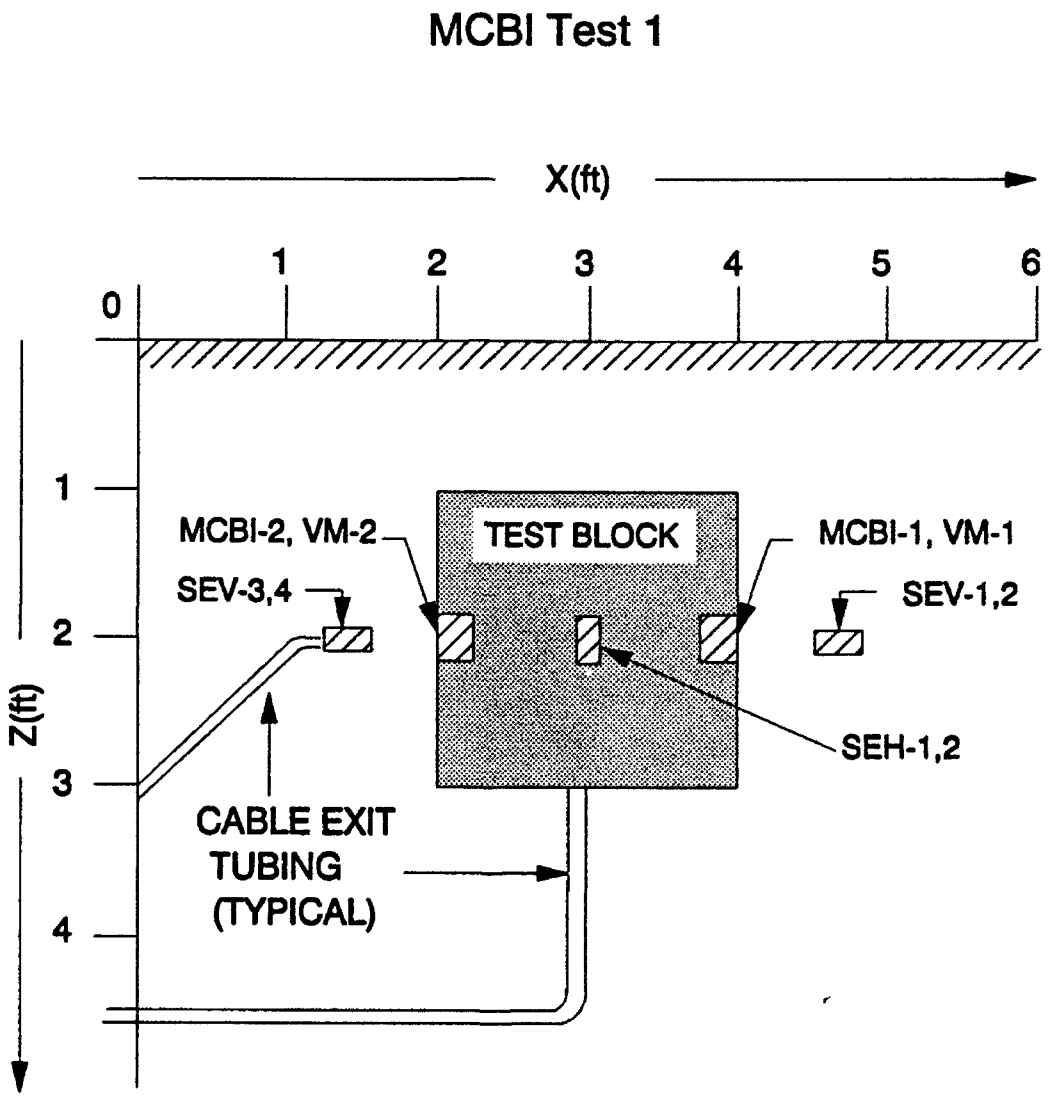

Figure 27. Cross-section of the testbed for MCBI Gage Validation Test 1

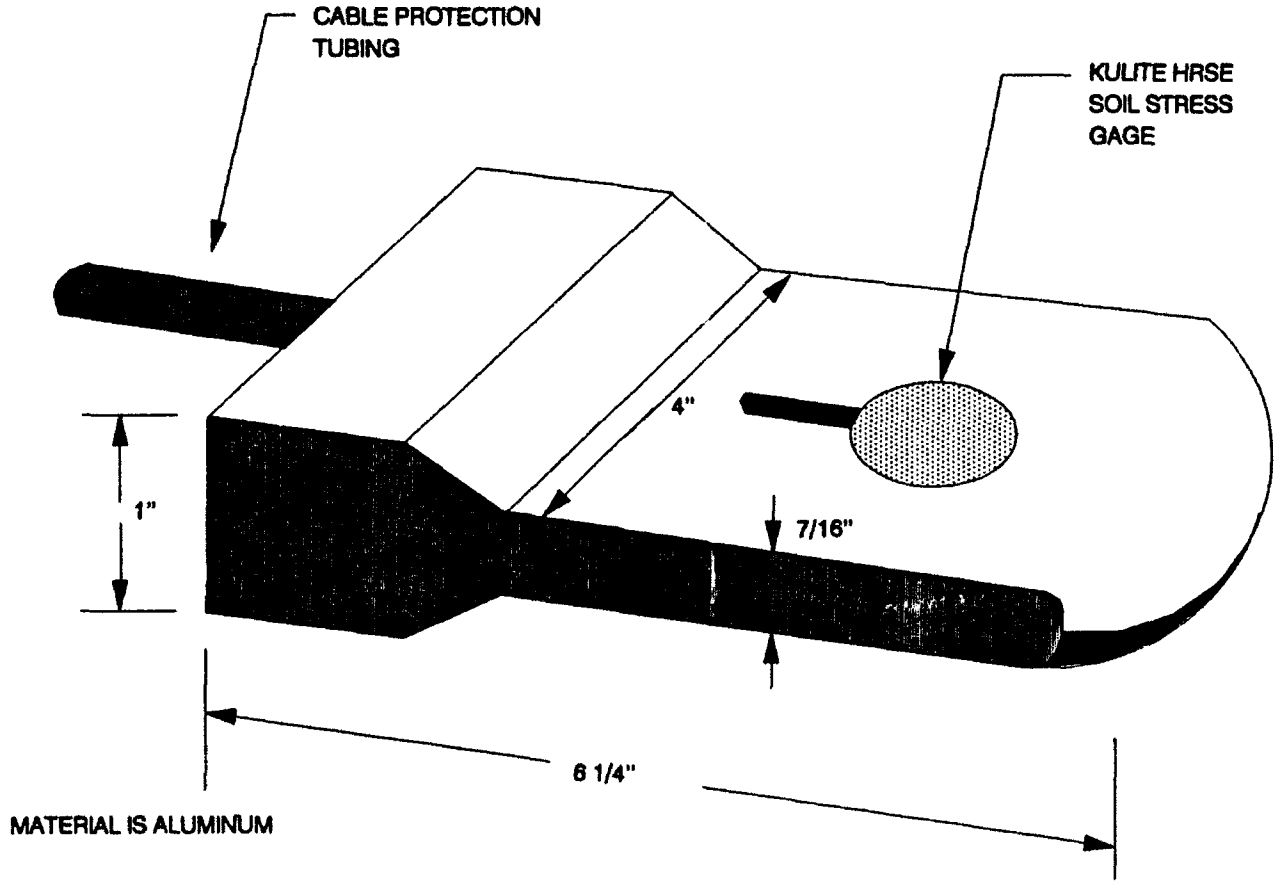

Figure 28. Kulite high-range soil stress gage and WES-designed "paddle" mount

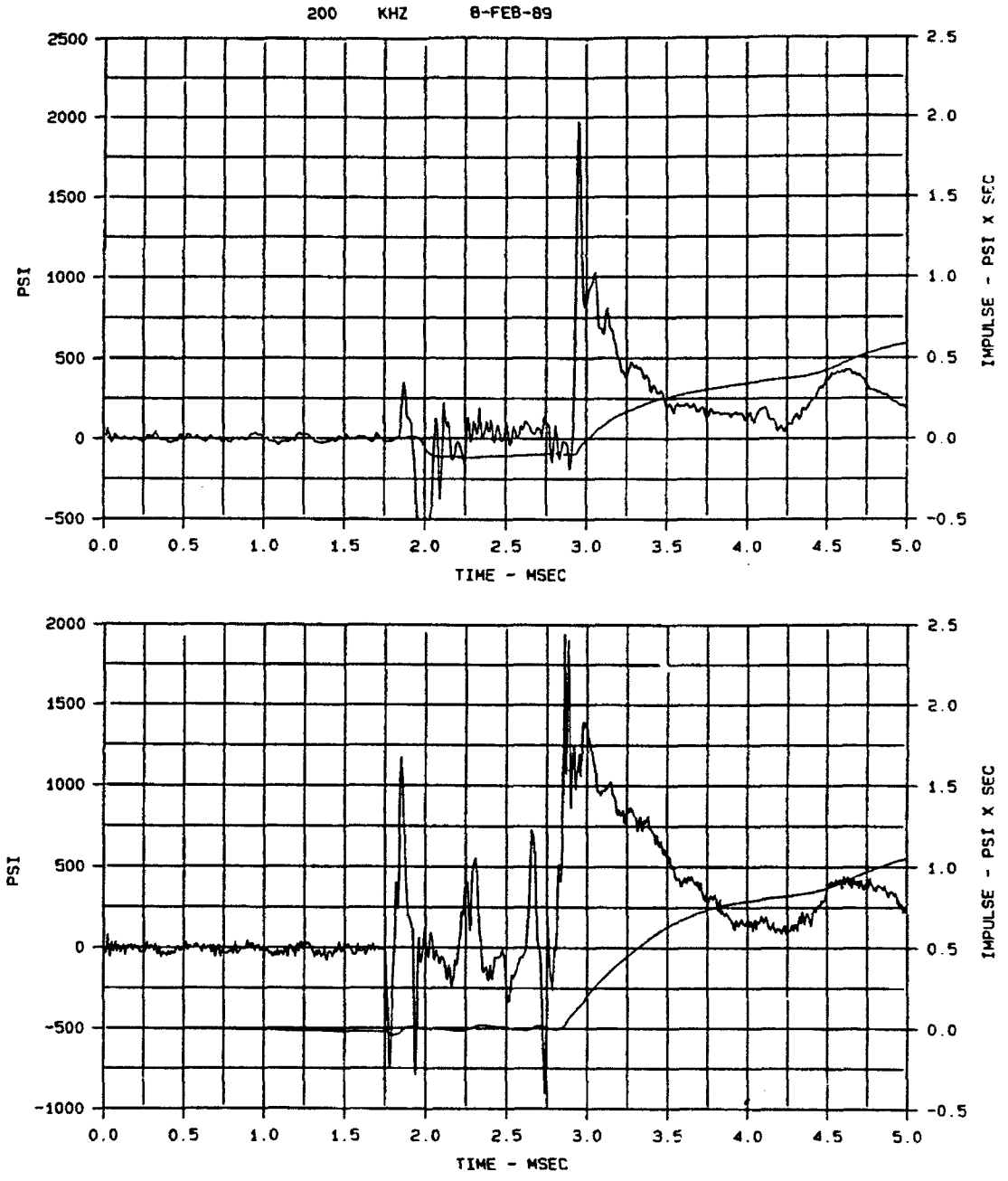

Figure 29. Comparison of MCBI-1 (bottom) and Kulite VM-1 interface stress records, 5 msec duration, MCBI Gage Validation Test 1

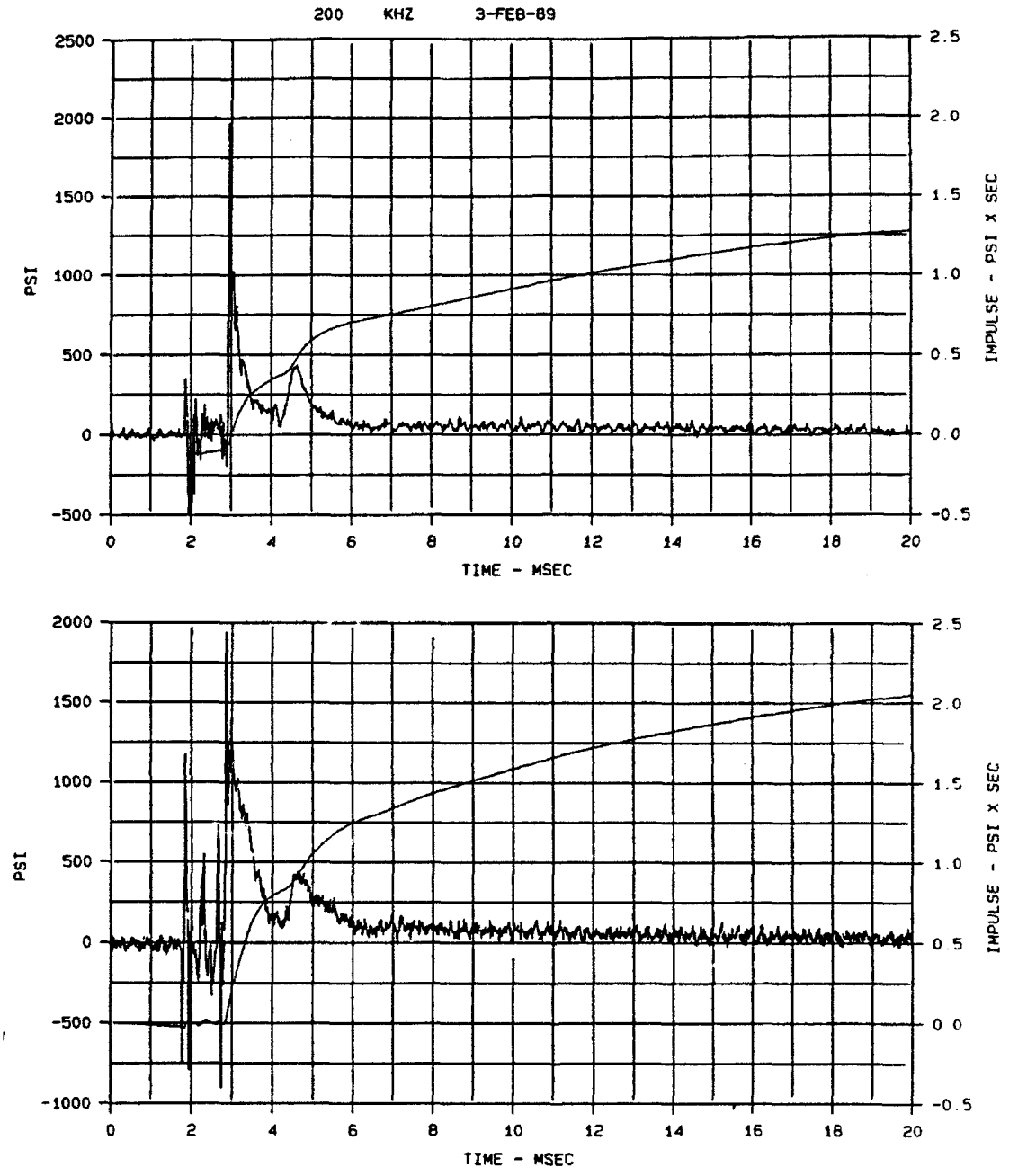

Figure 30. Comparison of MCBI-1 (bottom) and Kulite VM-1 interface stress records, 20 msec duration, MCBI Gage Validation Test 1

The other co-located interface gages were MCBI-2 and VM-2. Their stress wave forms were not in close agreement during the first millisecond after shock arrival (Figure 31). As was the case with the other interface stress measurements, the MCBI-2 and VM-2 wave forms exhibited acceleration-related, large amplitude spikes prior to stress wave arrival. Once again, the MCBI wave form was not significantly altered. The VM-750 wave form, however, was severely distorted by spikes occurring at 1.9 and 2.3 msec after 0-time. These spikes caused a positive 0.63 psi-sec impulse offset on the wave form.

MCBI-2 measured a peak initial stress of 1,410 psi, as opposed to the 2,180 psi measured by VM-2. The lower peak pressure and slower rise-time of the MCBI gage may have been caused by imperfect packing of the backfill material near the gage face. In addition, the initial stress pulse measured by VM-2 decayed much more rapidly than did the pulse measured by MCBI-2. The VM-2 stress measured one-half msec after the peak was 115 psi, versus 880 psi for MCBI-2. This resulted in a significant difference between the two impulse wave forms. At 20 msec after 0-time (Figure 32), the MCBI-2 impulse was 1.9 psi-sec, while the VM-2 impulse was 1.3 psi-sec. Without the spike-induced 0.63-psi-sec offset, the VM-2 impulse was only 0.67 psi-sec after 20 msec.

The vertical and horizontal free-field soil stress wave forms are presented in Figures 33 and 34. With the exception of gage SEV-2, the wave forms produced by the soil stress gages were quite similar in character to the interface stress wave forms produced by the MCBI gages during the first millisecond after stress arrival. The stress amplitude decayed from the measured peak value at approximately the same rate for both the MCBI and HRSE gages. This indicates that the MCBI gages measured the initial stress wave (and resulting impulse) accurately, while the VM-750 gages under-registered stress and impulse due to their more rapid decay from peak measurement values. Beyond 1 msec, the soil stress gages measured 2 to 4 times higher stress than did the interface stress gages, primarily due to separation of the test block from the backfill material.

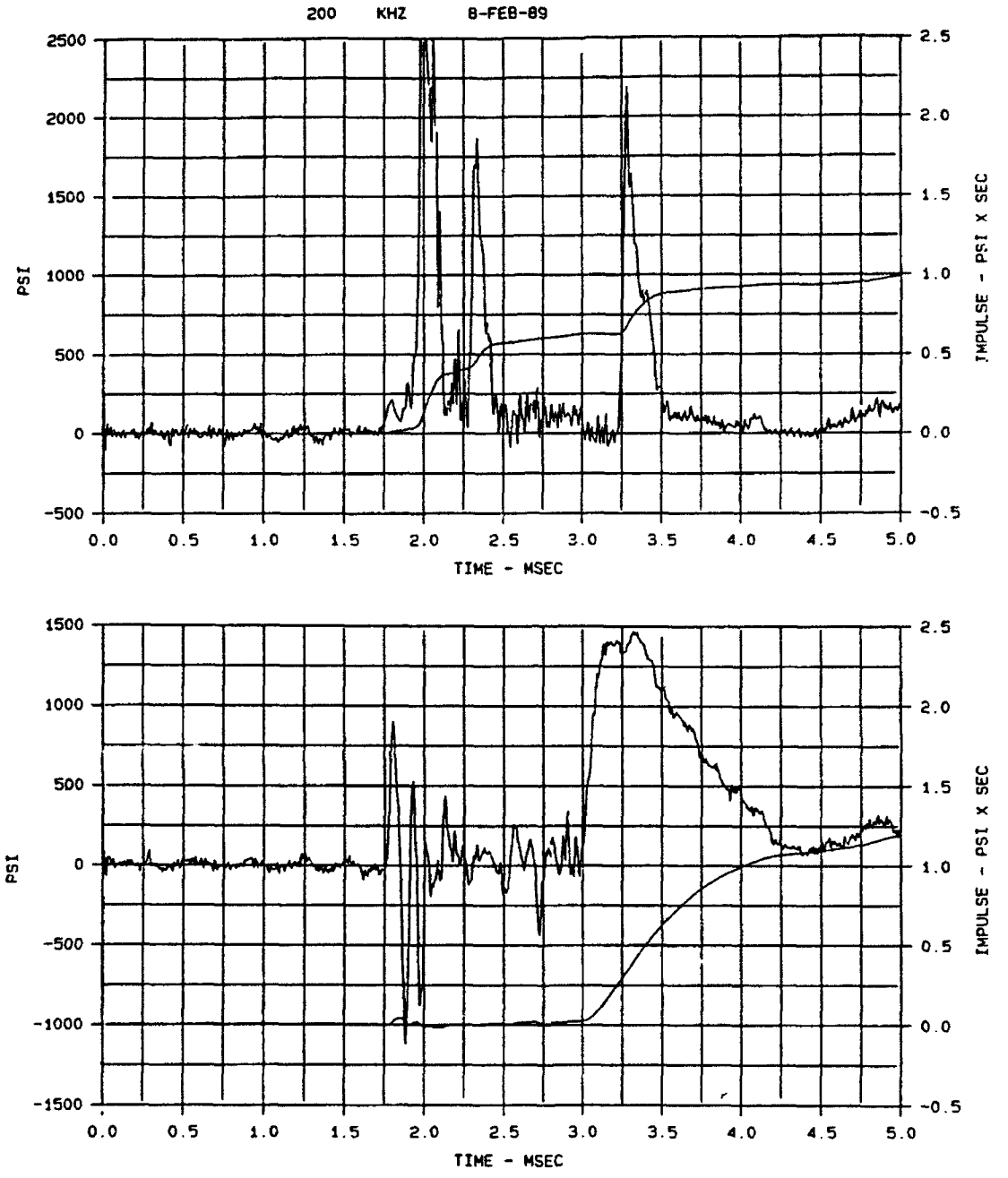

Figure 31. Comparison of MCBI-2 (bottom) and Kulite VM-2 interface stress records, 5 msec duration, MCBI Gage Validation Test 1

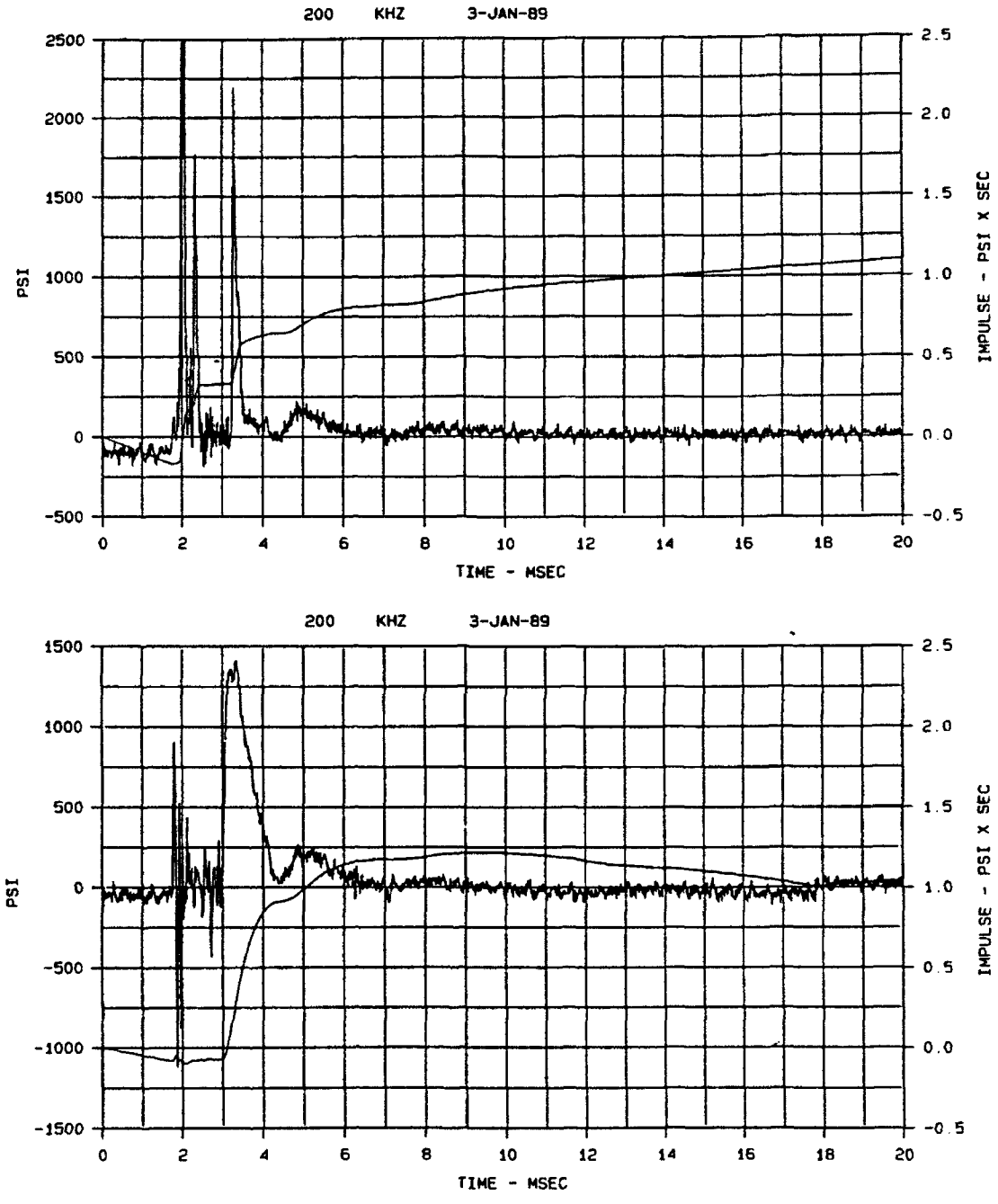

Figure 32. Comparison of MCBI-2 (bottom) and Kulite VM-2 interface stress records, 20 msec duration, MCBI Gage Validation Test 1

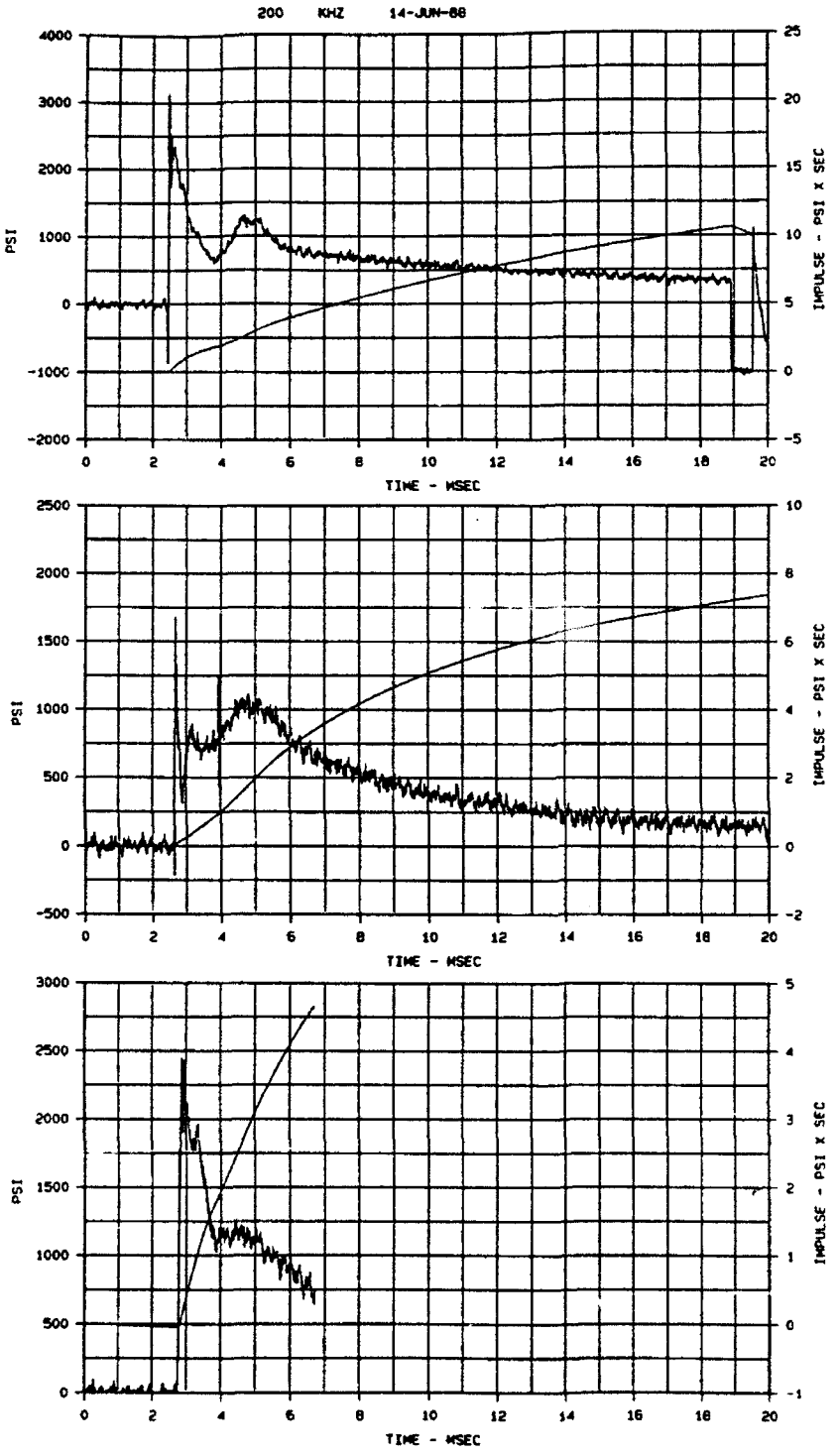

Figure 33. Vertical soil stress wave forms, MCBI Gage Validation Test 1

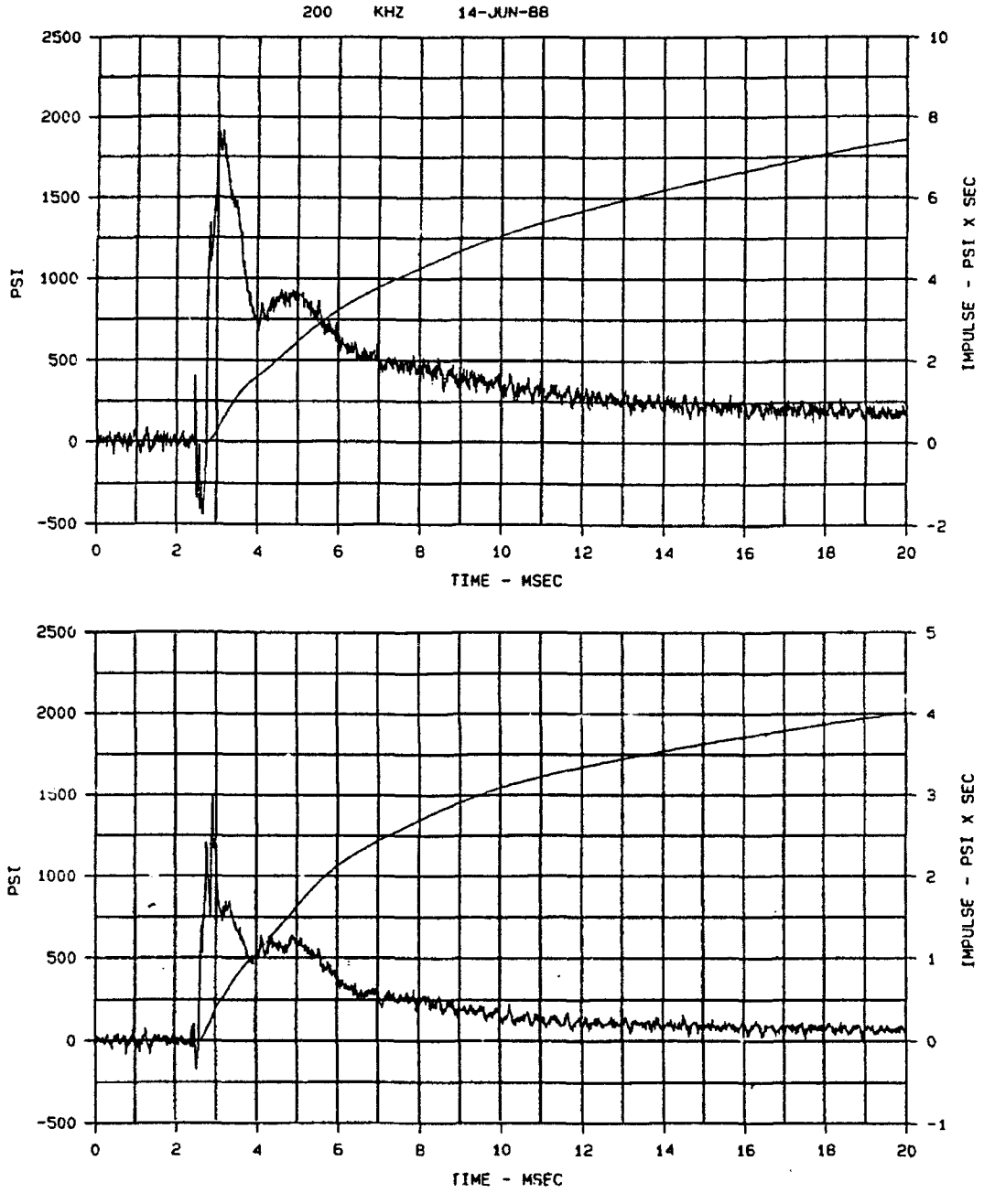

Figure 34. Horizontal soil stress wave forms, MCBI Gage Validation Test 1

4.2.2 MCBI Test 2.

The objective of the second validation test was to make a direct comparison between interface stress measurements produced by MCBI gages and theoretical interface stress wave forms constructed from soil stress data. The test concept was to place a concrete slab in a sand backfill, over which a HEST charge would be detonated to provide dynamic loading. As illustrated in Figure 35, sand was designated as Medium 1 and 3, and concrete as Medium 2.

Upon charge detonation, the initial free-field stress wave, σ_{ff}, propagating downward into the sand, creates a reflected stress wave, $R_{12}\sigma_{ff}$, and a transmitted stress wave $T_{12}\sigma_{ff}$ when it strikes the concrete pad. The magnitude and phase of the reflected and transmitted stress waves are defined by the reflection coefficient R_{12} and the transmission coefficient T_{12}, which are:

$$R_{12}=(\rho_2 c_2-\rho_1 c_1)/(\rho_2 c_2+\rho_1 c_1),\ T_{12}=2\rho_2 c_2/(\rho_2 c_2+\rho_1 c_1) \qquad (1)$$

where ρ_1 is the density and c_1 is the compressional wave velocity of the sand, and ρ_2 is the density and c_2 is the compressional wave velocity of the concrete.

The transmitted stress wave, $T_{12}\sigma_{ff}$, traveling downward through the concrete, creates an additional reflected wave, $R_{21}T_{12}\sigma_{ff}$, when it strikes the bottom concrete/sand interface. $R_{21}T_{12}\sigma_{ff}$ travels upward through the concrete, ultimately striking the upper concrete/sand interface and transmitting a stress wave $T_{21}R_{21}T_{12}\sigma_{ff}$ into the sand while simultaneously creating reflected stress wave $R_{21}T_{21}R_{21}T_{12}\sigma_{ff}$, which

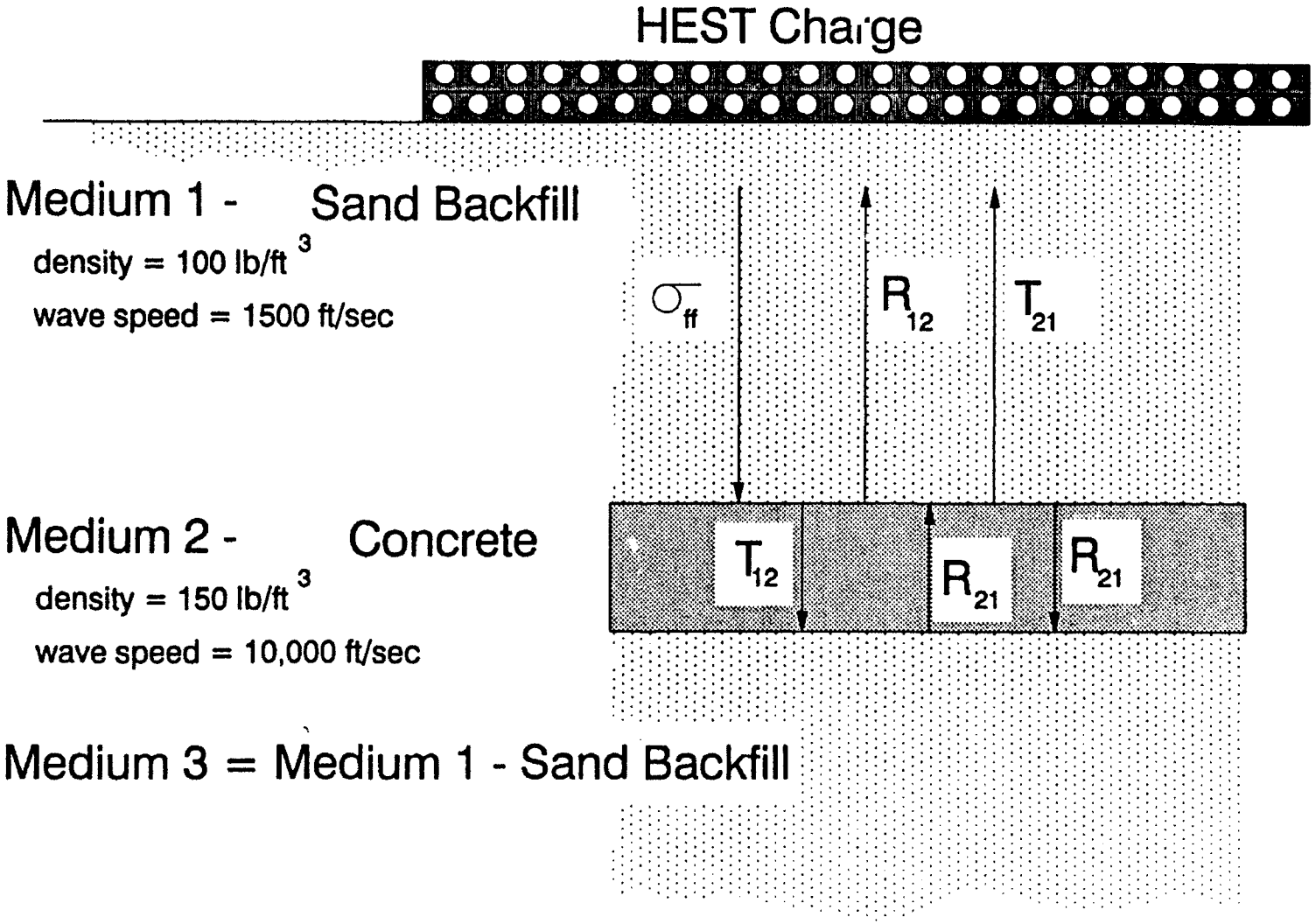

Figure 35. Design concept for MCBI Gage Validation Test 2

travels back through the concrete. The reflection and transmission coefficients R_{21} and T_{21} are defined as:

$$R_{21}=(\rho_1 c_1-\rho_2 c_2)/(\rho_2 c_2+\rho_1 c_1),\ T_{21}=2\rho_1 c_1/(\rho_2 c_2+\rho_1 c_1) \tag{2}$$

Assuming that the stress waves in the concrete continue to transmit and reflect as illustrated above, and that the stress wave, σ_{1f}, at the upper sand/concrete interface is equal to the incident free-field stress plus the stress transmitted back into the sand from reflections running through the concrete slab, σ_{1f} is given by:

$$\begin{aligned}\sigma_{1f}(t)=\sigma_{ff}(t)+R_{12}\sigma_{ff}(t)+T_{12}R_{21}T_{21}\sigma_{ff}(t-2l/c_2)\\ +T_{12}R_{21}R_{21}R_{21}T_{21}\sigma_{ff}(t-4l/c_2)+\ldots\end{aligned} \tag{3}$$

so:

$$\sigma_{1f}(t)=(1+R_{12})\sigma_{ff}(t)+T_{12}T_{21}\sum_{n=1}^{\infty}R_{21}^{2n-1}\sigma_{ff}(t-2nl/c_2) \tag{4}$$

The nominal densities of sand and concrete are ρ_1 = 100 lb/ft^3 and ρ_2 = 150 lb/ft^3, and the respective compressional wave velocities are c_1 = 1500 ft/sec and c_2 = 10,000 ft/sec. Using these values, the calculated stress wave reflection and transmission coefficients are R_{12} = 0.8182, T_{12} = 1.8182, R_{21} = -0.8182, and T_{21} = 0.1818. The negative sign of R_{21} indicates that it is a rarefaction. Substituting these values for the reflection and transmission coefficients into Equation 4,

$$\sigma_{1f}(t)=1.8182\sigma_{ff}(t)+0.3305\sum_{n=1}^{\infty}(-0.8182)^{2n-1}\sigma_{ff}(t-2nl/c_2) \tag{5}$$

This is the method used to compute the theoretical interface stress waves.

The testbed configuration for the MCBI Test 2 is shown in Figures 36 and 37. A 6-ft long by 6-ft wide excavation was first made in native BBTS soil. Flume sand, with an approximate compacted density of 100 lb/ft^3 was placed in the bottom 2 ft of the excavation. A 1-ft thick concrete test slab, containing three MCBI gages, was then placed in the backfill so that the interface gages were positioned 3 ft below surface grade. The remainder of the excavation was then filled with compacted flume sand which was compacted to approximately 100 lb/ft^3 following each 6-in. lift. A total of three vertically-oriented HRSE gages (SEV-1, -2, and -3) were placed in the backfill at a depth of 1.5 ft below surface grade to provide a measure of the free-field soil stresses loading the concrete pad.

MCBI Test 2 was conducted during December 1988. Appendix C contains all wave forms obtained from the test. MCBI gages MCBI-1 and MCBI-2 produced good wave forms, as did all three soil stress gages. Gage MCBI-3 suffered an internal electrical failure at shock arrival and did not yield usable data.

Following the test, the soil stress data were processed and then used to provide the input to Equation 5 for calculation of the theoretical stress at the upper sand/concrete interface. Soil stress data from gages SEV-1 and SEV-2 appeared to be representative of the free-field environment, and were the only data used to drive the calculations. The soil stress wave forms were sampled at a frequency of 40 kHz starting at shock arrival. Beyond 2 msec after shock arrival, the soil stress wave forms were affected by reflected stresses from the concrete slab, thus limiting the useful duration for input to the calculation to approximately 2 msec.

The calculated interface stress derived from soil stress gage SEV-1 is plotted versus the measurement produced by MCBI-1 in Figure 38. The wave forms were in good overall agreement during the first 2 msec after shock arrival. The MCBI-1 wave form indicated initial stress spikes of well over 10,000 psi during the first 200 μsec, while the calculated stress varied from 1,500 to 4,500 psi. This discrepancy was probably

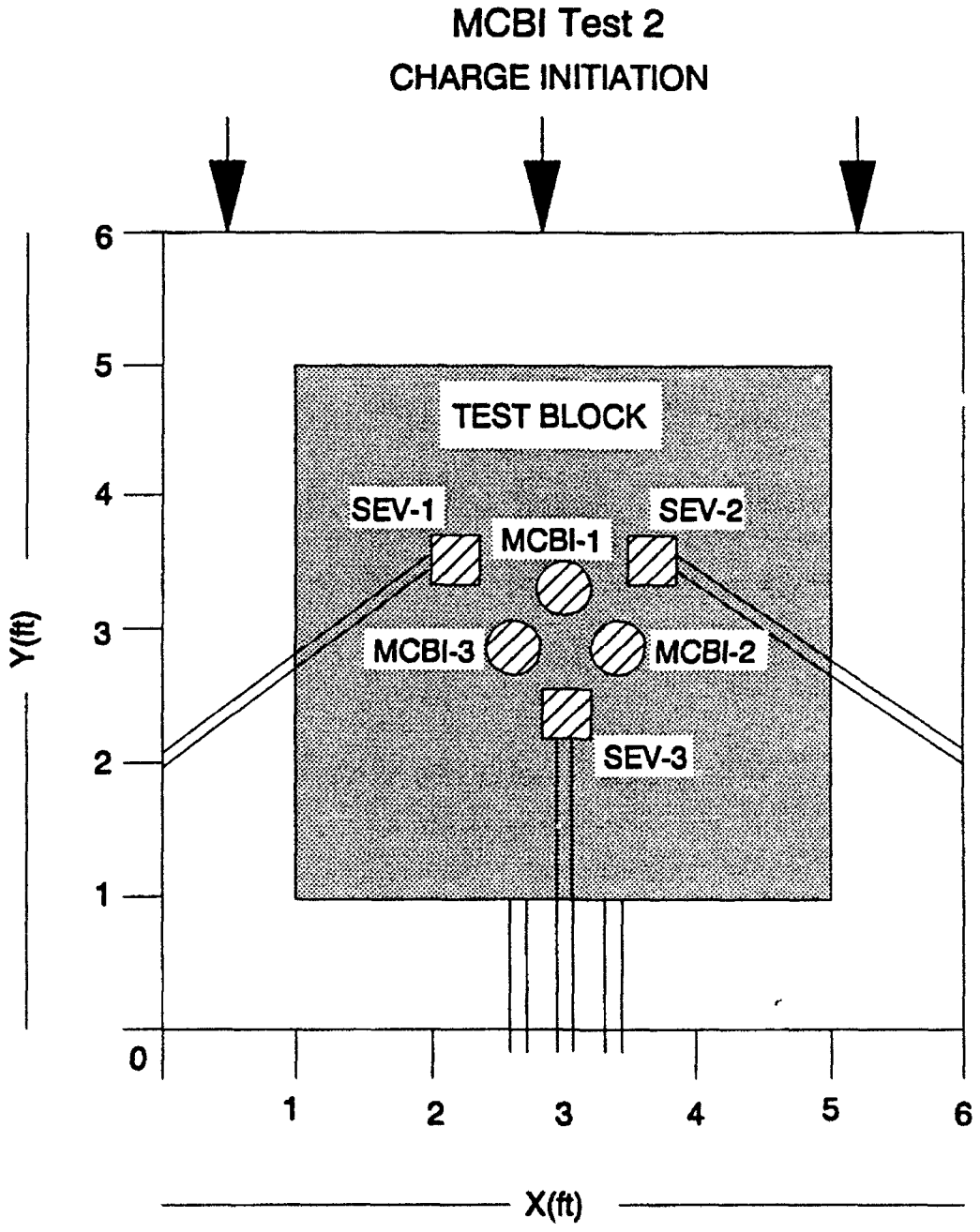

Figure 36. Plan view of the testbed layout for the MCBI Gage Validation Test 2

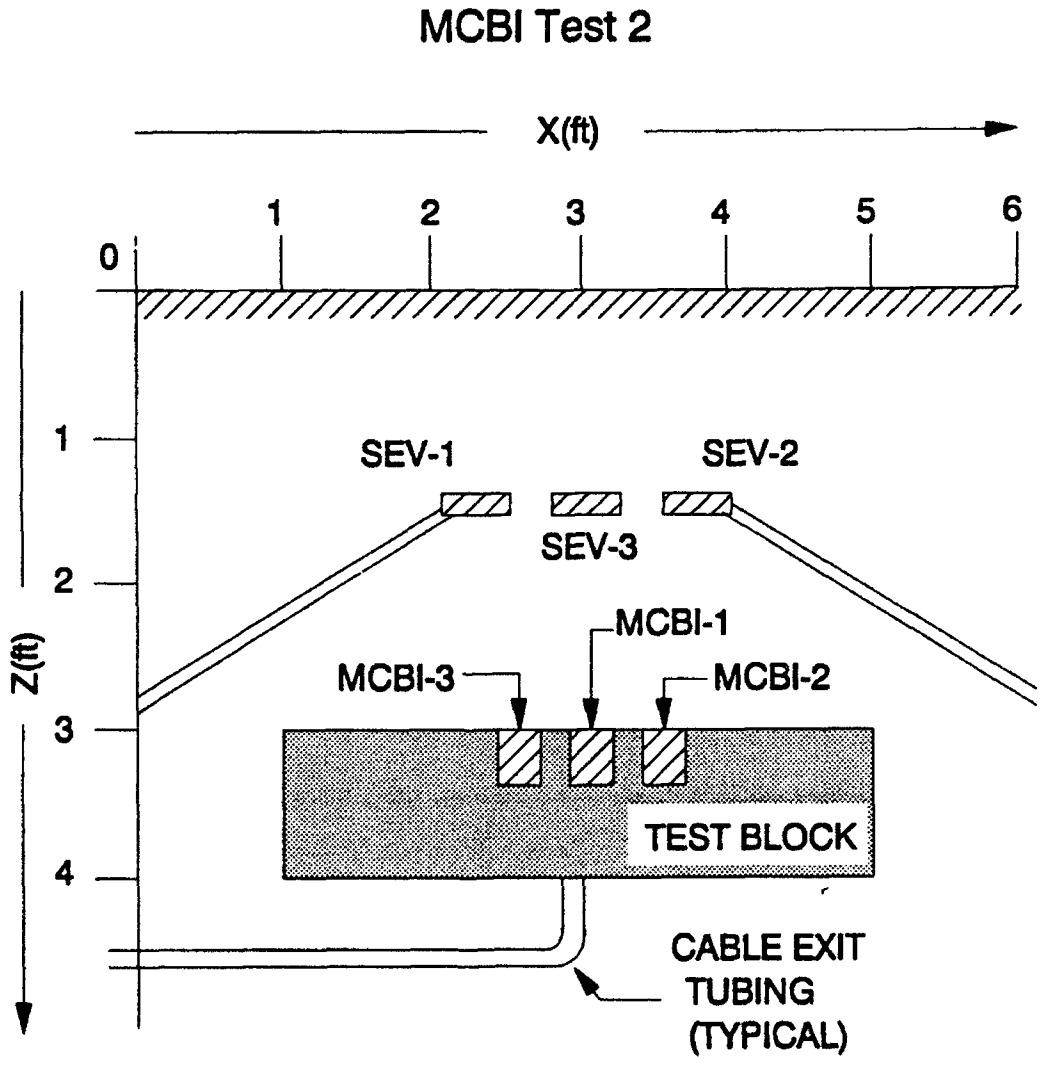

Figure 37. Cross-section of the testbed layout for the MCBI Gage Validation Test 2

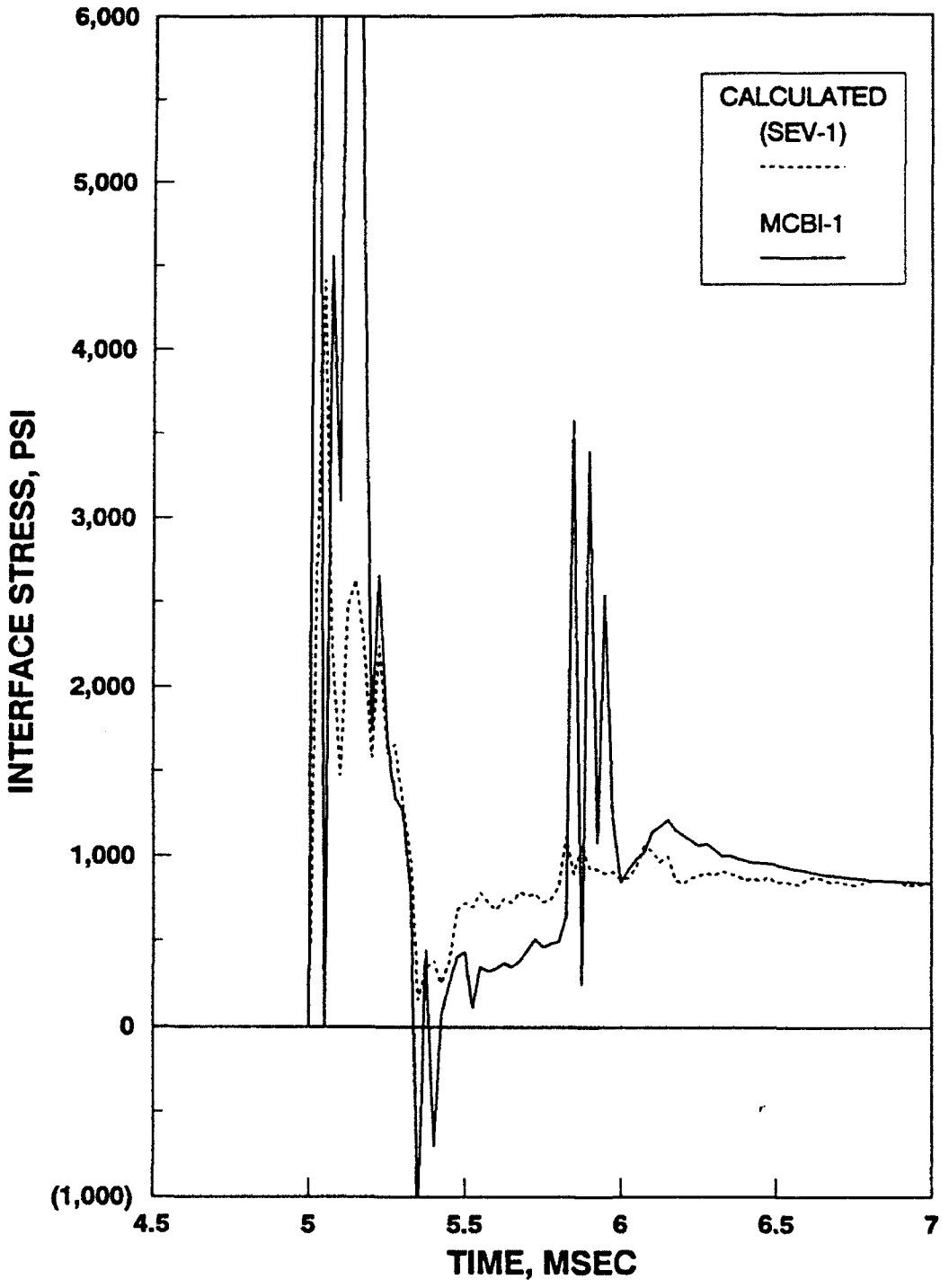

Figure 38. Comparison of measured (MCBI-1) and calculated (from SEV-1) interface stress wave forms, MCBI Test 2

due to the normal acceleration sensitivity of the MCBI gage, and possibly to the action of nonlinear soil effects.

At 350 to 450 μsec after shock arrival, MCBI-1 indicated negative stress spikes (tension), due to tensile relief effects from the bottom side of the slab. The calculated stress wave form also tracked the arrival of the tensile wave, although it did not indicate negative stress values. From approximately 450 to 800 μsec after shock arrival, both wave forms measured slowly increasing stress, although the calculated stress was typically 100 to 400 psi higher than that measured by MCBI-1. This is consistent with the onset of downward displacement of the slab, which is not modeled by the calculated wave form, but would result in a lower level of interface stress.

From 800 to 1,000 μsec after shock arrival, MCBI-1 indicated a series of positive stress spikes which were much higher than the essentially flat, calculated stress wave form. This behavior appears to be consistent with the arrival at the MCBI gage of a second reflected stress wave emanating from the bottom of the concrete. This tensile wave would travel through the MCBI gage's sensing column, causing the positive stress spikes. Beyond 1 msec after shock arrival, at which time the slab and backfill have more or less come into a state of equilibrium, the measured and calculated interface stress wave forms compare quite favorably.

The calculated interface stress derived from SEV-1 is compared to the MCBI-2 measurement in Figure 39. The wave forms did not, in general, compare favorably, although there was good agreement of the onset and magnitude of the relief wave effects beginning approximately 350 μsec after shock arrival. As was the case of MCBI-1, MCBI-2 exhibited severe acceleration-related stress spikes in the first 200 μsec, and negative stress spikes at 300 to 350 μsec after shock arrival. MCBI-2 indicated a much lower interface stress than did the calculated wave form at 500 to 750 μsec after shock arrival. This was likely due

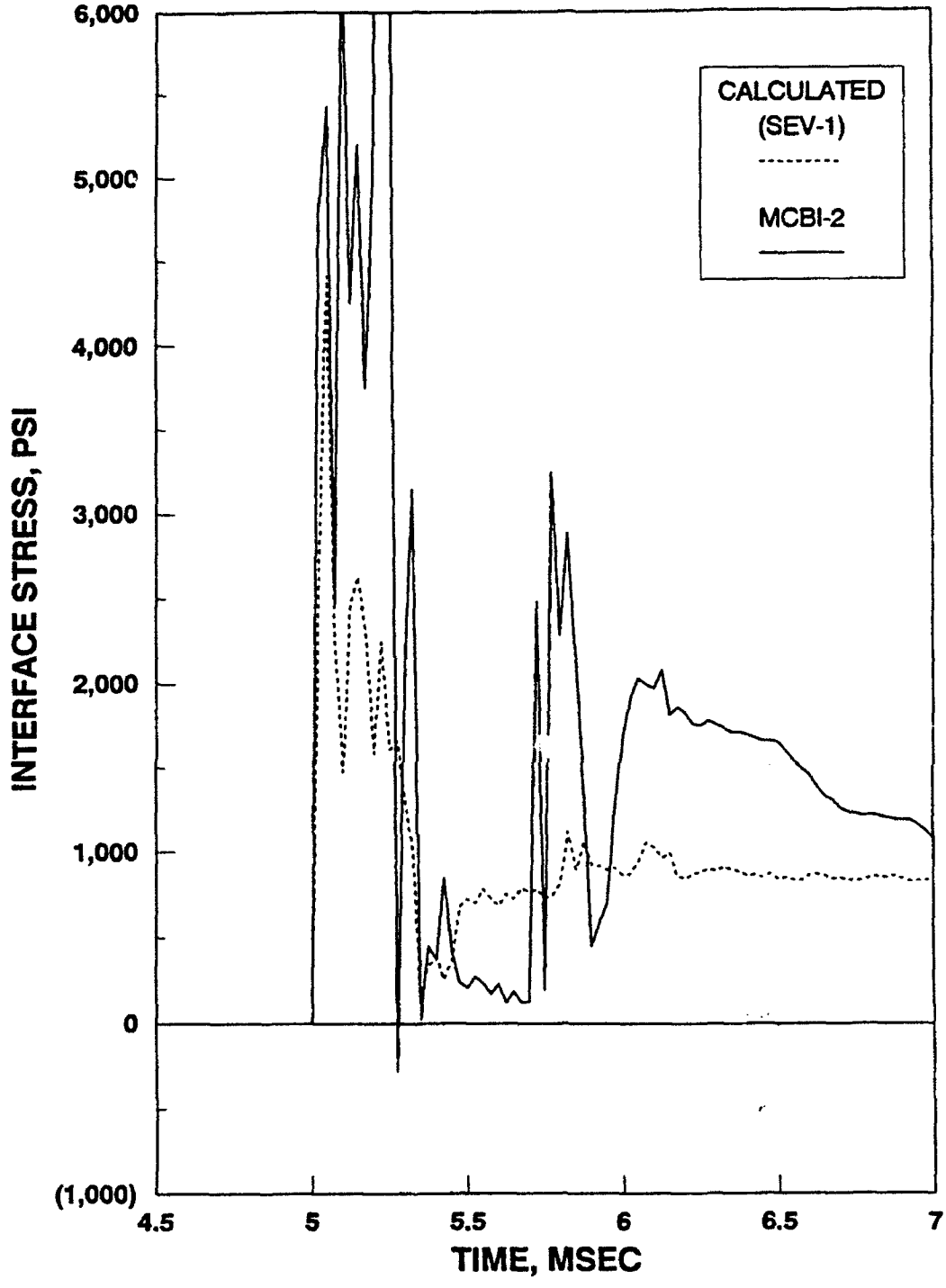

Figure 39. Comparison of measured (MCBI-2) and calculated (from SEV-1) interface stress wave forms, MCBI Test 2

to the onset of slab displacement. MCBI-2 then measured interface stresses much higher than the calculated values beyond 1 msec after shock arrival.

Based upon the above comparison, the measurement from soil stress gage SEV-1 did not appear to accurately represent the loading wave applied to MCBI-2. Because of this, a second calculation was done using the input wave form measured by soil stress gage SEV-2. This calculated wave form is compared to the MCBI-2 wave form in Figure 40. Overall, the calculated SEV-2 interface stress wave form was quite similar to that measured by MCBI-2 during the first millisecond after shock arrival. The calculated and measured wave forms both indicated high-amplitude stress spikes during the initial 250 μsec, and the arrival of the relief wave at 350 to 400 μsec. The wave forms continued to agree well until the onset of large positive stress spikes on the MCBI-2 wave form at 750 μsec after shock arrival. This phenomenon was also evident on the calculated wave form, but was of a much lower magnitude.

After approximately 1 msec, the interface stress measured by MCBI-2 was significantly higher than the calculated values. The agreement was better beyond 1.6 msec after shock arrival, but the measured stress was still 30 to 50 percent psi higher than the calculation. The reason for this discrepancy is unclear. However, the MCBI-2 measurement was also much higher than the MCBI-1 measurement beyond 1 msec after shock arrival.

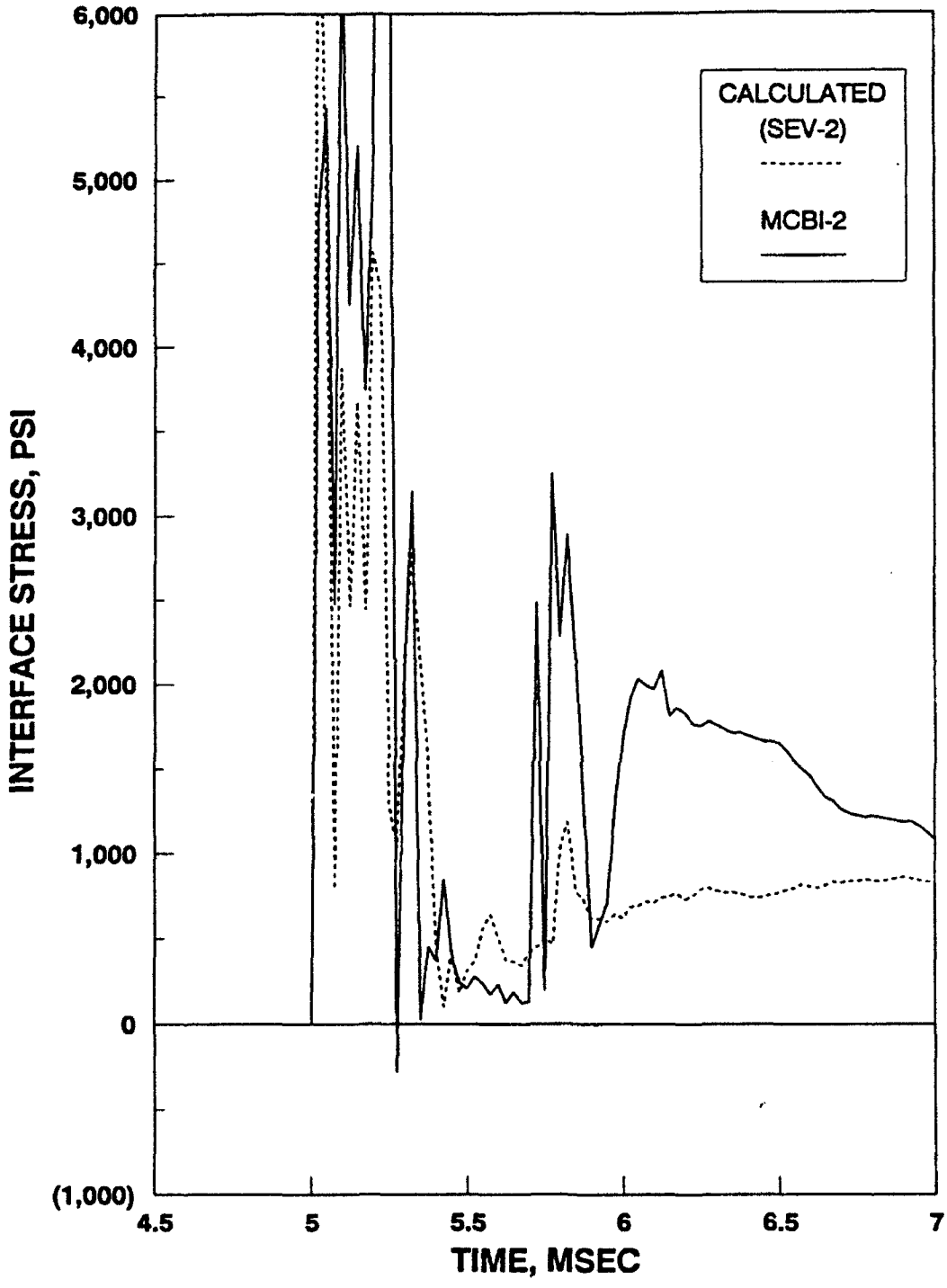

Figure 40. Comparison of measured (MCBI-2) and calculated (from SEV-2) interface stress wave forms, MCBI Test 2

SECTION 5
FINITE ELEMENT ANALYSIS

5.1 CALCULATIONAL OBJECTIVES

In this section, calculations are presented that investigate strain gradients which occur in the MCBI gage sensing column (due to cross-sectional changes) during dynamic load application, and assess the effects of these strain gradients on the sensitivity of the transducer. The overall objective of these calculations was to determine the accuracy with which the MCBI gage is capable of measuring dynamic, normal stresses.

5.2 FINITE ELEMENT ANALYSIS OF MCBI GAGE RESPONSE

A numerical analysis of MCBI gage response was performed with the finite element computer program DYNA2D (Reference 9). The input parameters for the calculation were first entered into the MAZE pre-processing program (Reference 10), which prepared a output file in the proper format for input into DYNA2D. Post-processing of the solution generated by DYNA2D was done with the ORION program (Reference 11).

5.2.1 Calculation Set-up.

In order to simplify calculations, the MCBI gage was modeled as being axisymmetric. The sensing column is only approximately axisymmetric due to the presence of the four machined flats for placement of the strain gages. These flats are not large enough, however, to compromise the validity of the calculations. Calculations were further simplified by modeling only the MCBI gage sensing column and gage housing. Inclusion of the gage mount was not considered necessary, since its primary function is to provide lateral stress isolation for the gage and should not, because of its design, affect normal stress sensitivity.

The MAZE input file (provided in Appendix D) contained instructions which defined the geometry, finite element mesh, material properties, and applied loads. Figure 41 illustrates the gage parts which were modeled, and the finite element mesh generated by MAZE is shown in Figure 42. The MCBI gage was modeled with 4-node solid elements arranged in an axisymmetric geometry. The gage housing and sensing column were modeled as an elastic steel with the following properties:

Mass density: 7.642×10^{-4} lb-sec^2/in.^{4}

Elastic modulus: 30×10^6 psi

Poisson's ratio: 0.3

Pressure boundary conditions were applied on the upper surface of the mesh. The applied pressure history was a step function with a rise-time from 0 to 10,000 psi of 100 μsec (Figure 43). This rise-time was selected because it was the fastest rise-time that did not produce unacceptably severe and unreasonable "ringing" in the calculated parameter-history plots. The applied pressure was then held constant at 10,000 psi for 1 msec. The bottom surface of the mesh was treated as a rigid boundary, which approximates the condition created when the MCBI gage is cast into a massive concrete structure.

Interfaces between the sensing column and gage housing were modeled by merging the two parts. This approximates the actual loading condition in which the column and gage housing expand laterally, effectively eliminating the space between the opposing surfaces.

A series of initial DYNA2D calculations were run to determine the adequacy of the grid sizes used. These calculations indicated that a mesh consisting of 410 elements was adequate to describe the response of the sensing column and gage housing.

5.2.2 Calculation Results

Axial stress contour plots from the finite element solution were produced to check the validity of the DYNA2D calculation, and to obtain information on the concentration of stresses within the sensing column. Figures 44-47 follow the propagation of axial stress down the MCBI gage in 2-μsec time increments, beginning at 2 μsec after zero-time. These plots show that the calculation is accurately modeling the stress wave

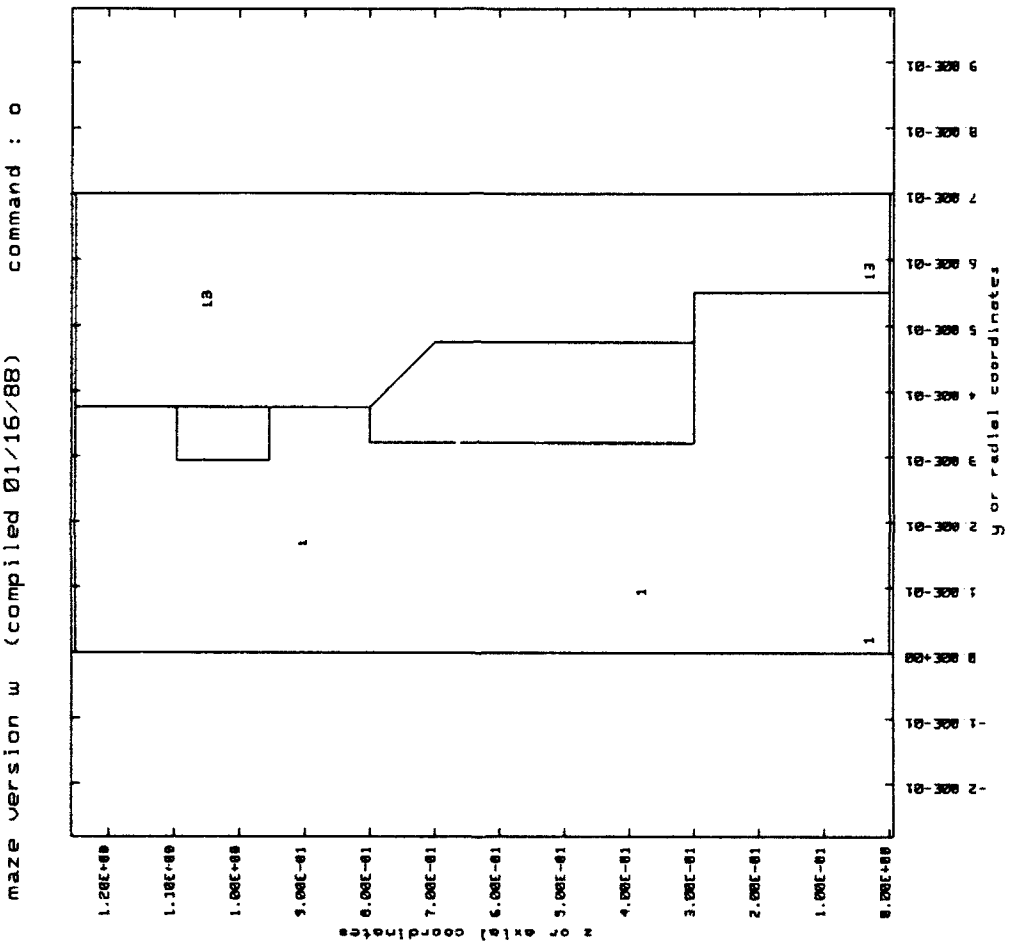

Figure 41. MCBI gage parts modeled using DYNA2D

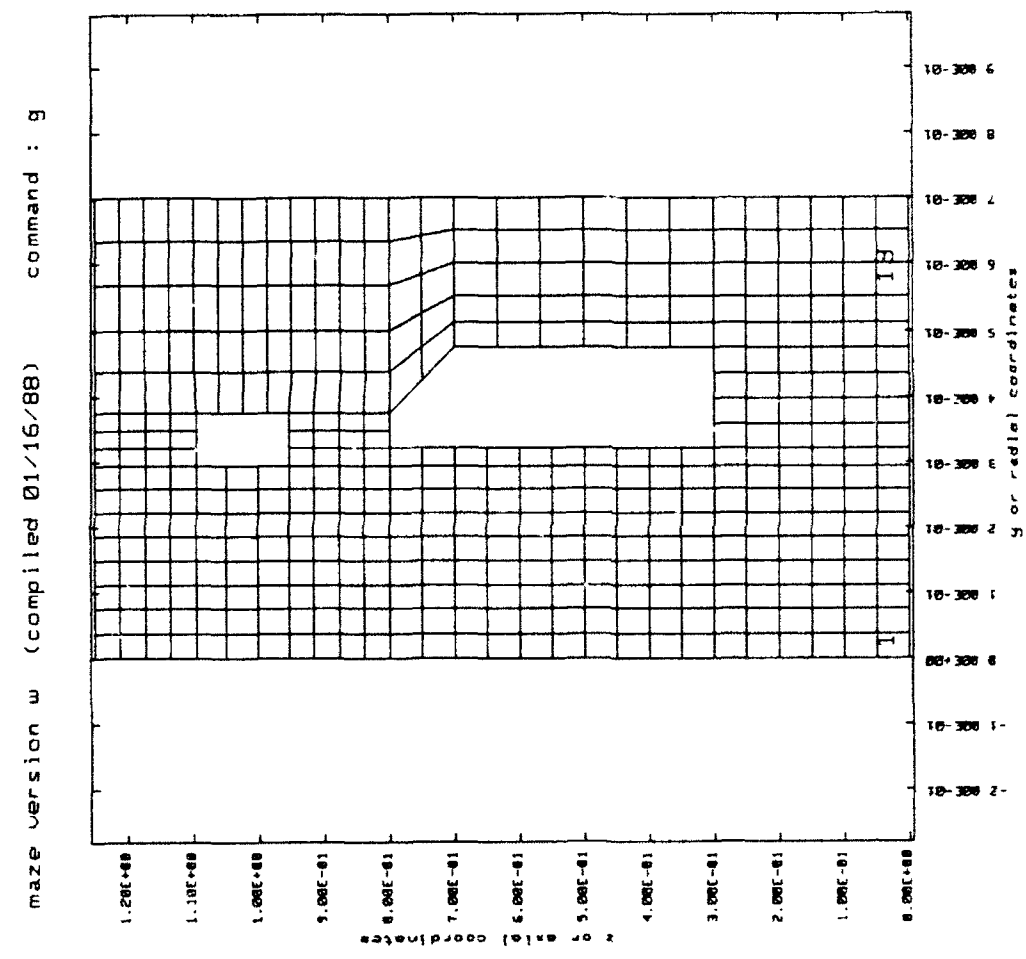

Figure 42. Finite element mesh of the MCBI gage generated by MAZE

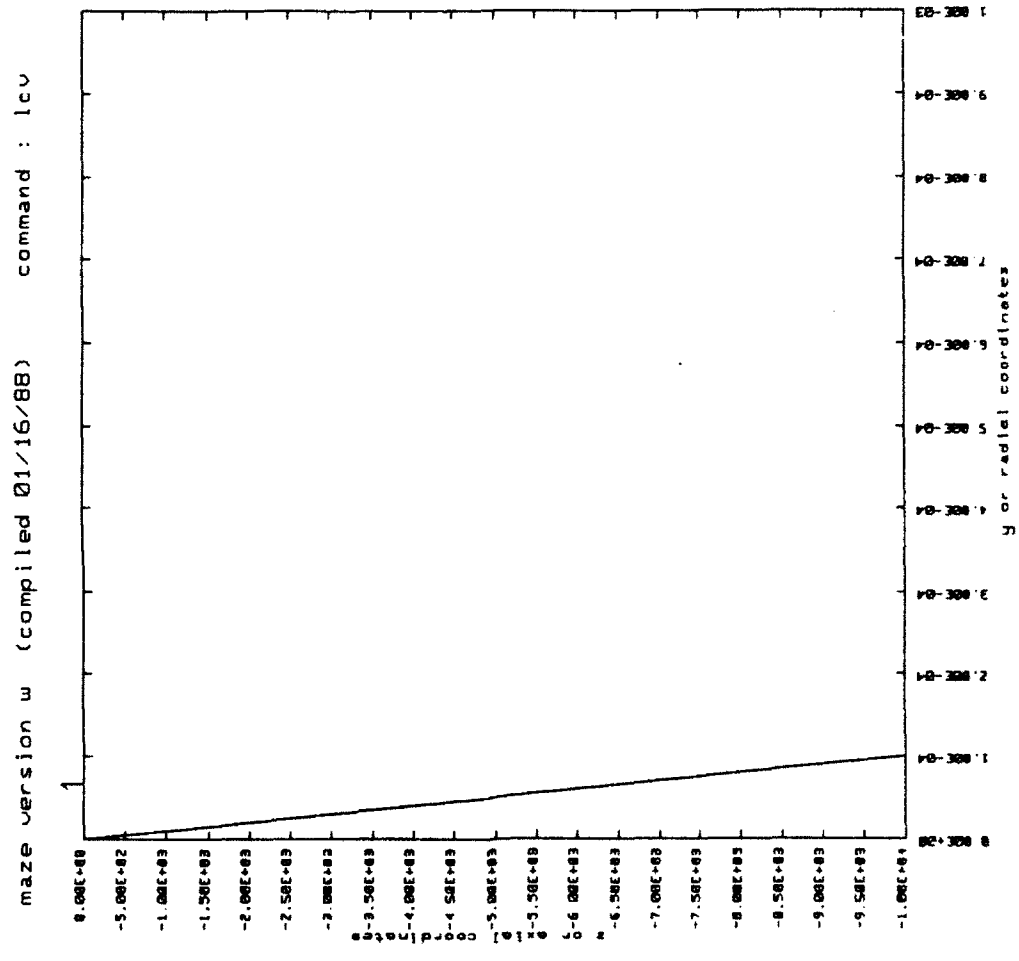

Figure 43. Stress loading curve applied to the top of the MCBI gage during finite element calculations

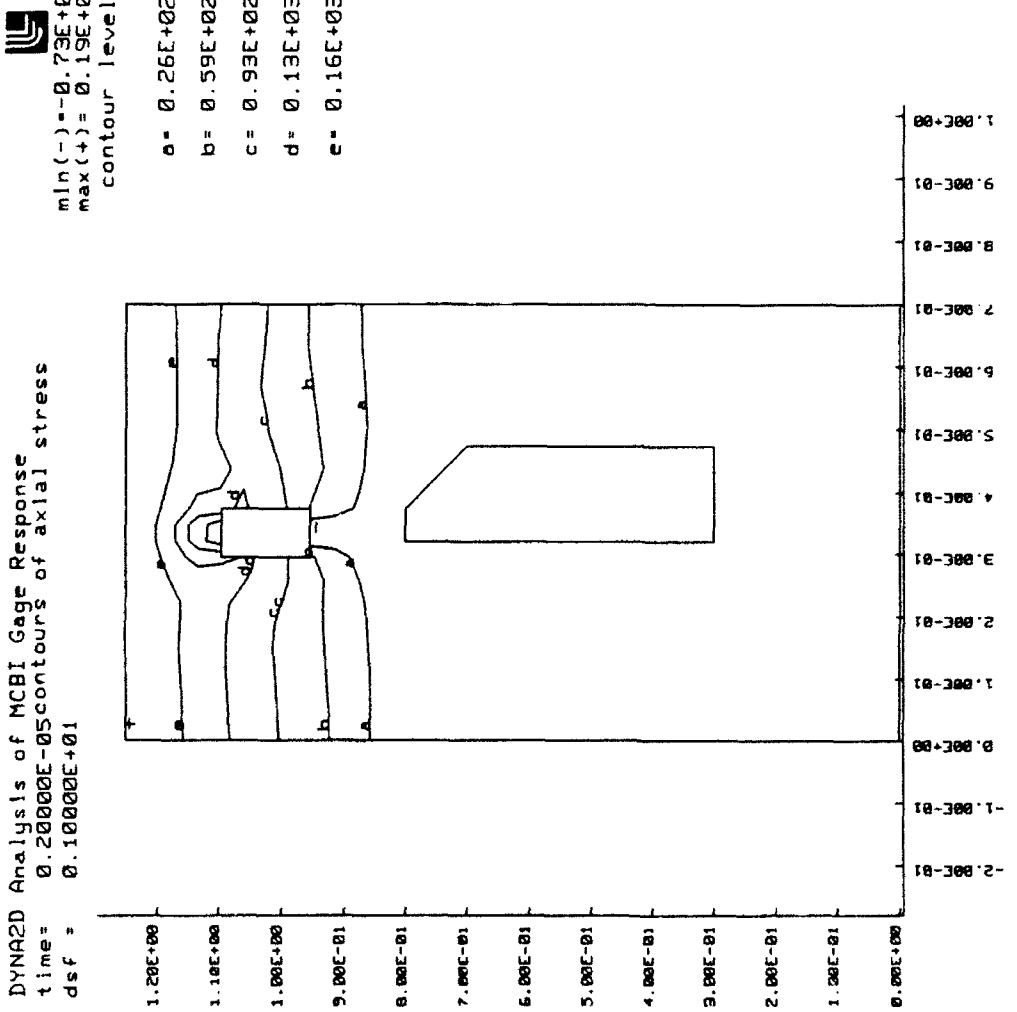

Figure 44. Axial stress contours inside the MCBI gage at 2 μsec after zero-time, as calculated by DYNA2D

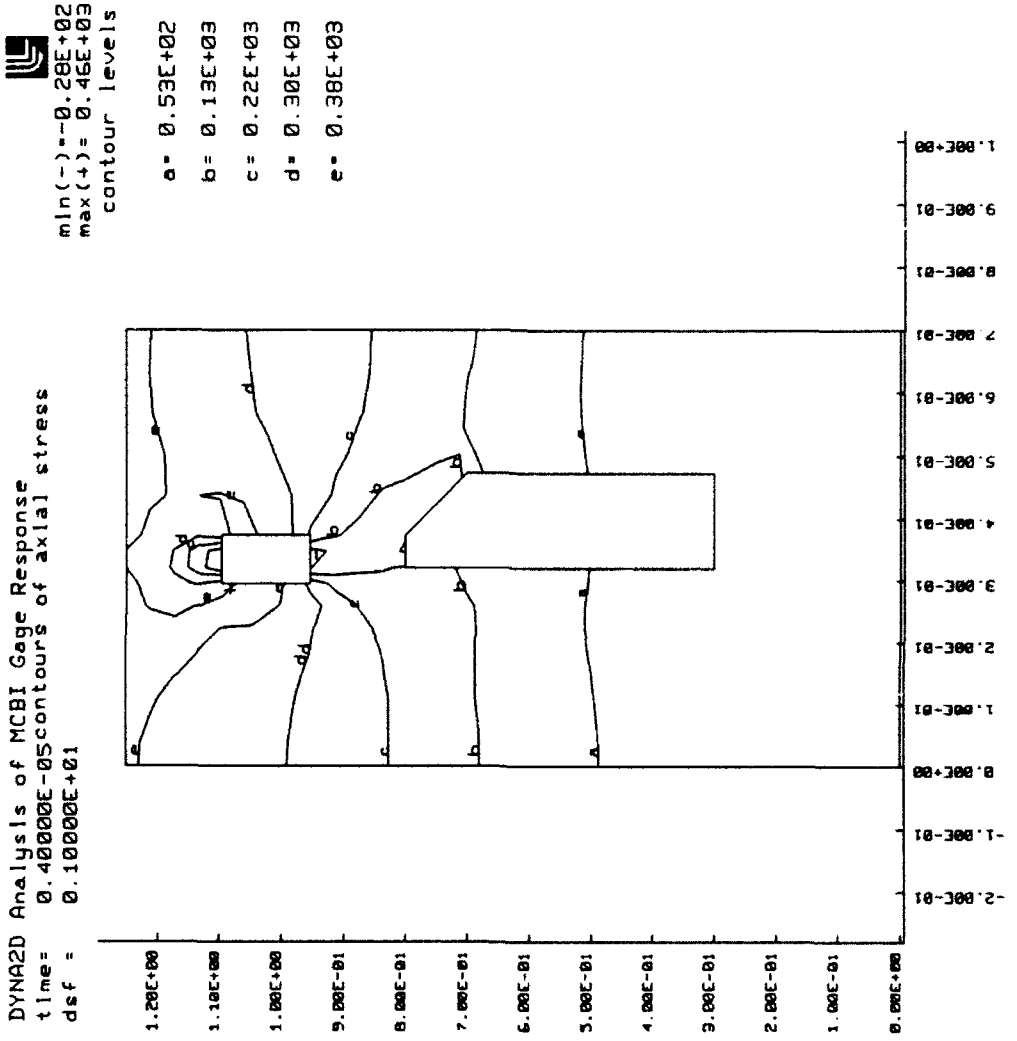

Figure 45. Axial stress contours inside the MCBI gage at 4 μsec after zero-time, as calculated by DYNA2D

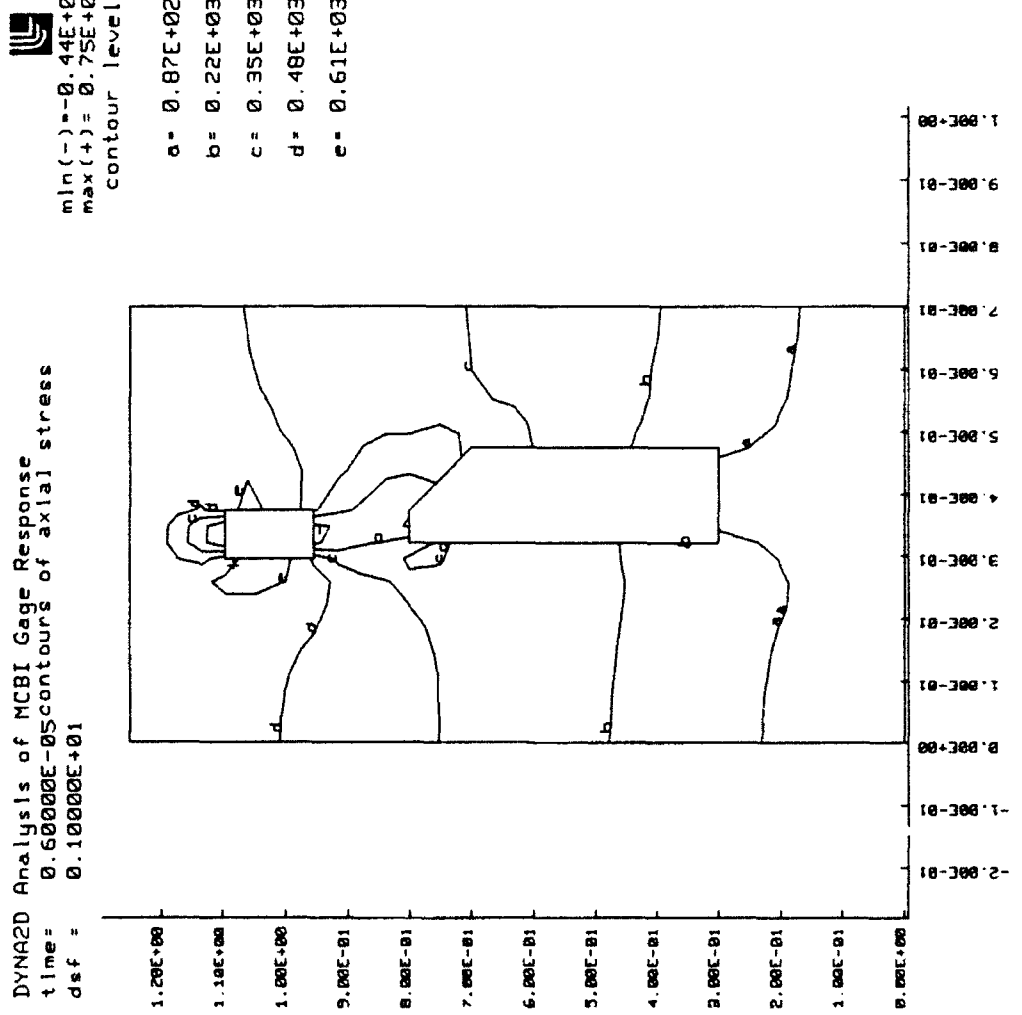

Figure 46. Axial stress contours inside the MCBI gage at 6 μsec after zero-time, as calculated by DYNA2D

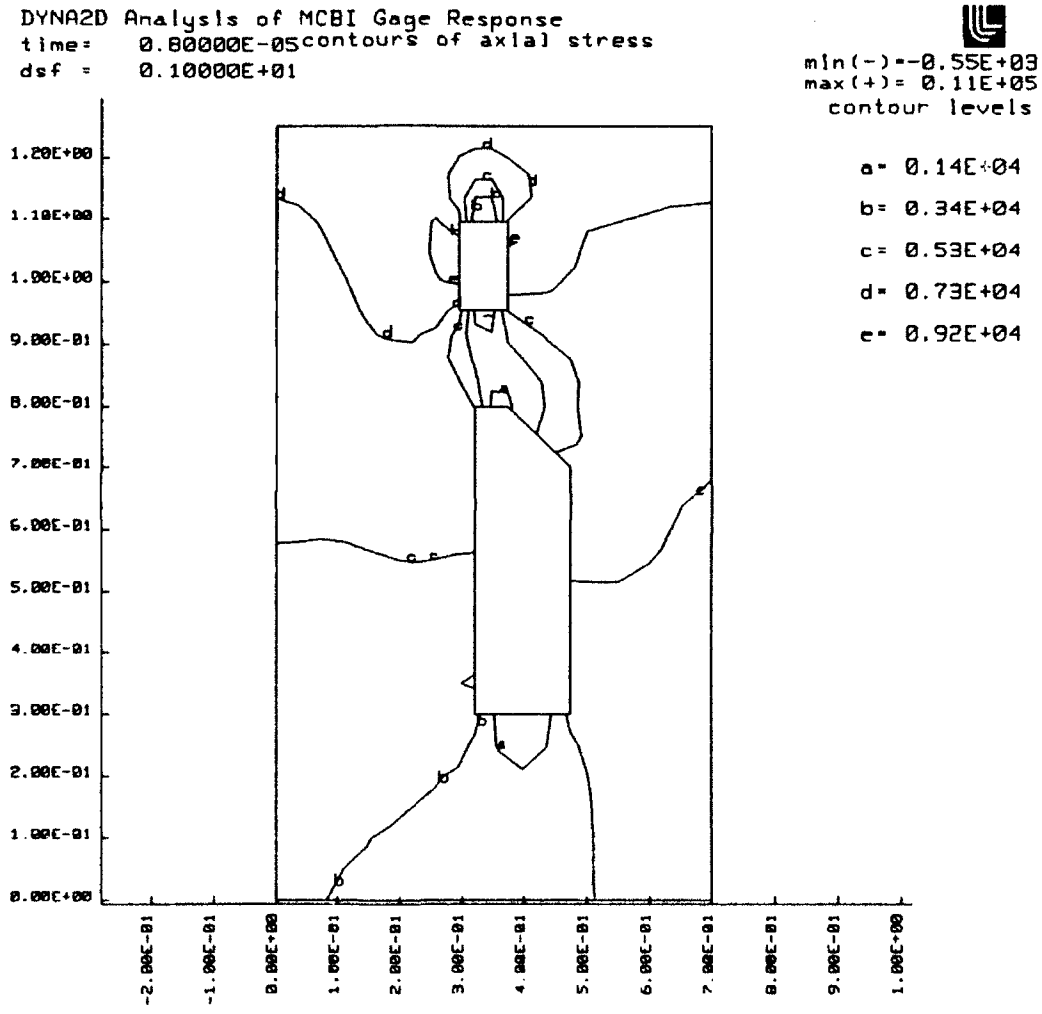

Figure 47. Axial stress contours inside the MCBI gage at 8 μsec after zero-time, as calculated by DYNA2D

velocity in steel (approximately 16,500 ft/sec), and that the incide stress is reflected at the lower boundary of the gage (Figure 47).

Additional plots of axial stress are shown at 0.2 and 0.4 msec after zero-time in Figures 48 and 49, respectively. These plots indicate that no axial stress concentrations exist at late times in the area where the strain gages are located on the sensing column. Similar plots of hoop stress are shown in Figures 50 and 51. Some hoop stress concentration is present at 0.2 msec in the strain-gaged area. However, this stress concentration disappears at 0.4 msec after zero-time. Thus, no long-term stress concentrations should affect the measurements produced by the strain gages.

5.3 TRANSDUCER RESPONSE TO DYNAMIC STRESS

The DYNA2D calculation yielded time histories of axial and transverse (hoop) strain in the sensing column due to the applied load. Strain-time histories were produced for the two grid elements which were closest to the actual locations of strain gages on the sensing column. The locations of these elements are shown in Figure 52. The strain-time histories were then used to calculate the implied stress loading on the top surface of the coulumn.

The axial and hoop strain histories of the two elements are plotted in Figures 53 and 54. Both plots indicate a pronounced oscillation or ringing. This is due to reflections from the calculation boundaries. The ringing has a higher amplitude than would occur in reality, due to the perfectly-reflecting boundary conditions.

For conditions of plane stress, axial strain (ϵ_z) and hoop strain (ϵ_h) are related to axial stress (σ_z) by

$$\sigma_z = E(\epsilon_z + \mu\epsilon_h)/(1 - \mu^2)$$

where μ is Poisson's ratio for steel, 0.3, and E is Young's modulus, 30 x 10^6 psi. Using this relation, the axial and hoop strain histories were used to derive the axial stress history which would be experienced by the MCBI gages.

It was necessary to correct the calculated axial stress history because of the change in cross-sectional area of the MCBI sensing column. The strain gages are located on a segment of the column with a cross-sectional area of 0.1024 $in.^2$, while the stress load is applied at

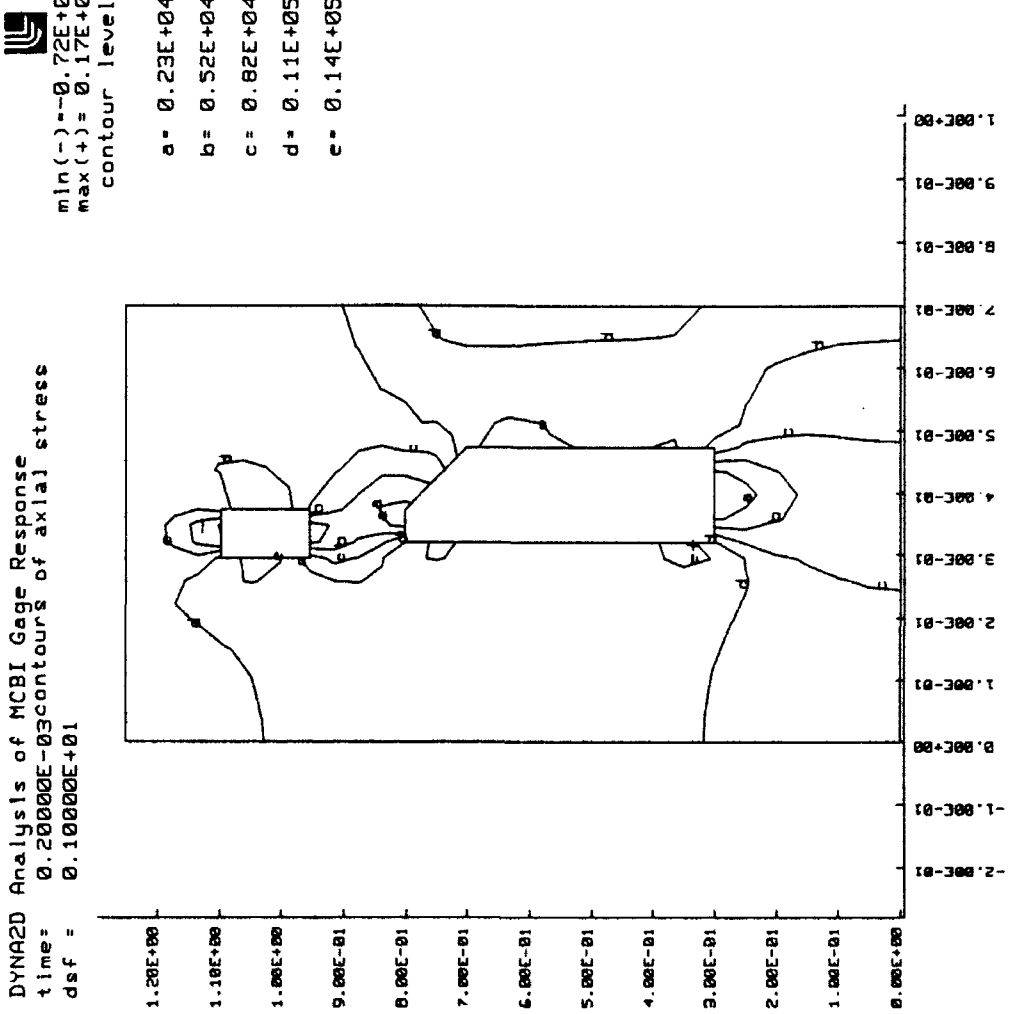

Figure 48. Axial stress contours inside the MCBI gage at 0.2 msec after zero-time, as calculated by DYNA2D

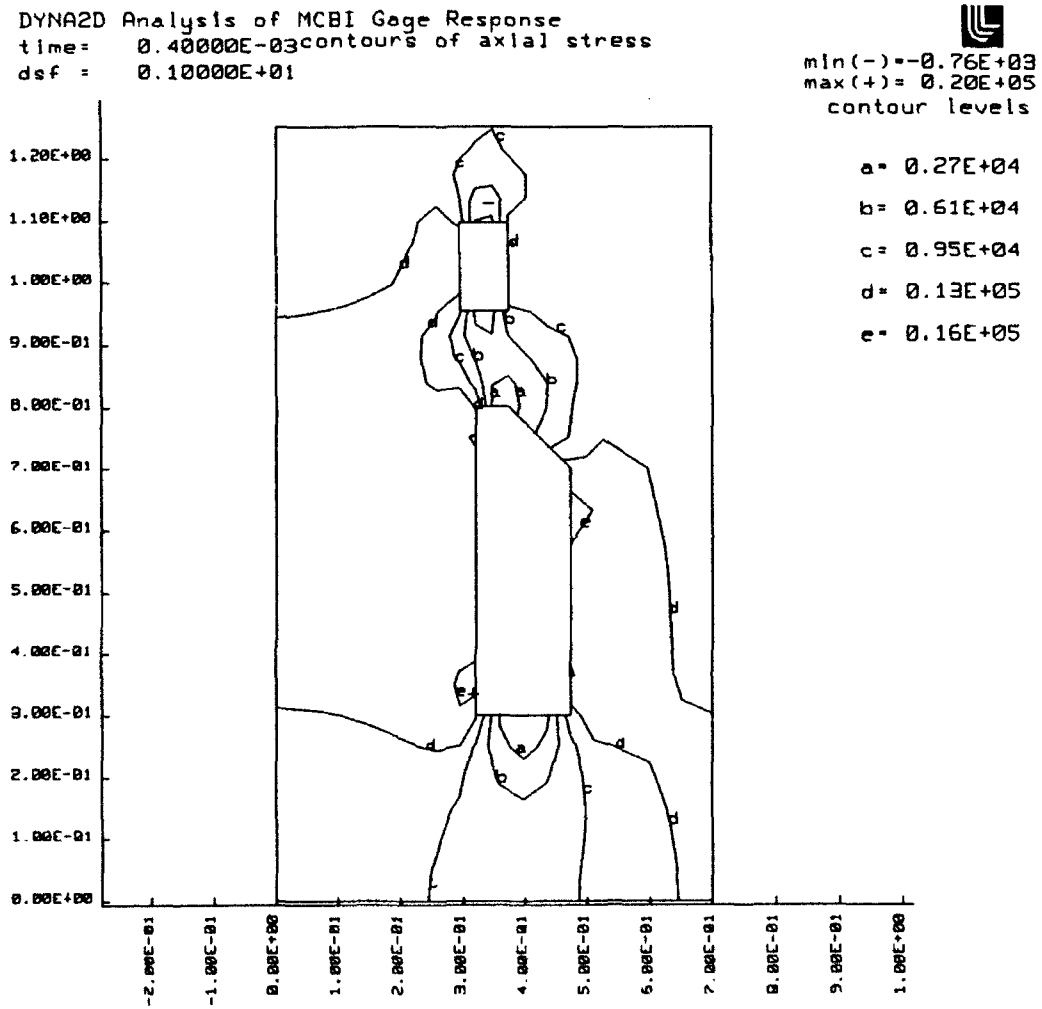

Figure 49. Axial stress contours inside the MCBI gage at 0.4 msec after zero-time, as calculated by DYNA2D

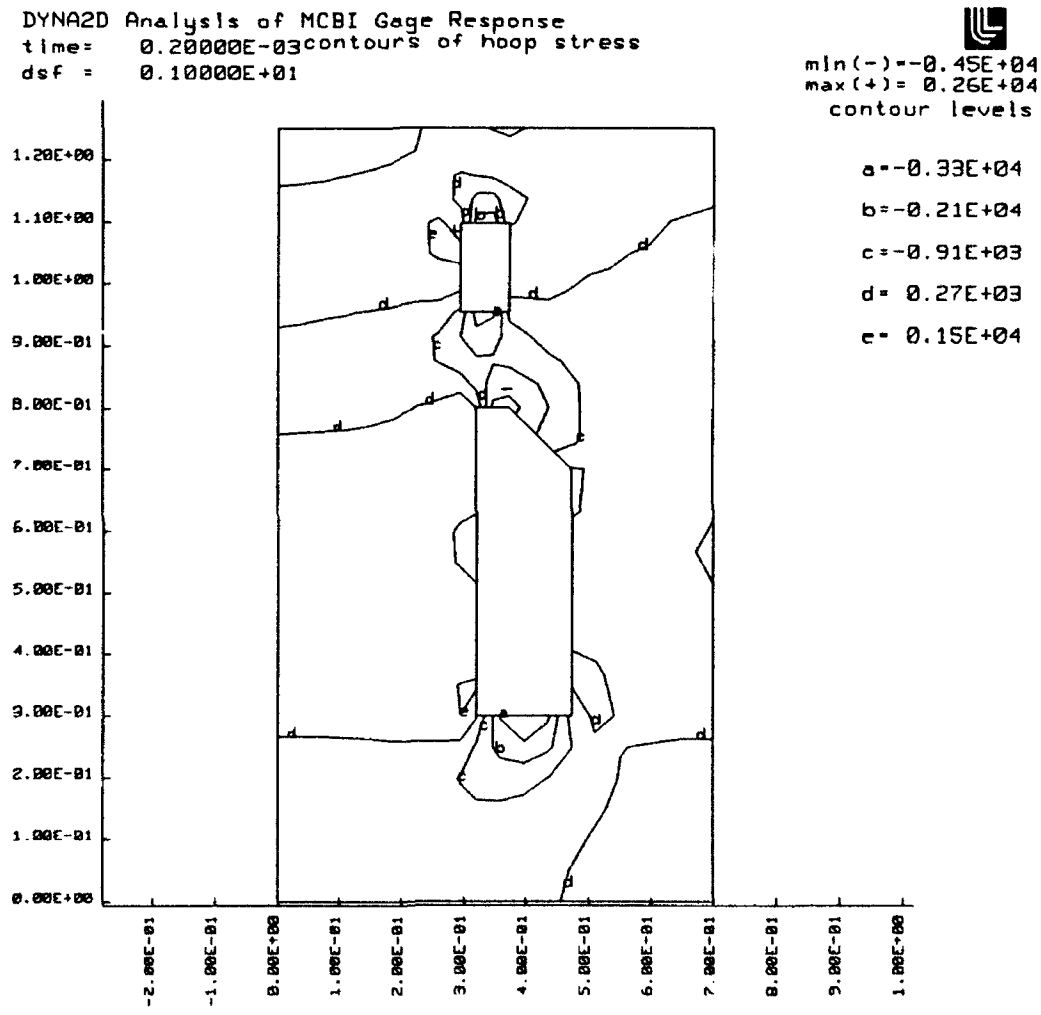

Figure 50. Hoop stress contours inside the MCBI gage at 0.2 msec after zero-time, as calculated by DYNA2D

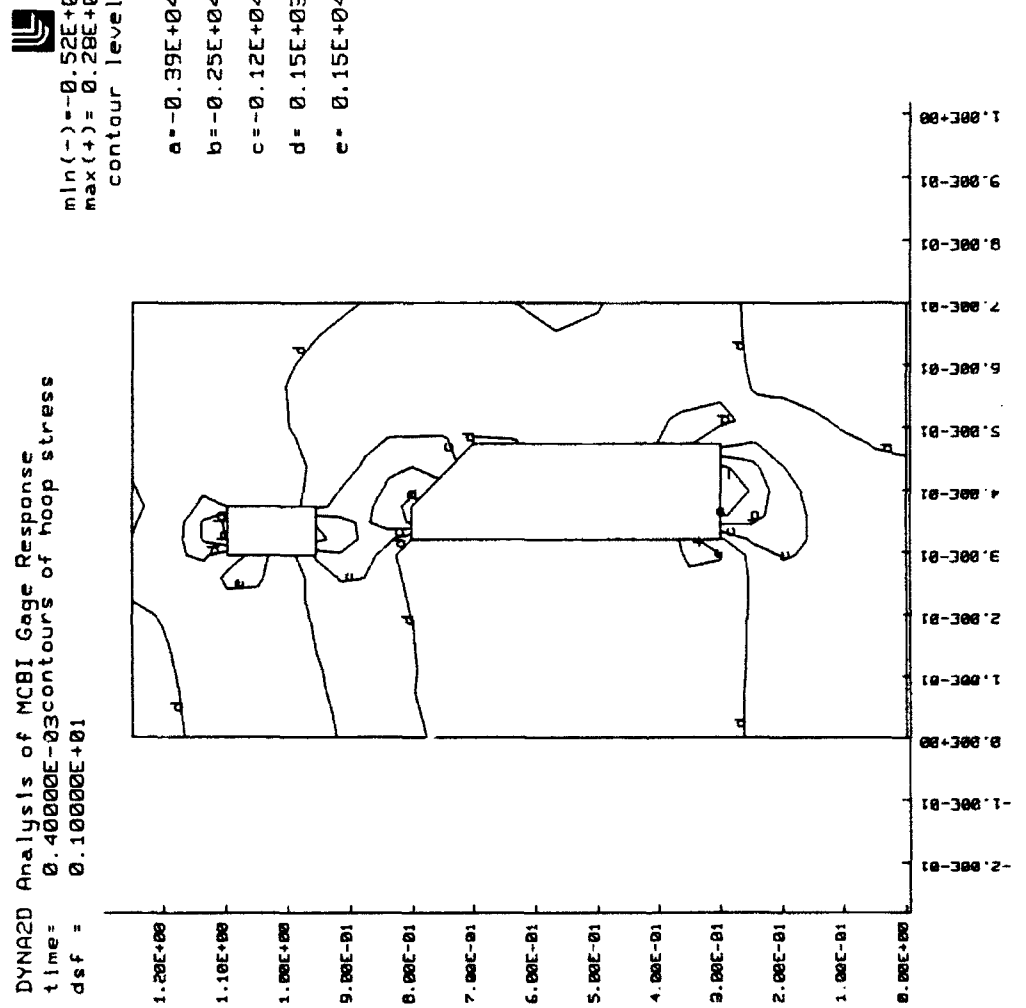

Figure 51. Hoop stress contours inside the MCBI gage at 0.4 msec after zero-time, as calculated by DYNA2D

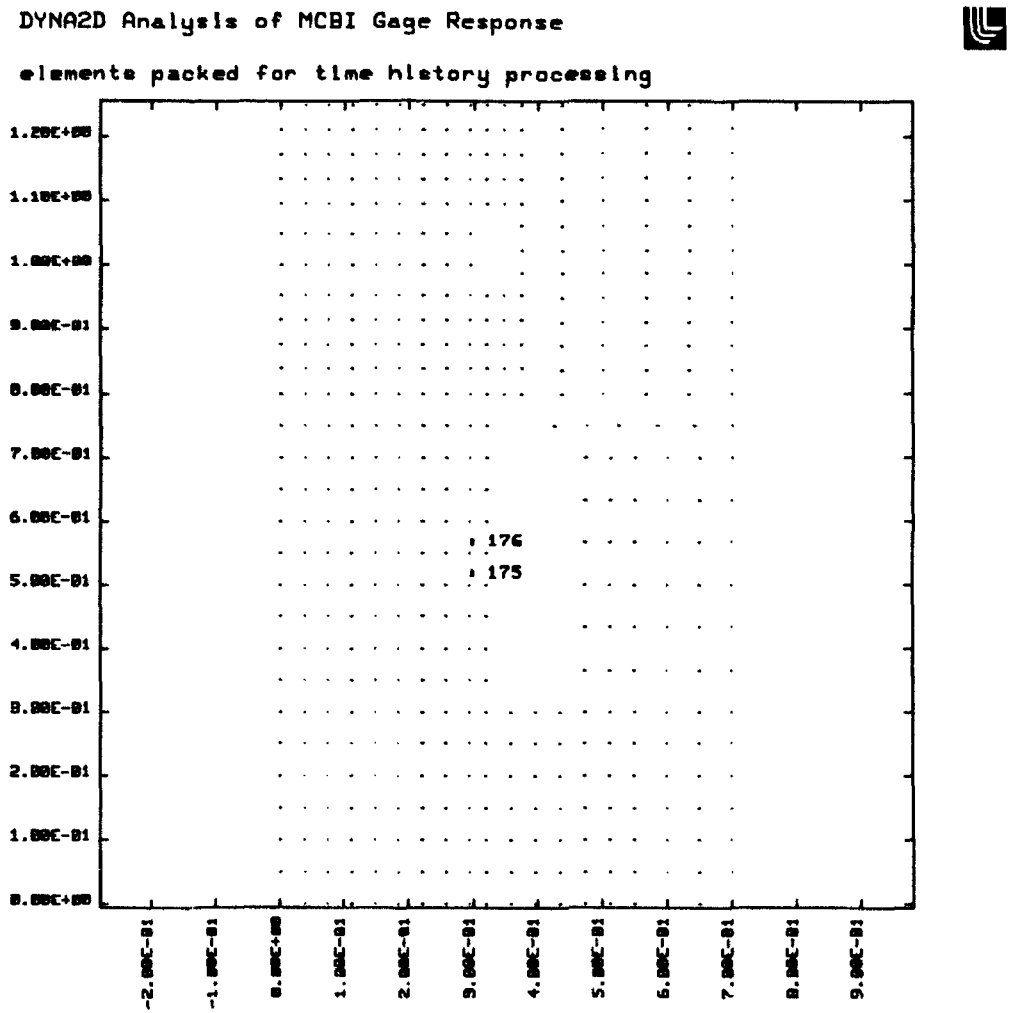

Figure 52. Location of mesh elements 175 and 176 selected for time-history plots

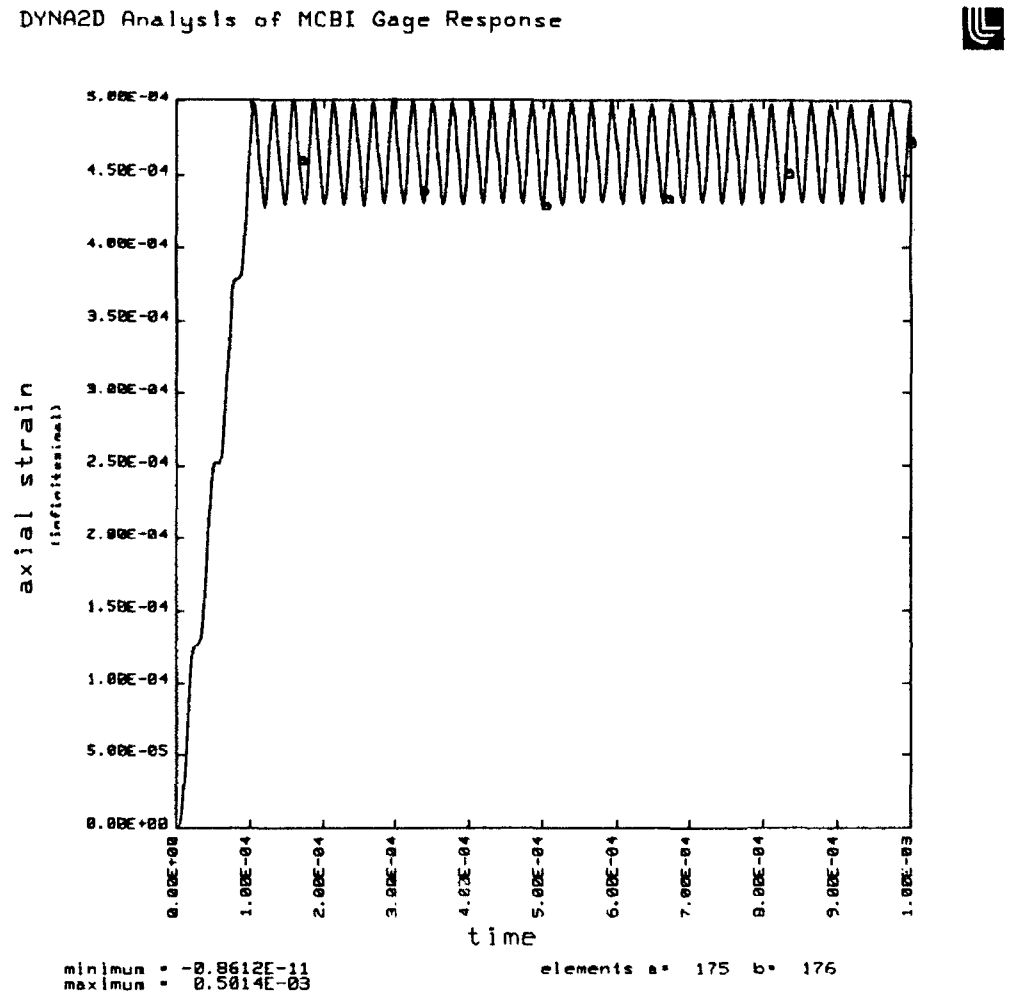

Figure 53. Axial strain-time histories for elements 175 and 176

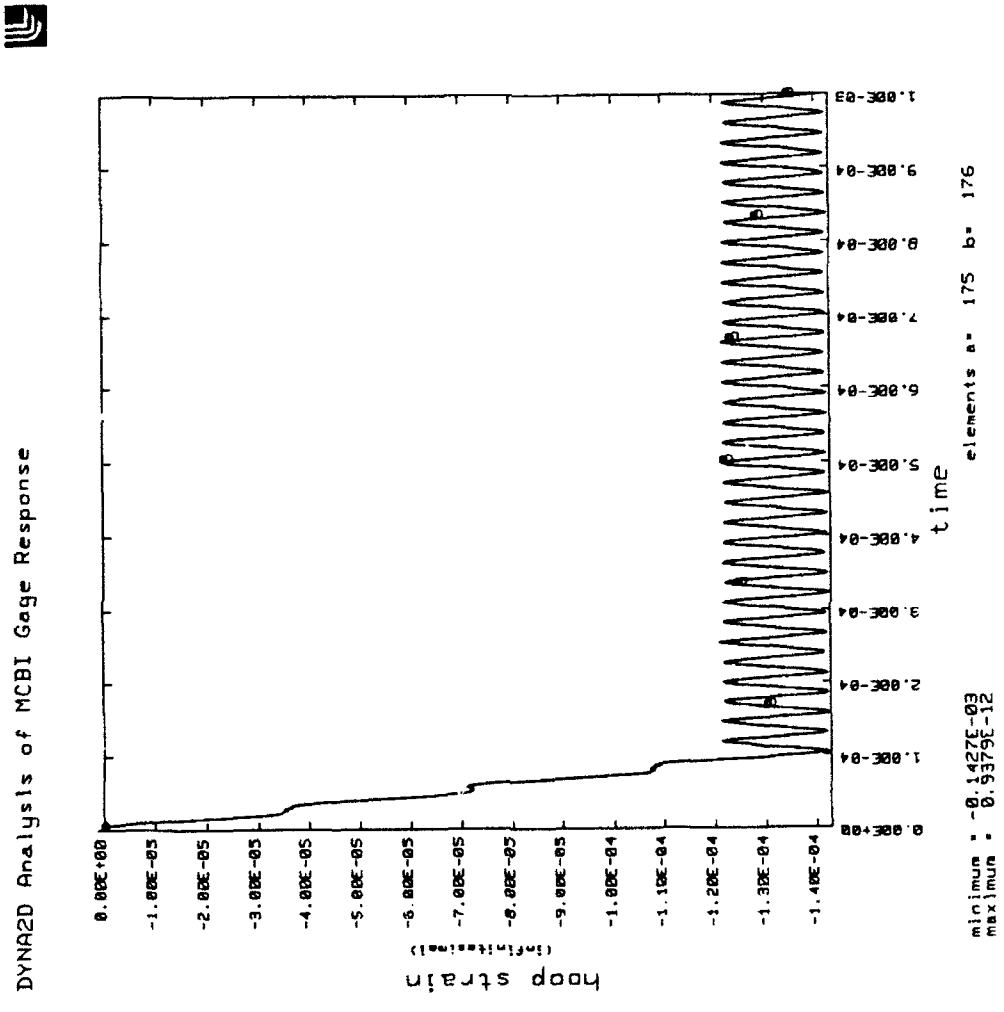

Figure 54. Hoop strain-time histories for elements 175 and 176

the top of the column over an area of 0.1406 $in.^2$. As a result of this, the stress in the sensing column is magnified by 0.1406/0.1024, or a factor of 1.373.

The corrected axial stress history is compared to the applied stress loading curve in Figure 55. Except for the ringing associated with reflections from the gage boundaries, the calculated stress history compares very well with the applied loading curve. This finding increases overall confidence in the ability of the MCBI gage to accurately measure dynamic normal stresses, and once again shows the absence of stress concentrations in the strain-gaged area of the sensing column.

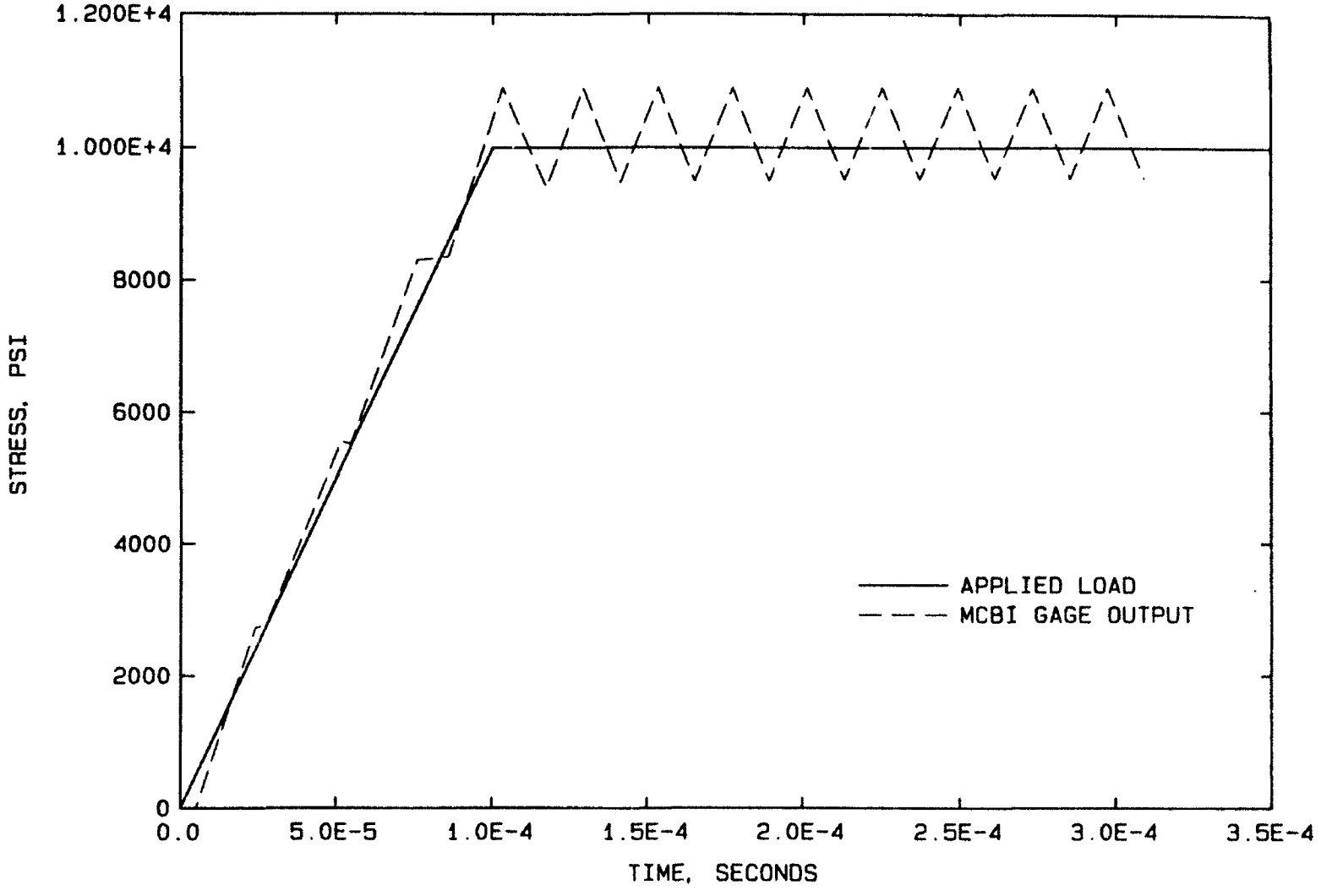

Figure 55. Comparison of calculated MCBI gage output versus applied stress loading curve

SECTION 6

CONCLUSIONS AND RECOMMENDATIONS

6.1 CONCLUSIONS

The MCBI gage appears to be a useful instrument for measuring normal interface stresses produced by explosion-induced loadings. It has the capacity to measure much higher stresses than currently used gages such as the Kulite VM-750, and is capable of measuring stresses in excess of 25,000 psi. During the MCBI Test 1, MCBI gages provided interface stress measurements which compared very favorably to those produced by similarly located VM-750 gages. In addition, the MCBI gage records suffered less distortion due to lateral acceleration than did the VM-750 interface gages.

MCBI gages produce an extremely linear and repeatable electrical output due to applied stress. MCBI gage lateral acceleration sensitivity is a relatively low 0.018 psi/g, and it is essentially insensitive to lateral stresses. The gage mounting hardware can be easily incorporated into most reinforced concrete structures, and the gage itself may be installed after the concrete is poured.

Finite element calculations show that the MCBI gage is capable of accurately measuring applied dynamic loads. These calculations also show that no axial or hoop stress concentrations are produced in the strain gaged-area of the sensing column.

In addition to its interface stress measurement capabilities, it is possible that the MCBI gage, or a variation of it, could be used to measure airblast pressures. One MCBI gage successfully measured airblast, producing an impulse record similar to that obtained from nearby bar gages. With some modification, the MCBI gage may be capable of measuring airblast pressures up to 70,000 psi.

6.2 RECOMMENDATIONS

Hydrocode calculations should be performed to more accurately model the second MCBI gage validation experiment. This would increase confidence in the performance of the MCBI gage. However, its small size, and the amount of validation work already performed, make the MCBI the preferred choice over the old CBI gage for interface stress measurements above 5000 psi.

It is recommended that MCBI gages be considered for use in all normal interface stress measurement applications where the expected peak stress is between 5,000 and 25,000 psi. While MCBI gages can accurately measure stresses lower than 5,000 psi, commercially available gages are quite good and are less expensive. For applications where the expected peak stress is greater than 25,000 psi, MCBI gages can be used, although gage behavior at those pressure levels is not well characterized and some modifications to the mounting hardware may be required.

Further testing is needed to determine MCBI gage behavior at applied stress levels in excess of 25,000 psi. Also, it would be advantageous to conduct a series of tests to determine if the MCBI gage, or some variant of it, can reliably measure airblast pressures in the 10,000 to 70,000-psi range.

LIST OF REFERENCES

1. KULITE Product Bulletin KS-1000A, KULITE Miniature IS Diaphragm Pressure Transducers, 1982, KULITE Semiconductor Products, Inc., Ridgefield, NJ.

2. Faust, R. W. and Ingram, J. K., 1967, "Development of On-Structure Stress Gages," Technical Report 1-801, U. S. Army Engineer Waterways Experiment Station, Vicksburg, MS.

3. Chan, B., 1963, "Design of a Transducer for Pressure Measurements on Buried Concrete Structures," Miscellaneous Paper No. 1-593, U.S. Army Engineer Waterways Experiment Station, Vicksburg, MS.

4. KULITE Semiconductor Strain Gage Manual, KSGM-1, 1989, KULITE Semiconductor Products, Inc., Ridgefield, NJ.

5. Modern Steels and Their Properties, Carbon and Alloy Steel Bars and Rods, Handbook 3310, Bethlehem Steel Corporation

6. Graff, Karl F., 1975, Wave Motion in Elastic Solids, Ohio State University Press.

7. Peekna, A., 1977, "Development of a Laterally-Isolated Diaphragm-Type Soil-Structure Interface Stress Gage," Technical Report DNA-4816F, U.S. Army Engineer Waterways Experiment Station, Vicksburg, MS.

8. Rickman, D. D., 1986, "CHT-3 Airblast Calibration Test, Data Report," Letter Report, U.S. Army Engineer Waterways Experiment Station, Vicksburg, MS.

9. Hallquist, J. D., 1978, "DYNA2D-An Explicit Finite Element and Finite Difference Code for Axisymmetric and Plane Strain Calculations, (User's Guide)", Report UCRL-52429, University of California, Lawrence Livermore National Laboratory.

10. Hallquist, J. D., 1983, "MAZE-An Input Generator for DYNA2D and NIKE2D", Report UCID-19029, Revision 2, University of California, Lawrence Livermore National Laboratory.

11. Hallquist, J. D., and Levatin, J. L., 1985, "ORION-An Interactive Color Post-processor for Two Dimensional Finite Element Codes", Report UCID-19310, Revision 2, University of California, Lawrence Livermore National Laboratory.

APPENDIX A

MCBI GAGE MACHINE DRAWINGS

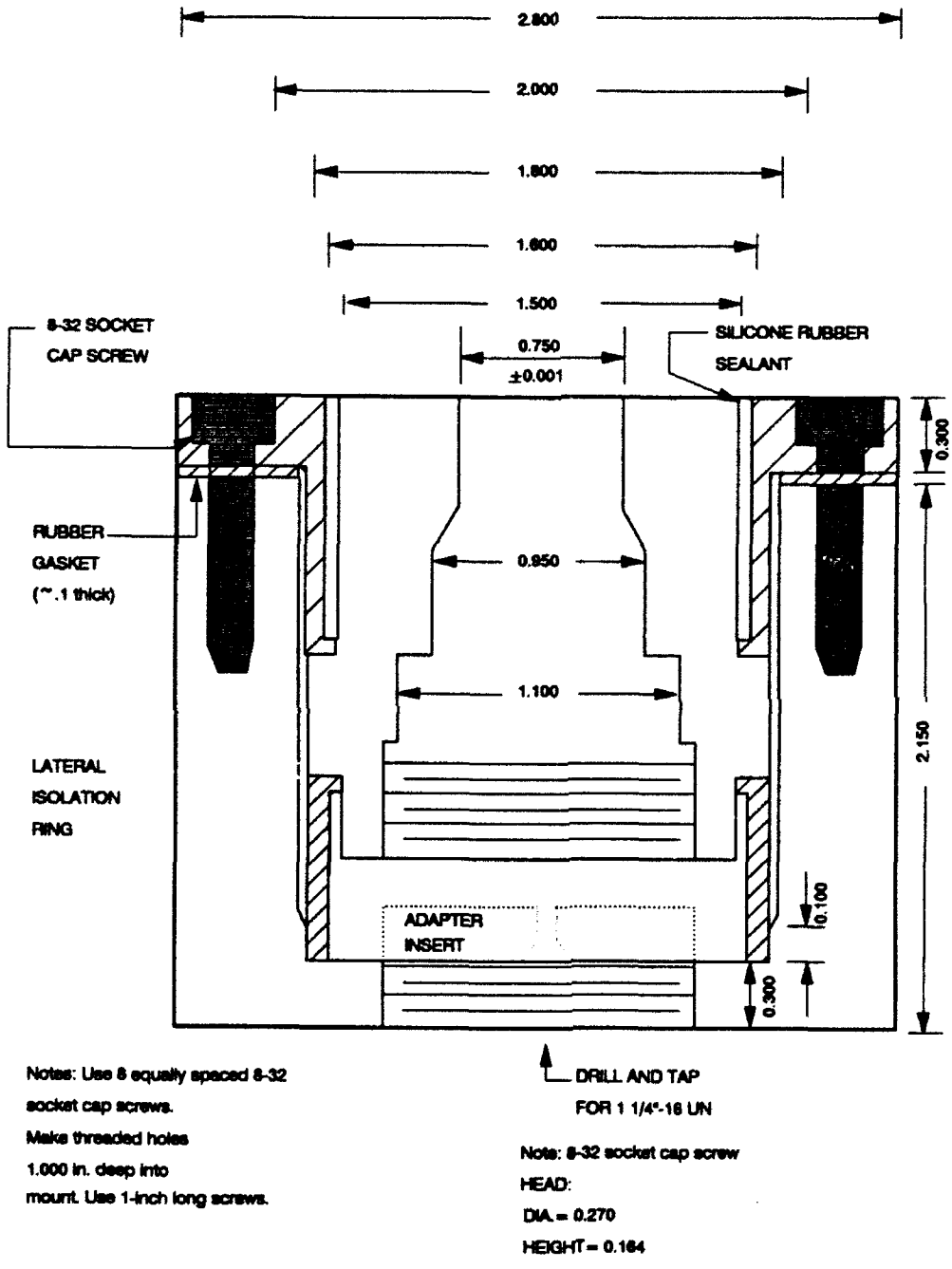

Figure 56. Machine drawing of assembled MCBI gage and mount

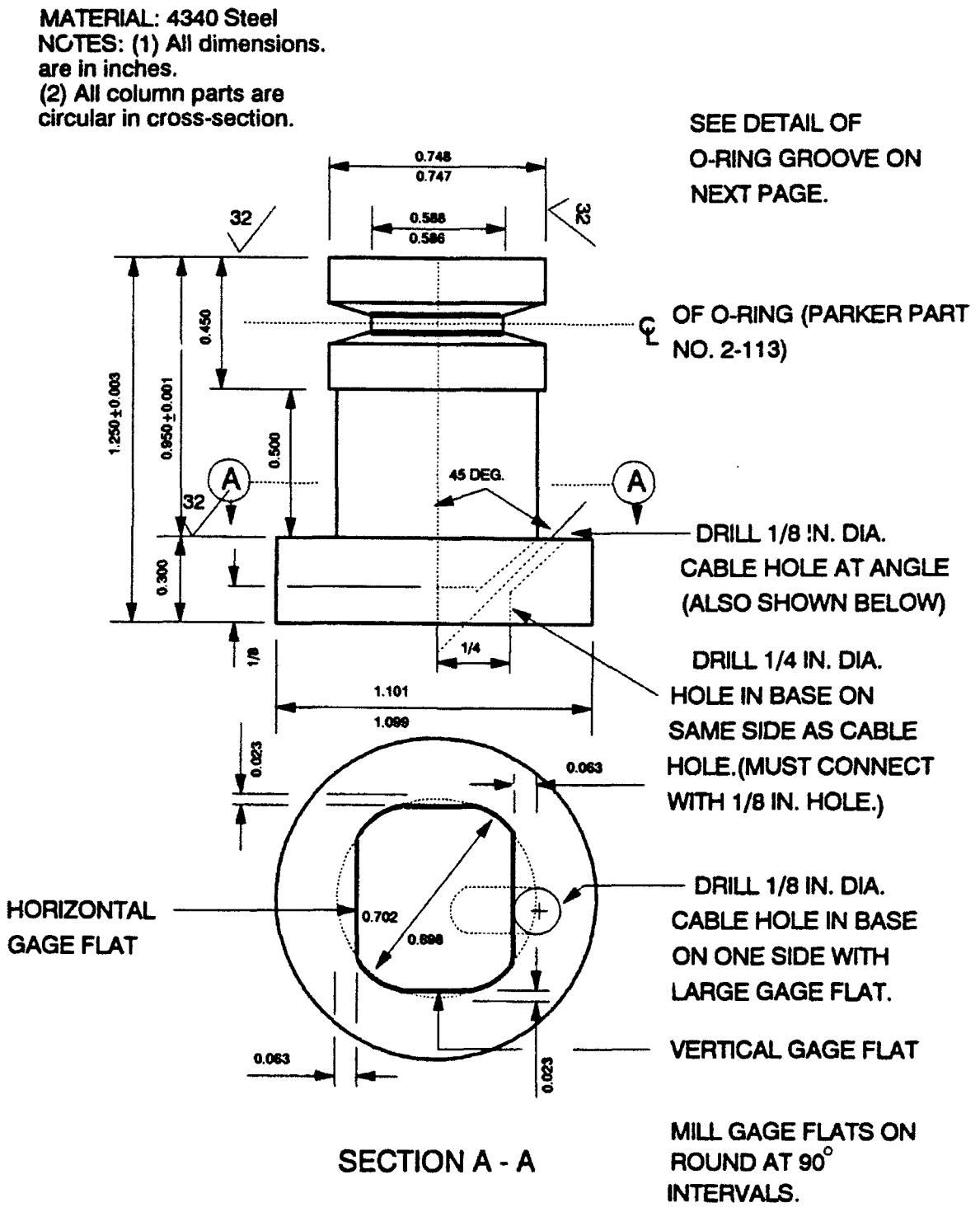

Figure 57. Machine drawing of MCBI gage sensing column

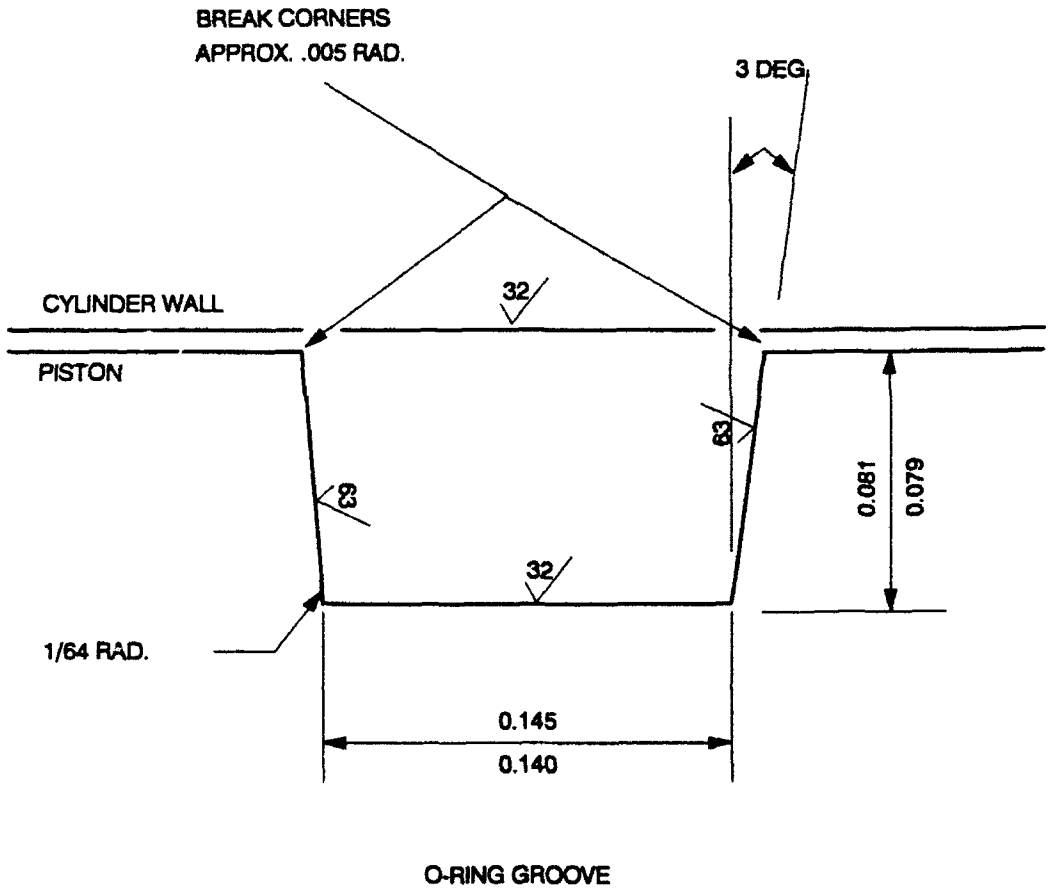

Figure 58. Machining details for the "O"-ring groove located on the MCBI gage sensing column

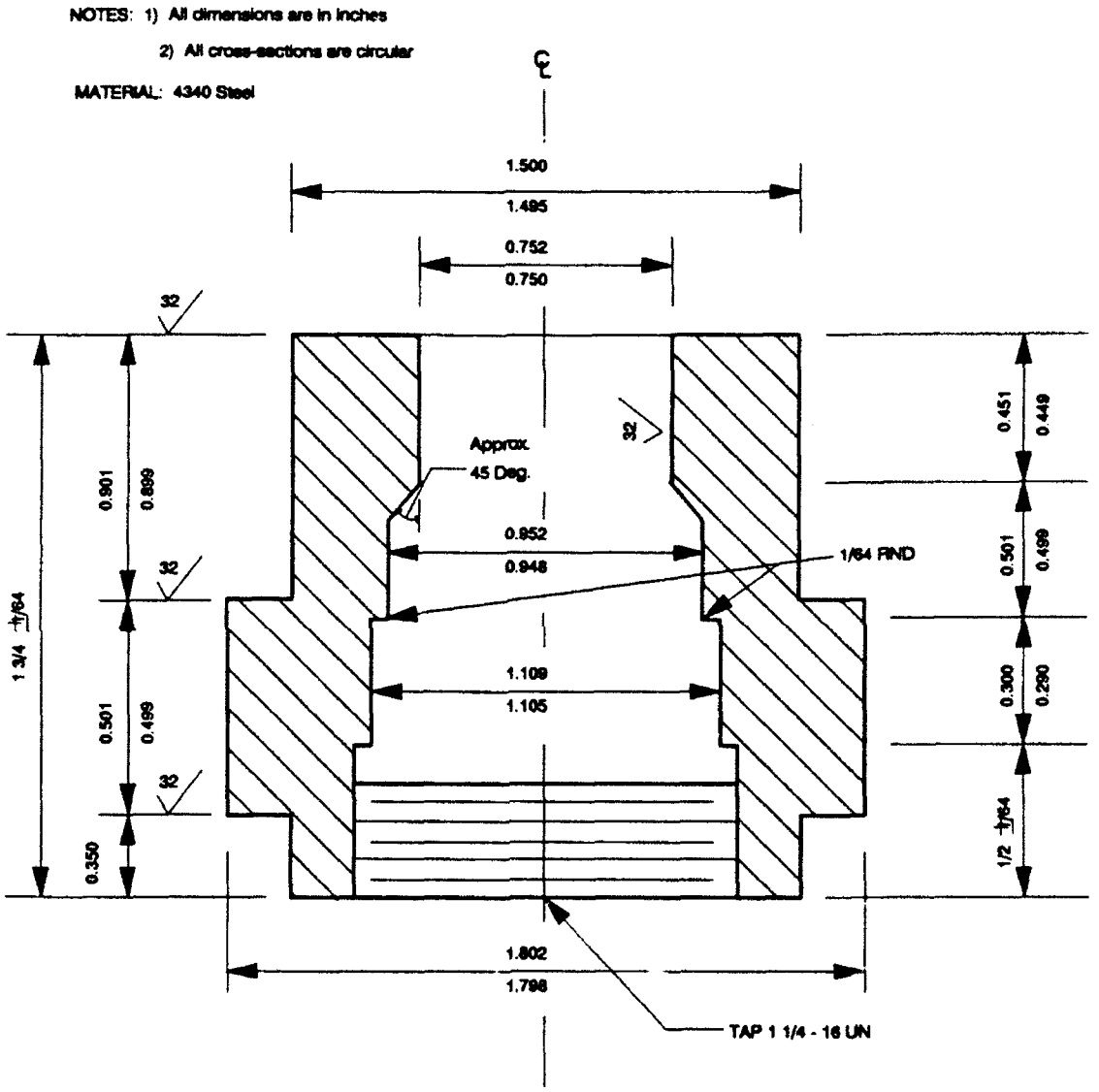

Figure 59. Machine drawing of the MCBI gage housing

MATERIAL: 4340 Steel

NOTE: All dimensions are in inches

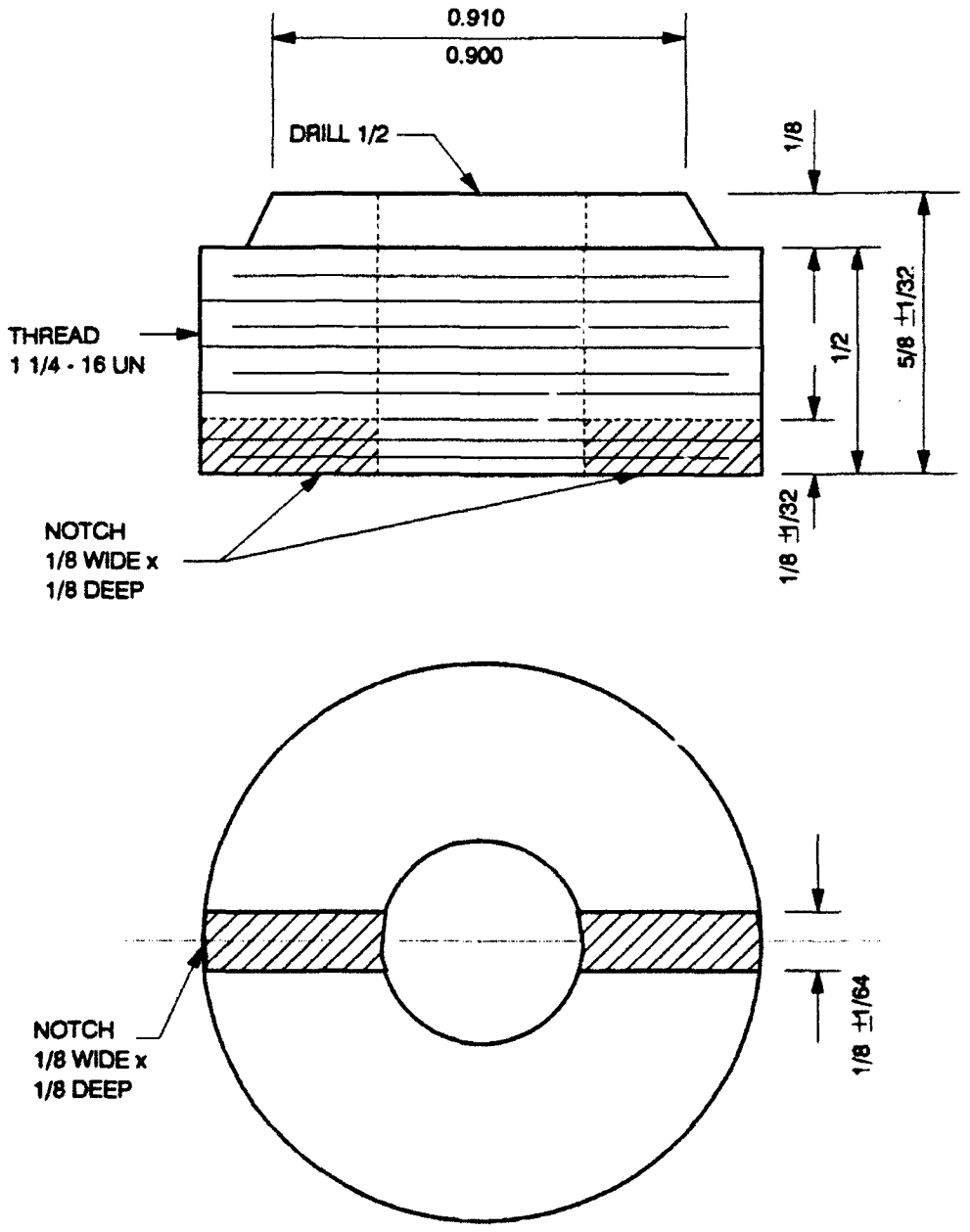

Figure 60. Machine drawing of the MCBI gage column support plug

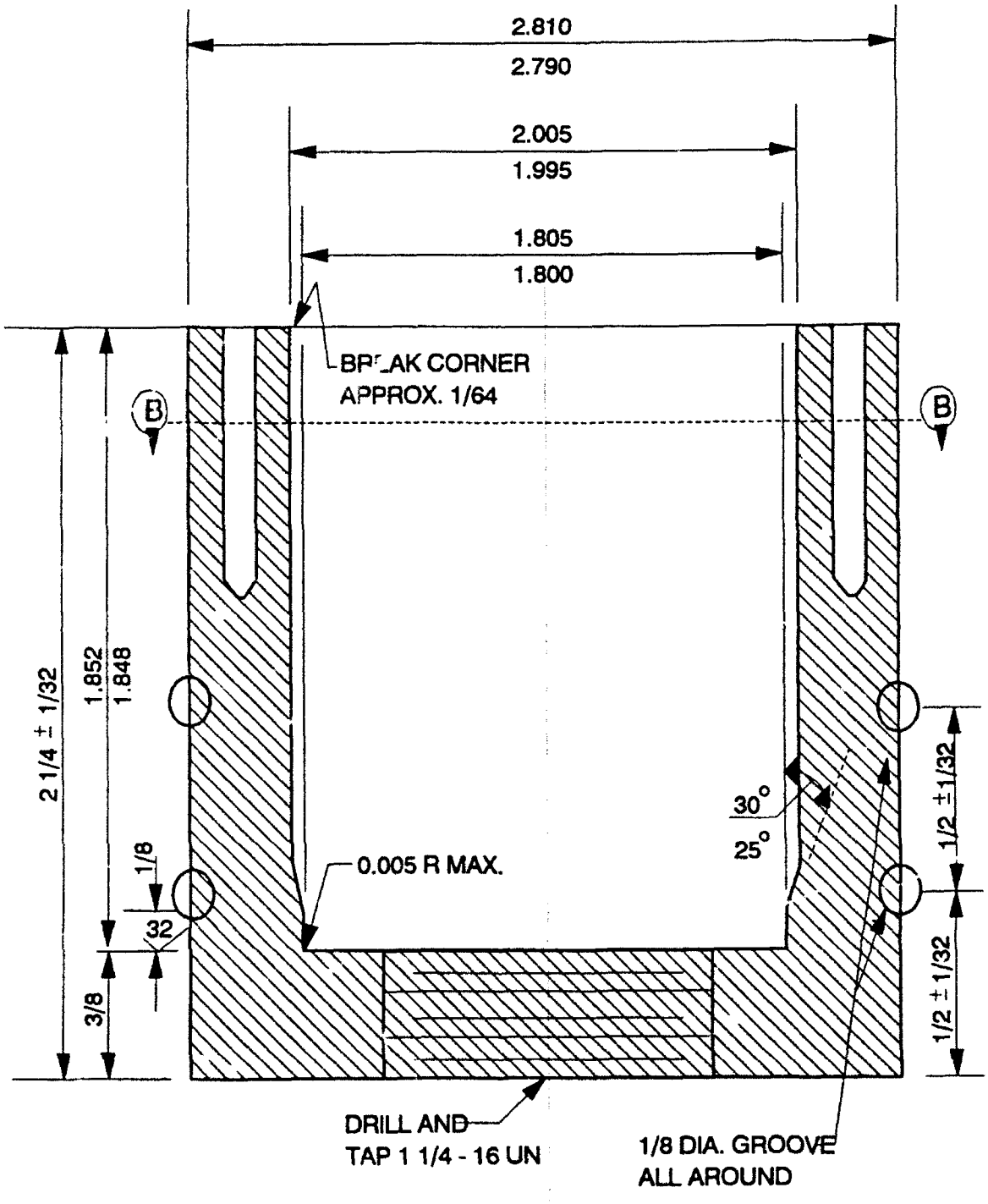

Figure 61. Machine cross-section of the MCBI gage mount

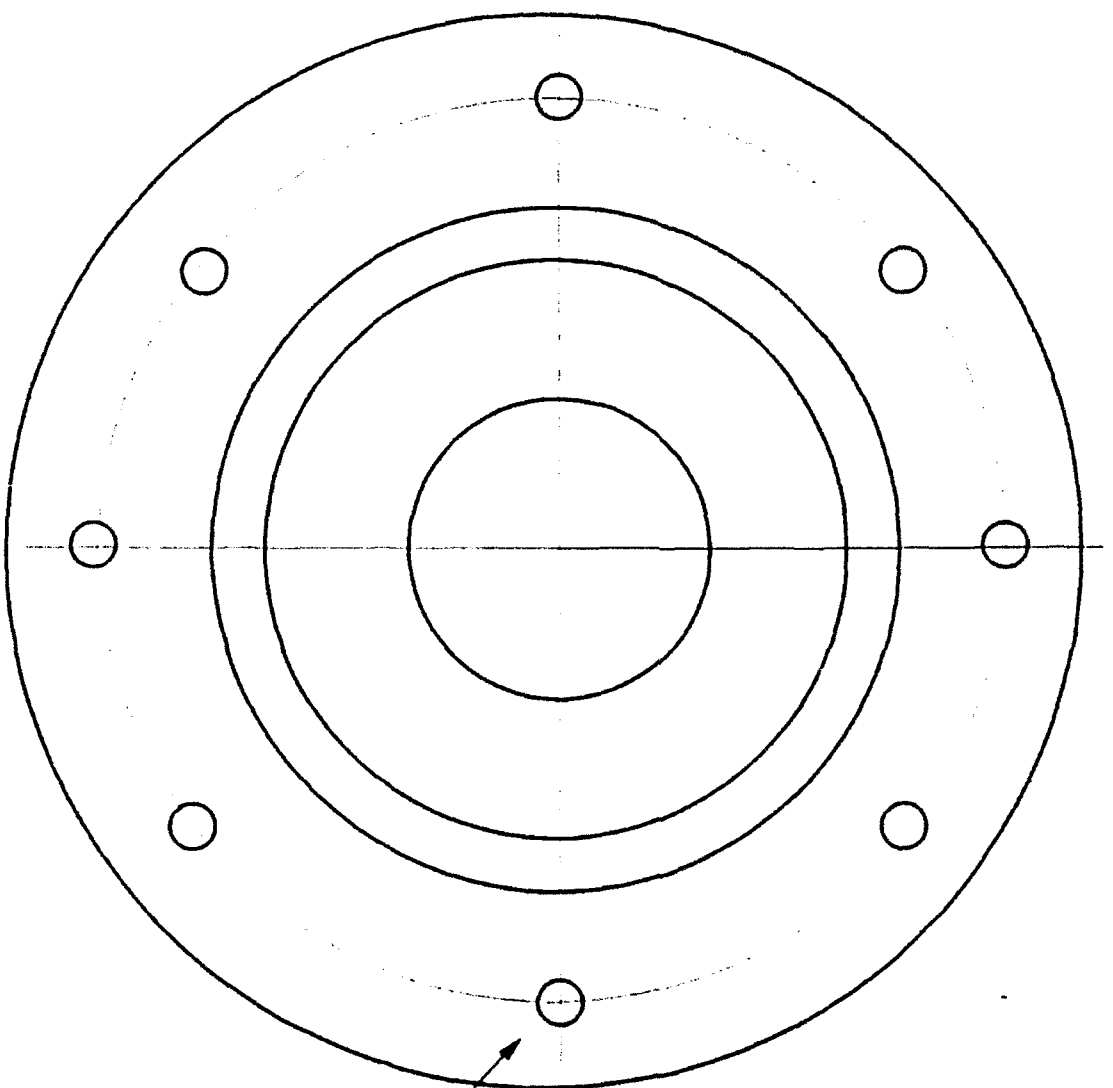

Figure 62. Top view of the MCBI gage mount

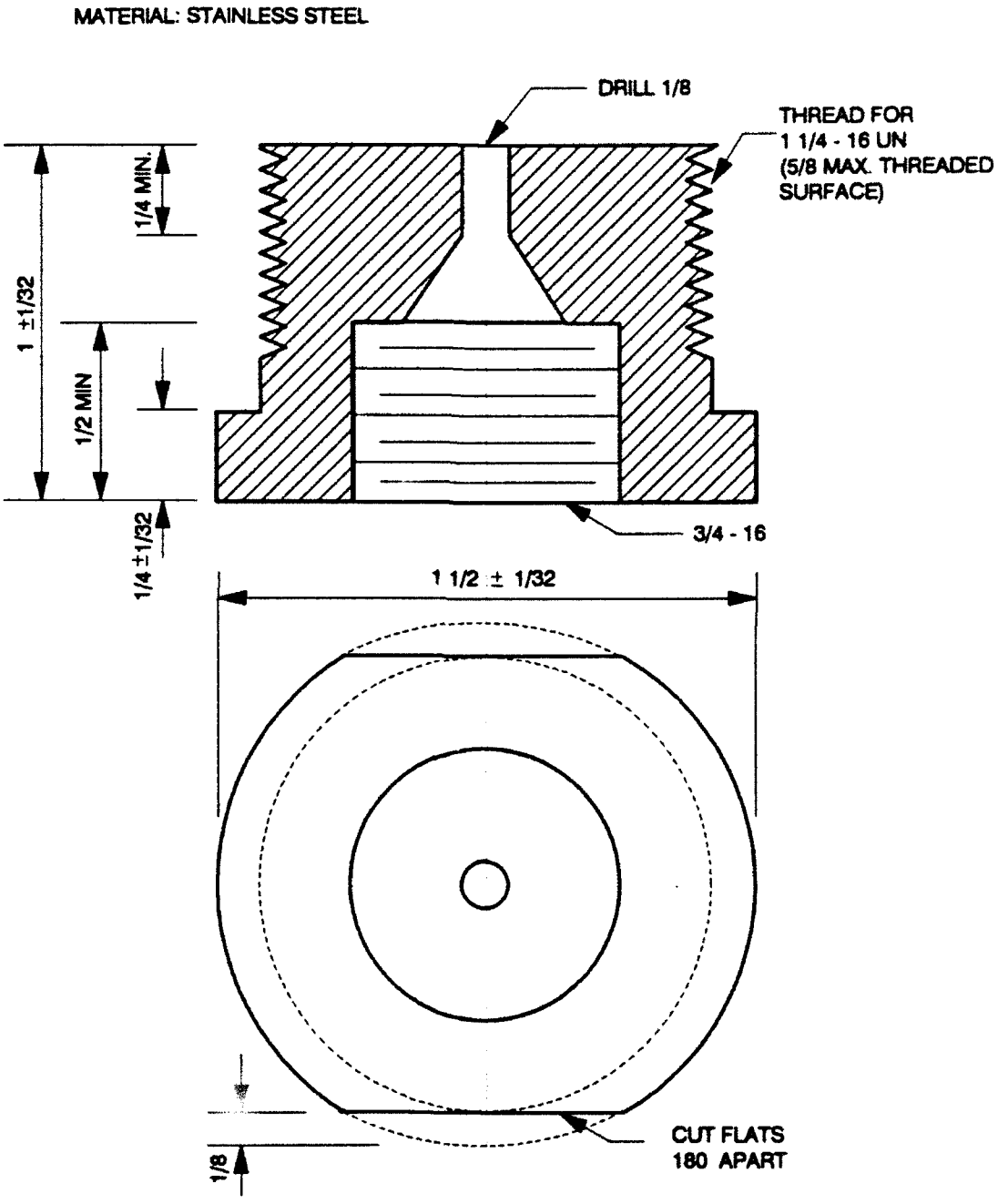

Figure 63. Machine drawing of the tubing adapter used with the MCBI gage mount

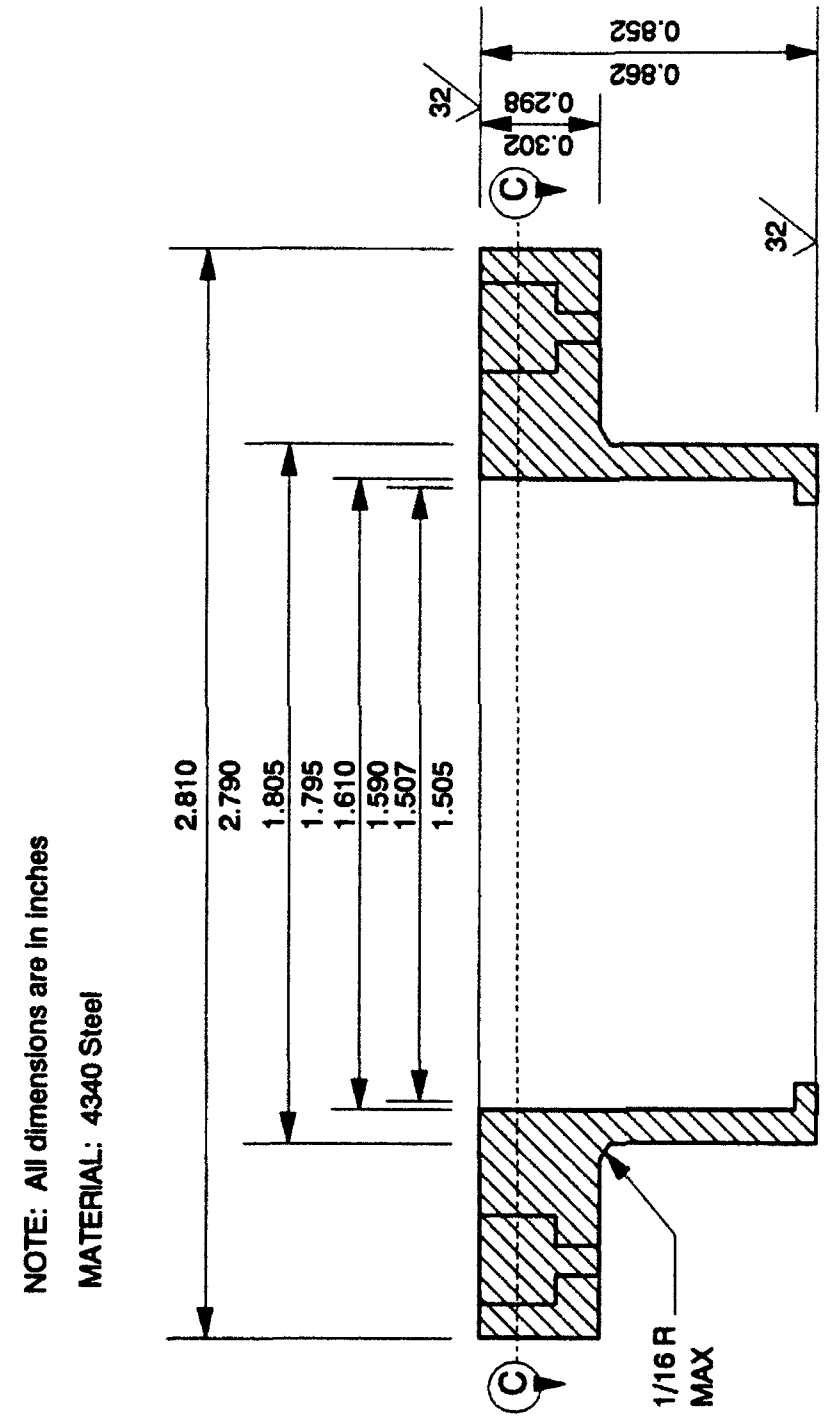

Figure 64. Machine drawing of the MCBI gage clamping ring

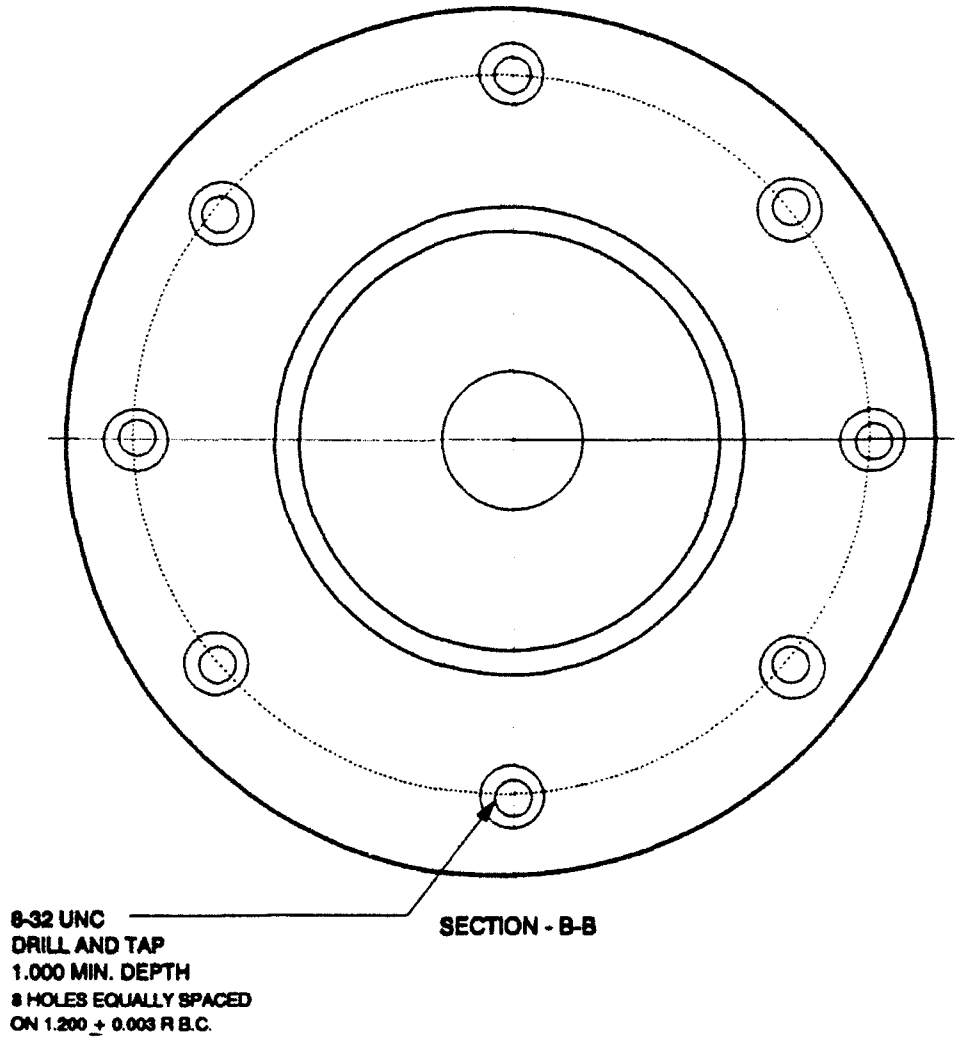

Figure 65. Top view of MCBI gage clamping ring

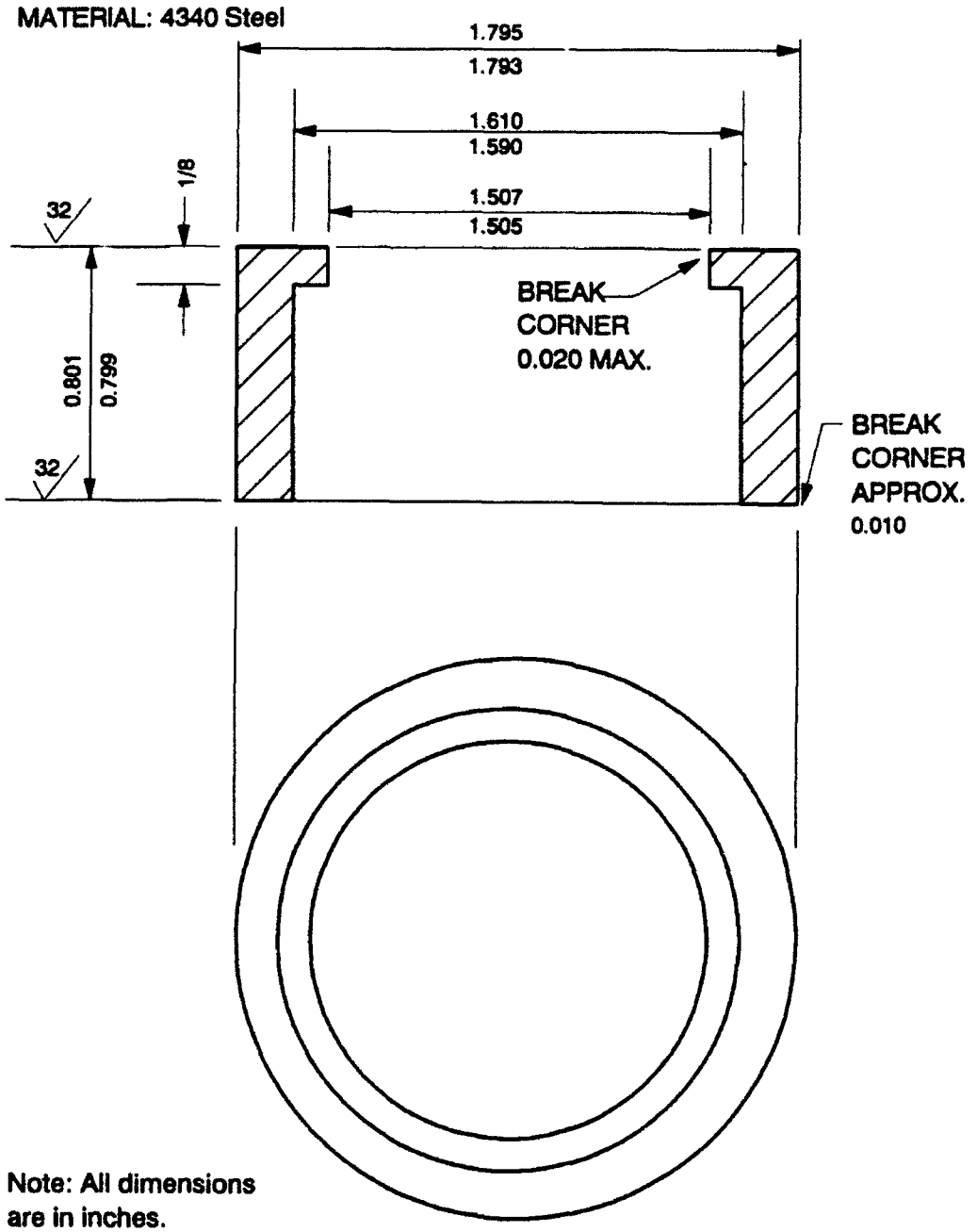

Figure 66. Machine drawing of MCBI gage lateral isolation ring

MATERIAL: Any available hard steel
NOTE: All dimensions are in inches

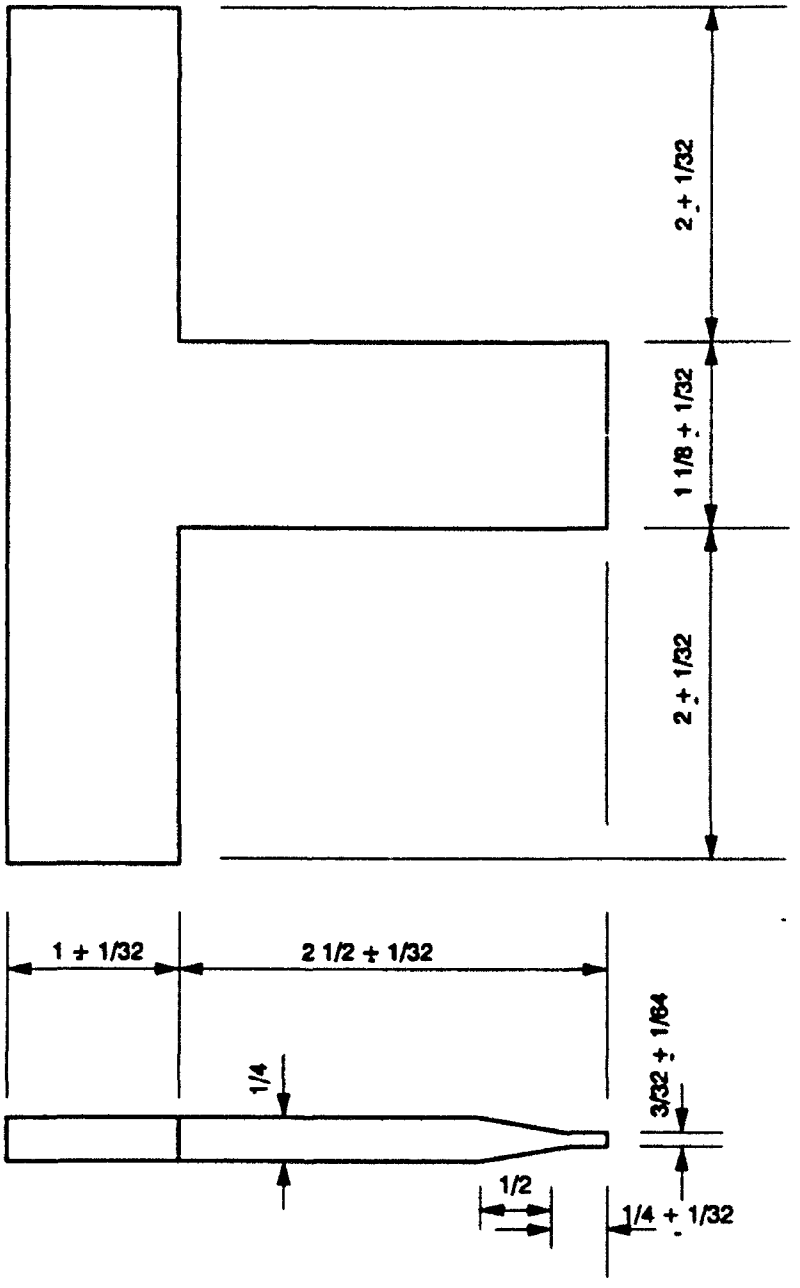

Figure 67. Machine drawing of MCBI gage assembly tool

APPENDIX B

MCBI TEST 1 DATA WAVE FORMS

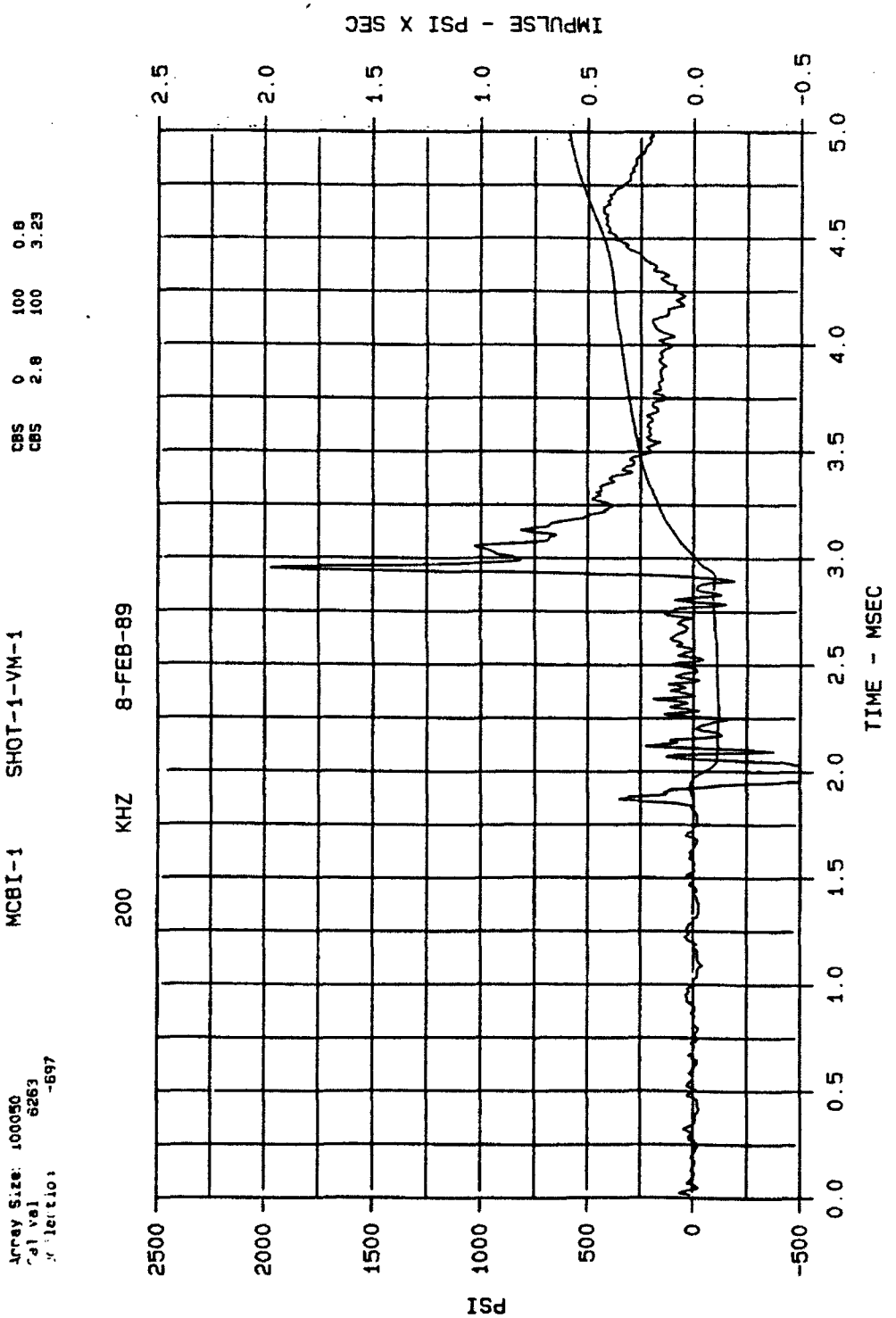

Figure 68. Interface stress wave form measured by gage VM-1, 5 msec duration, MCBI Gage Validation Test 1

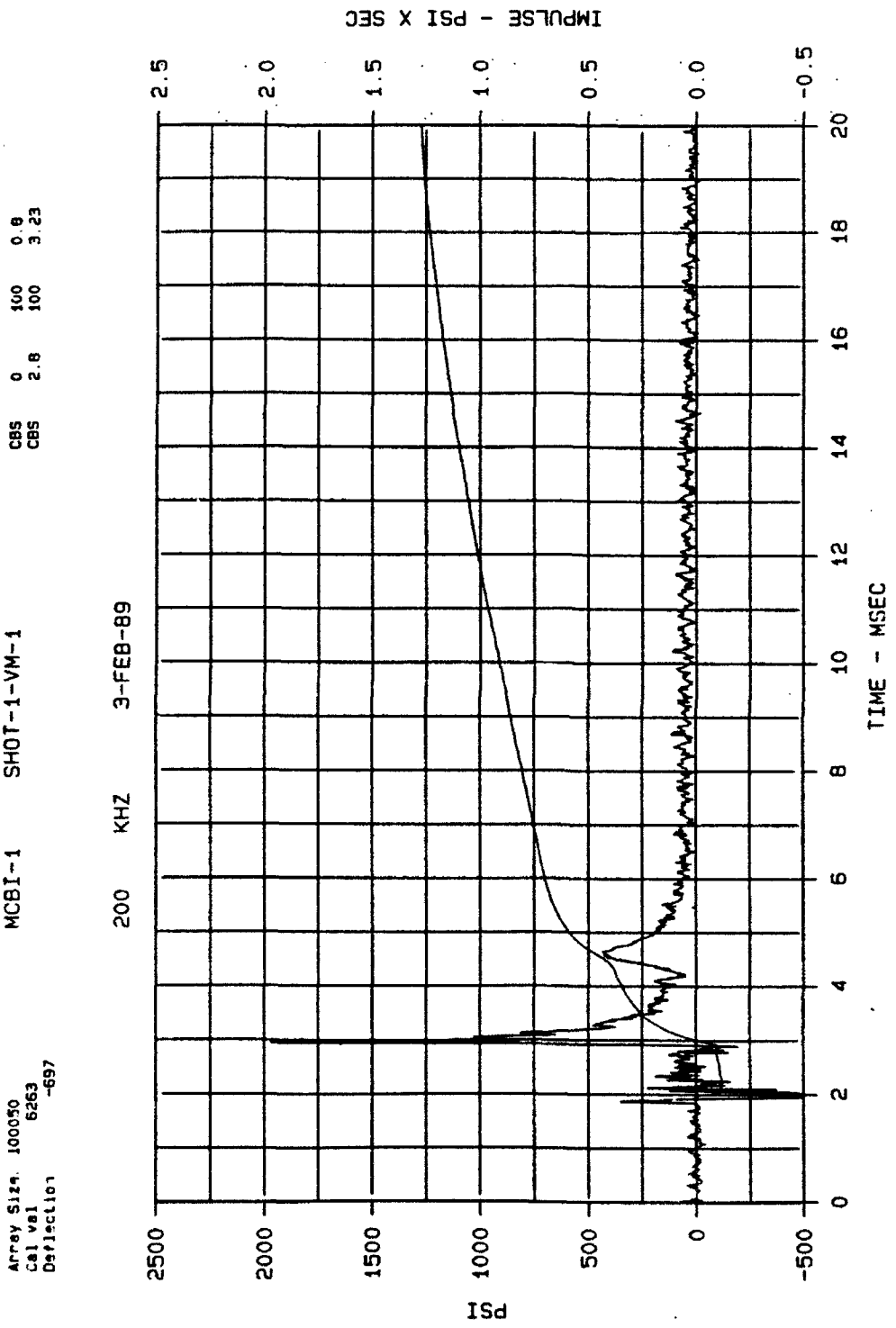

Figure 69. Interface stress wave form measured by gage VM-1, 20 msec duration, MCBI Gage Validation Test 1

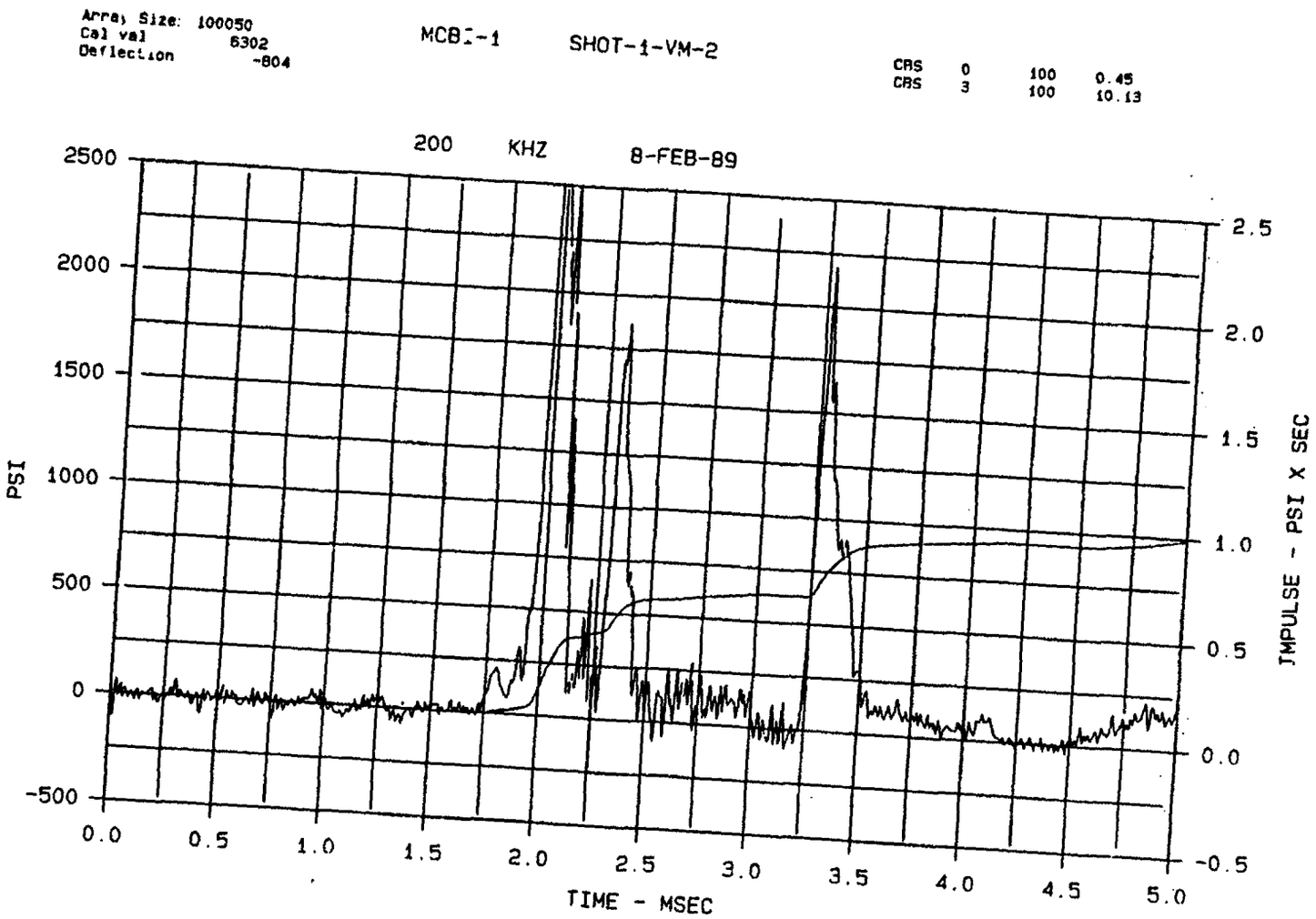

Figure 70. Interface stress wave form measured by gage VM-2, 5 msec duration, MCBI Gage Validation Test 1

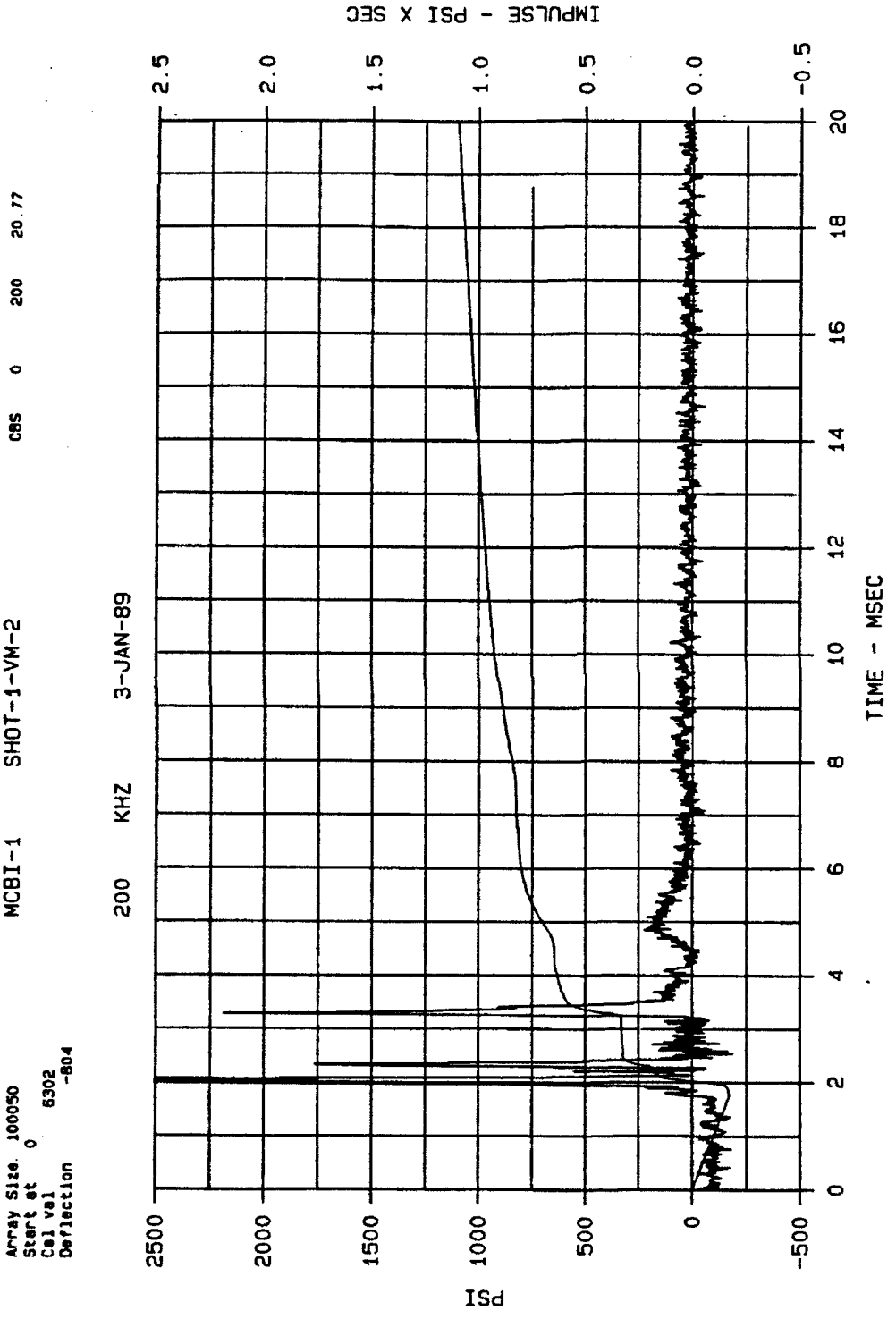

Figure 71. Interface stress wave form measured by gage VM-2, 20 msec duration, MCBI Gage Validation Test 1

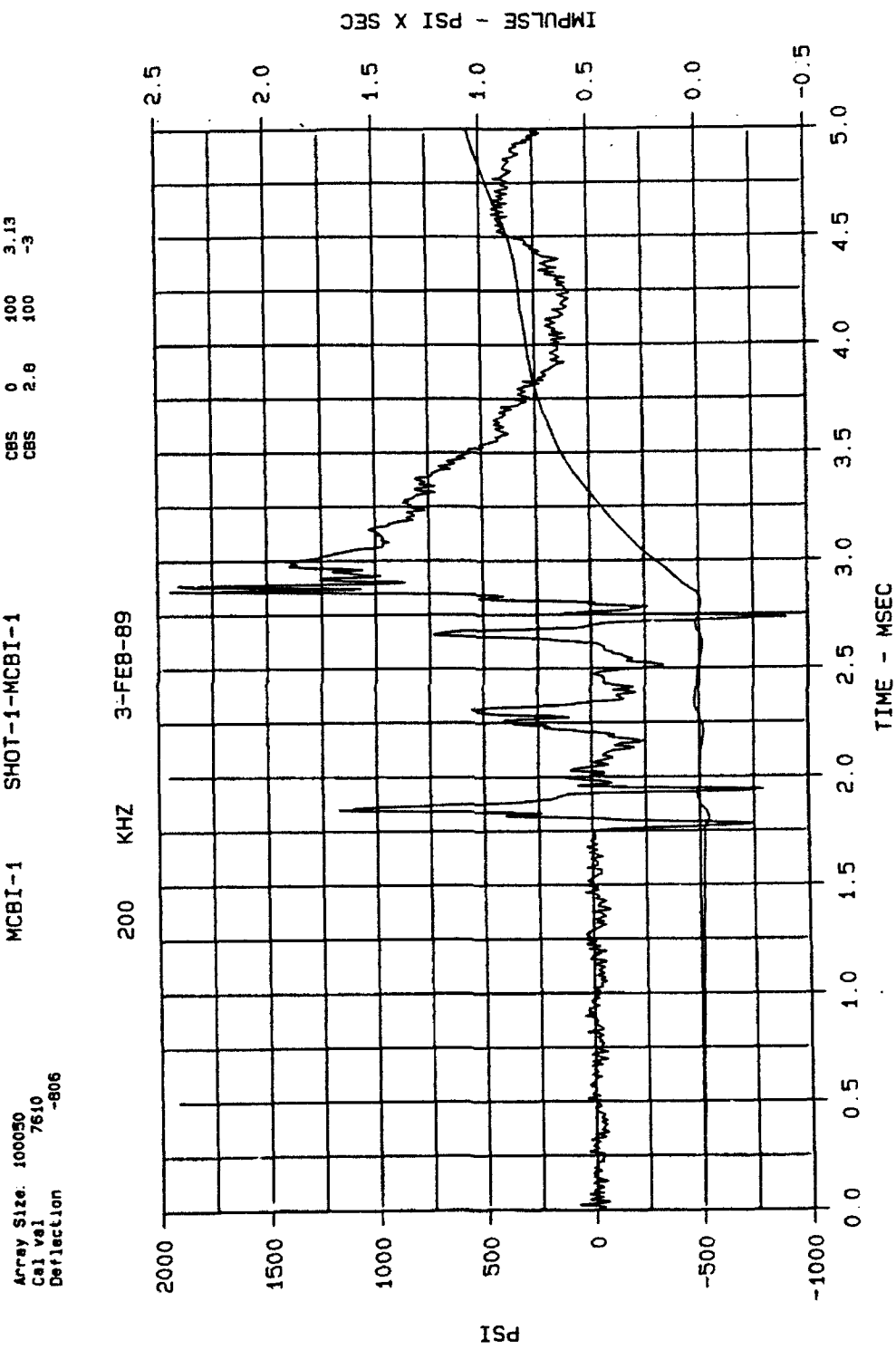

Figure 72. Interface stress wave form measured by gage MCBI-1, 5 msec duration, MCBI Gage Validation Test 1

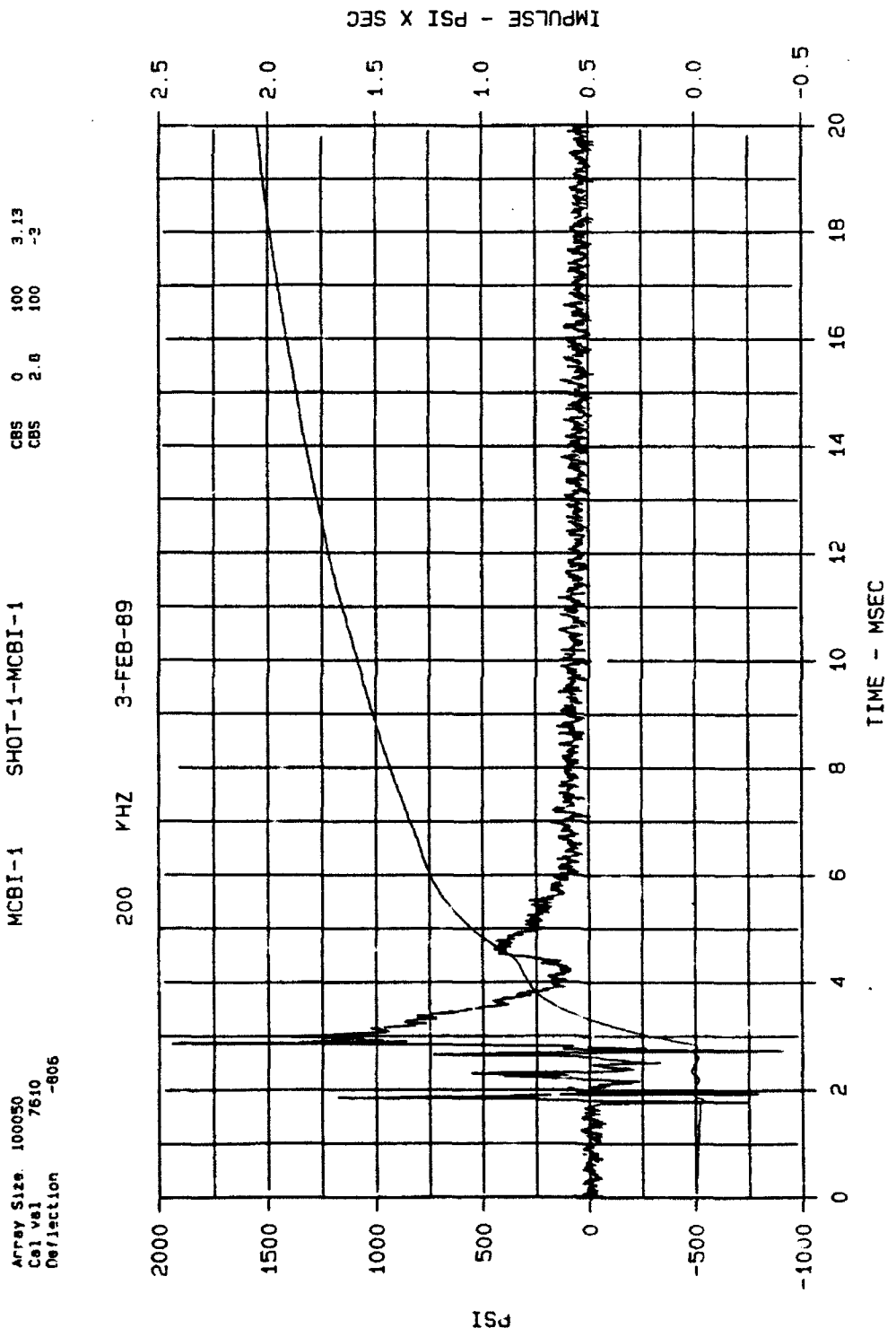

Figure 73. Interface stress wave form measured by gage MCBI-1, 20 msec duration, MCBI Gage Validation Test 1

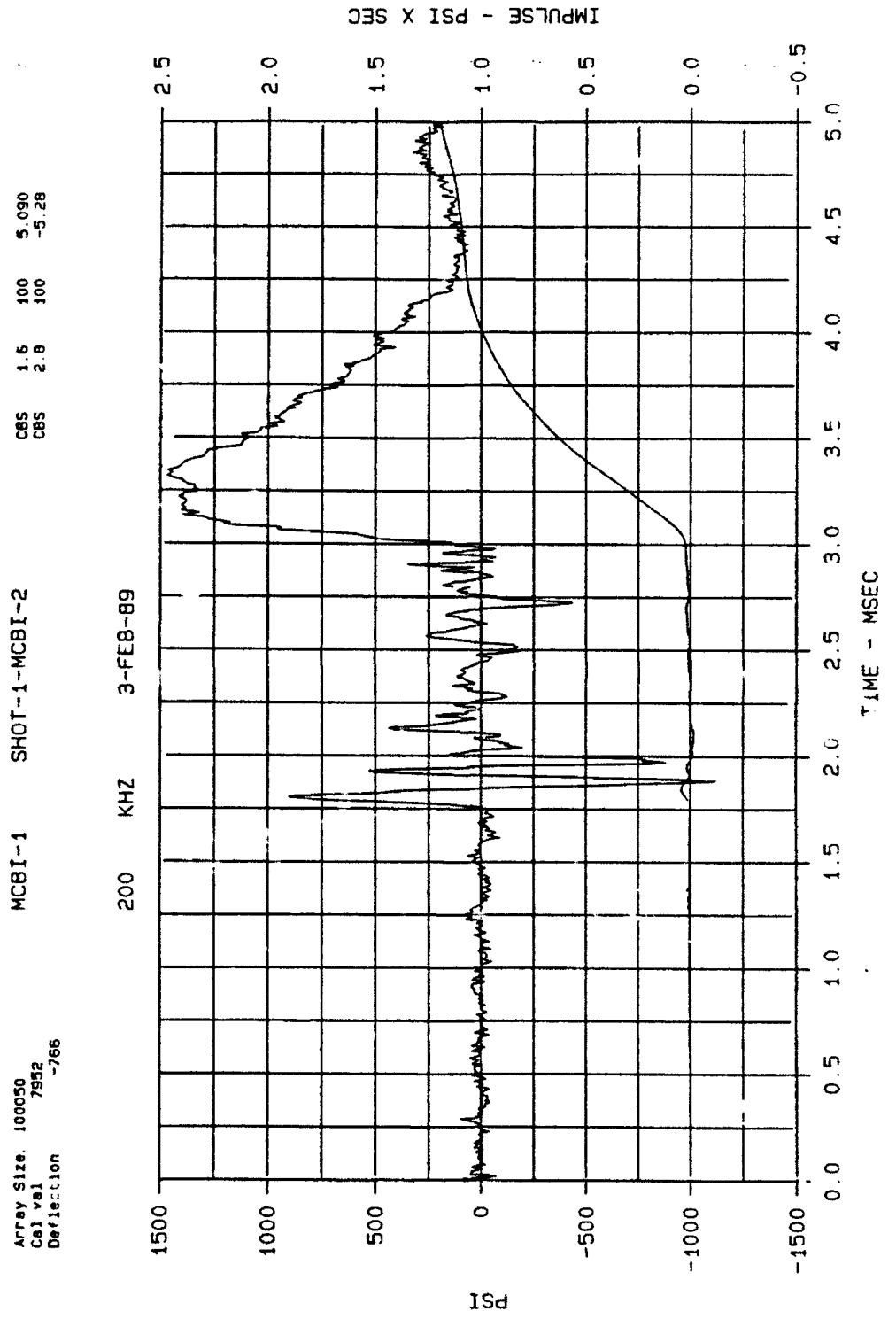

Figure 74. Interface stress wave form measured by Gage MCBI-2, 5 msec duration, MCBI Gage Validation Test 1

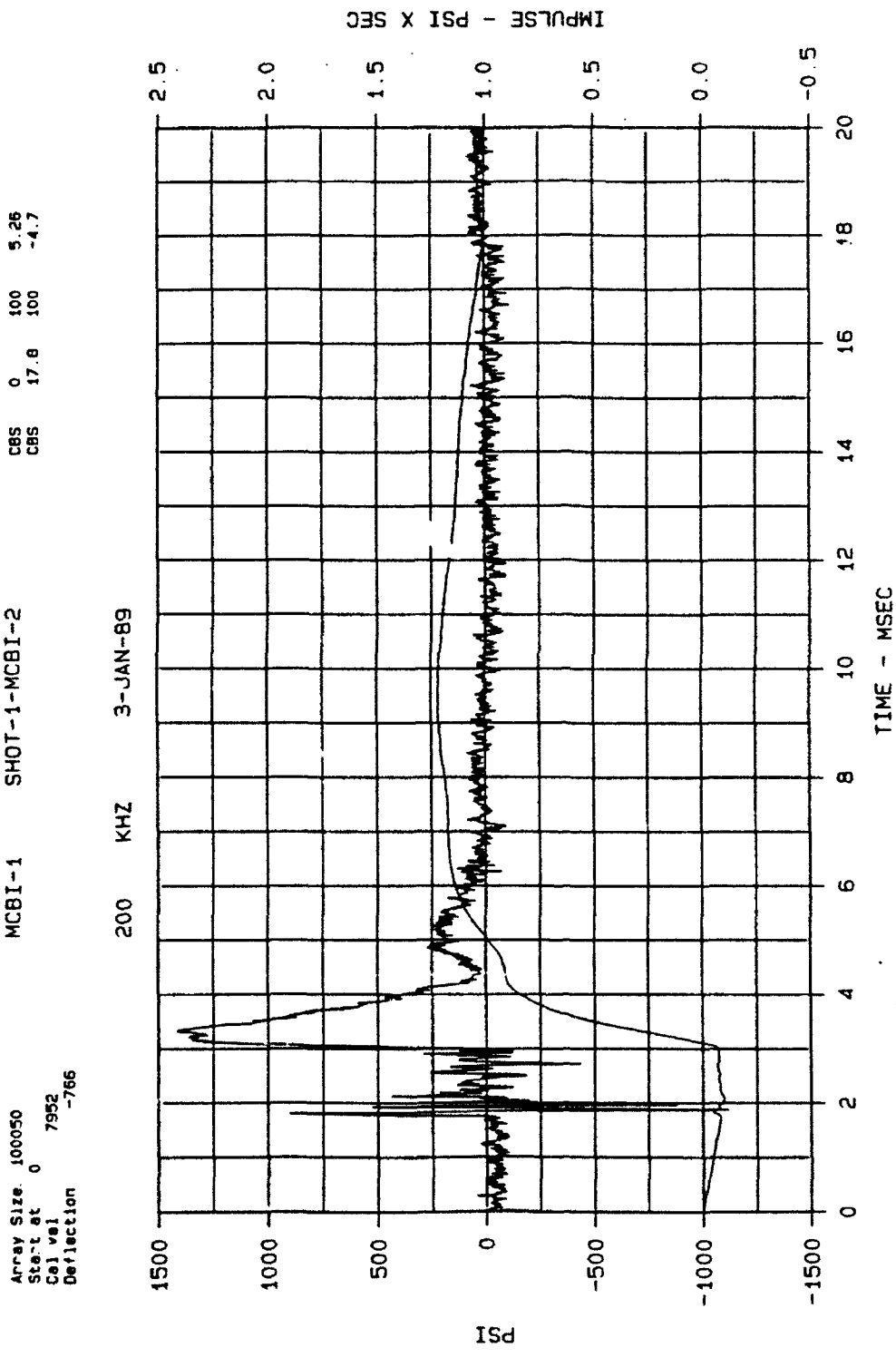

Figure 75. Interface stress wave form measured by gage MCBI-2, 20 msec duration, MCBI Gage Validation Test 1

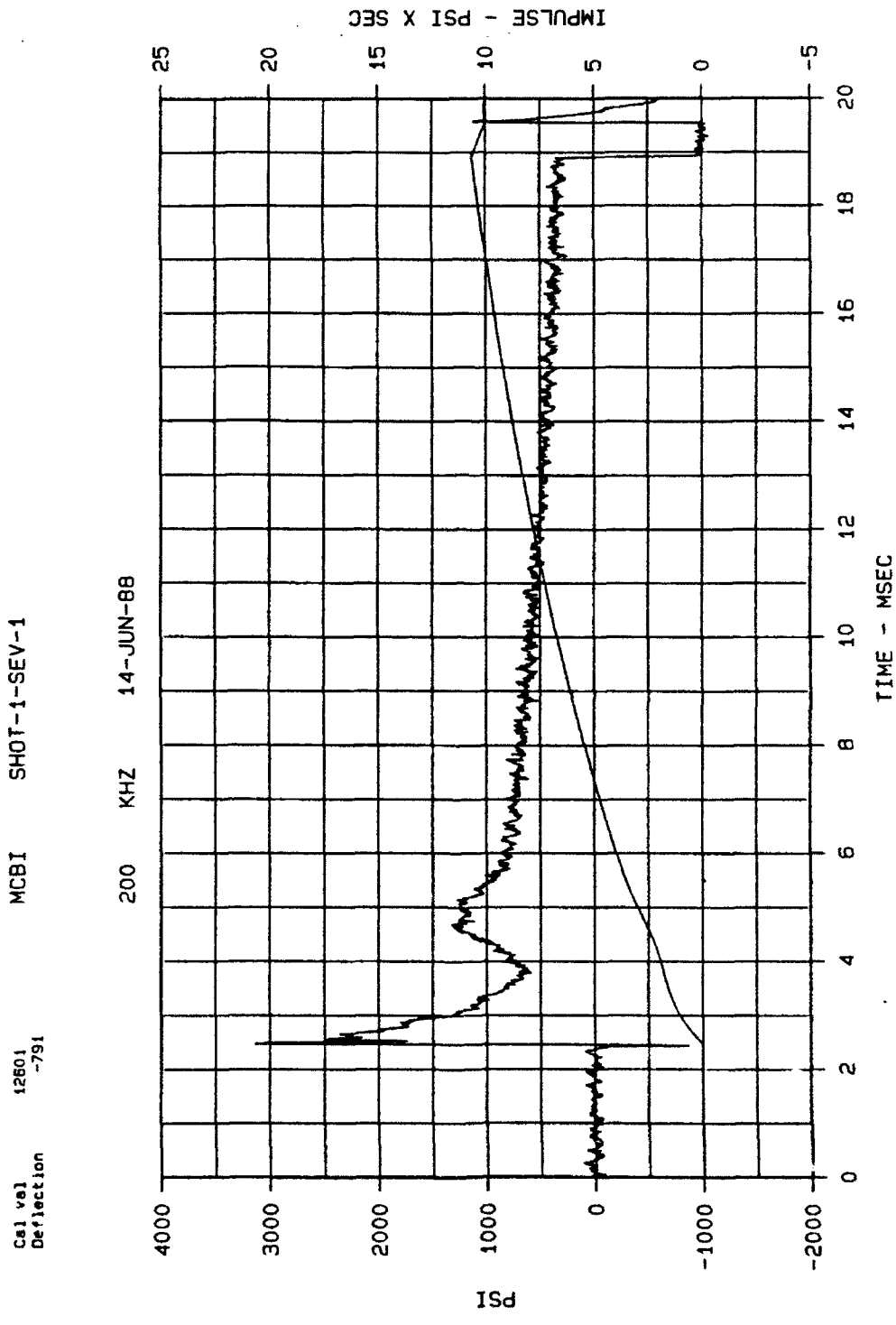

Figure 76. Soil stress wave form measured by gage SEV-1, 20 msec duration, MCBI Gage Validation Test 1

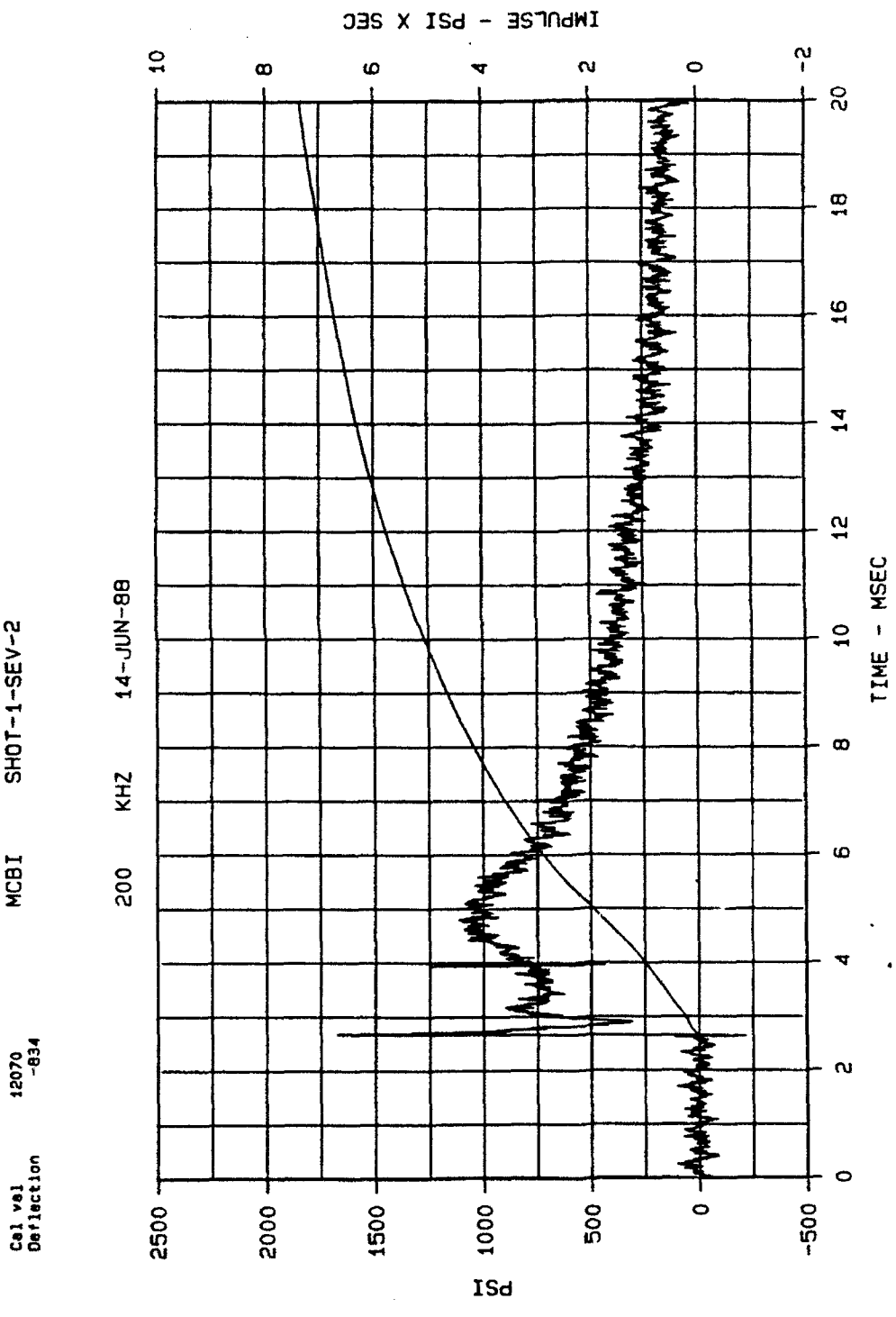

Figure 77. Soil stress wave form measured by gage SEV-2, 20 msec duration, MCBI Gage Validation Test 1

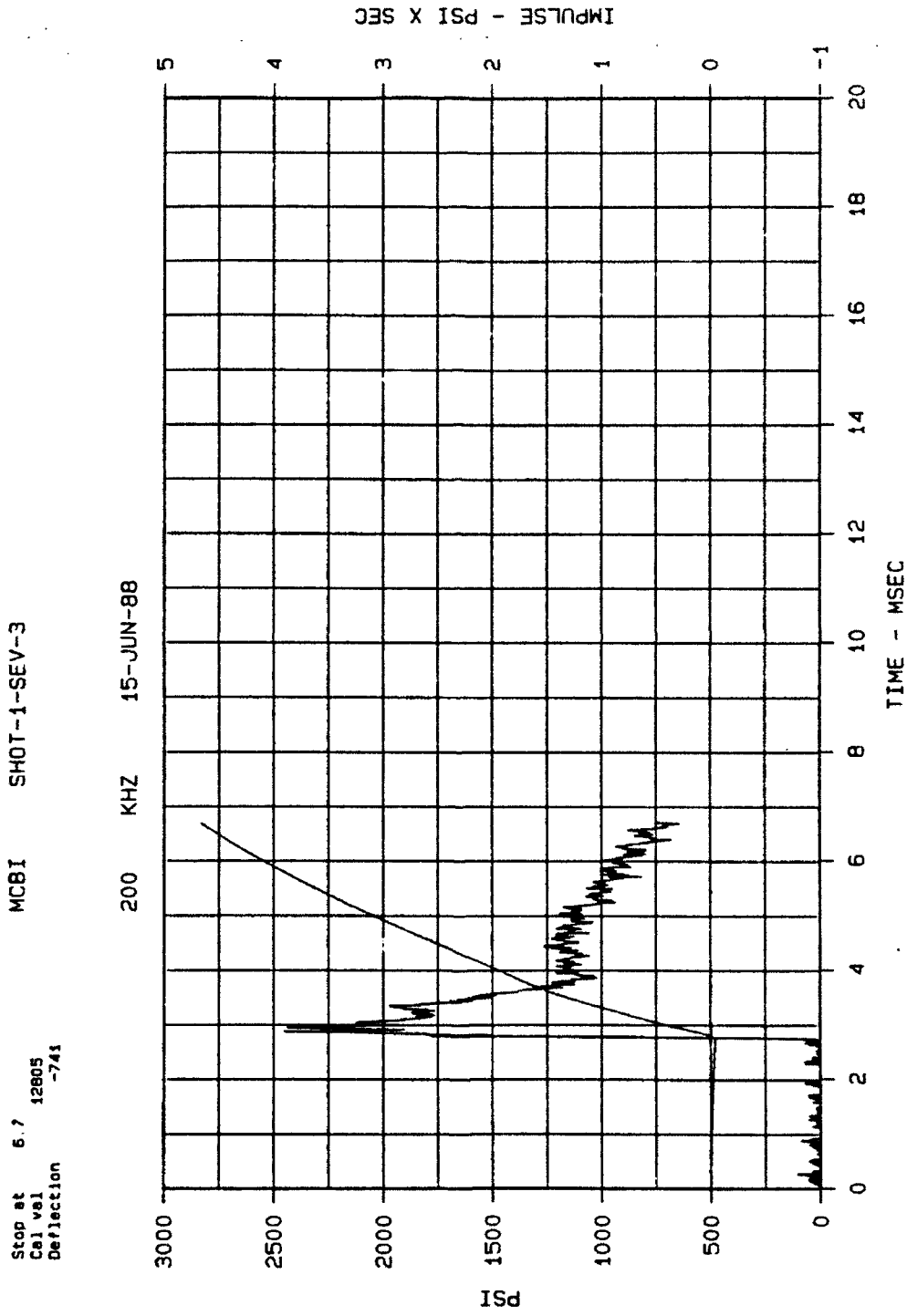

Figure 78. Soil stress wave form measured by gage SEV-3, 20 msec duration, MCBI Gage Validation Test 1

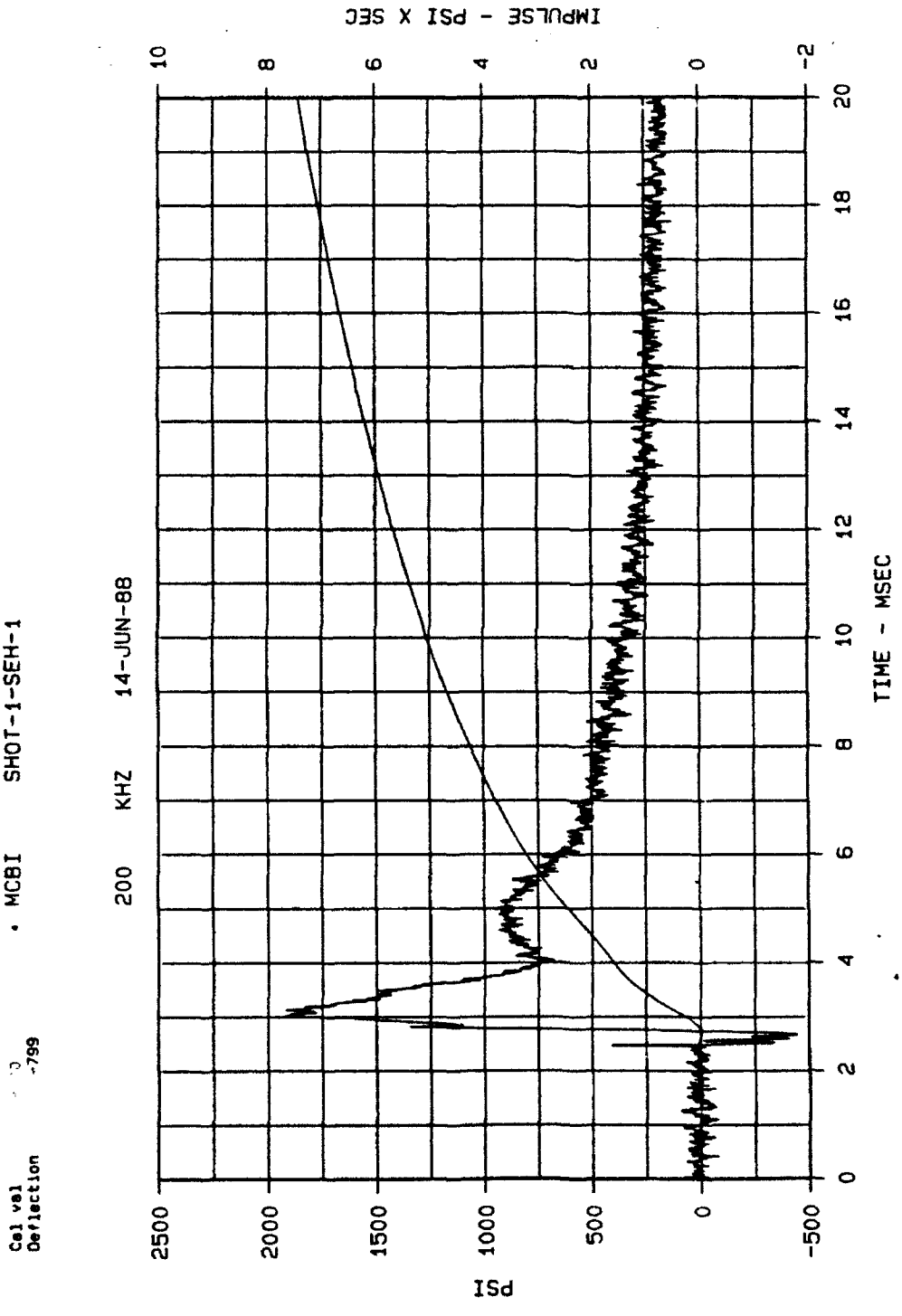

Figure 79. Soil stress wave form measured by gage SEH-1, 20 msec duration, MCBI Gage Validation Test 1

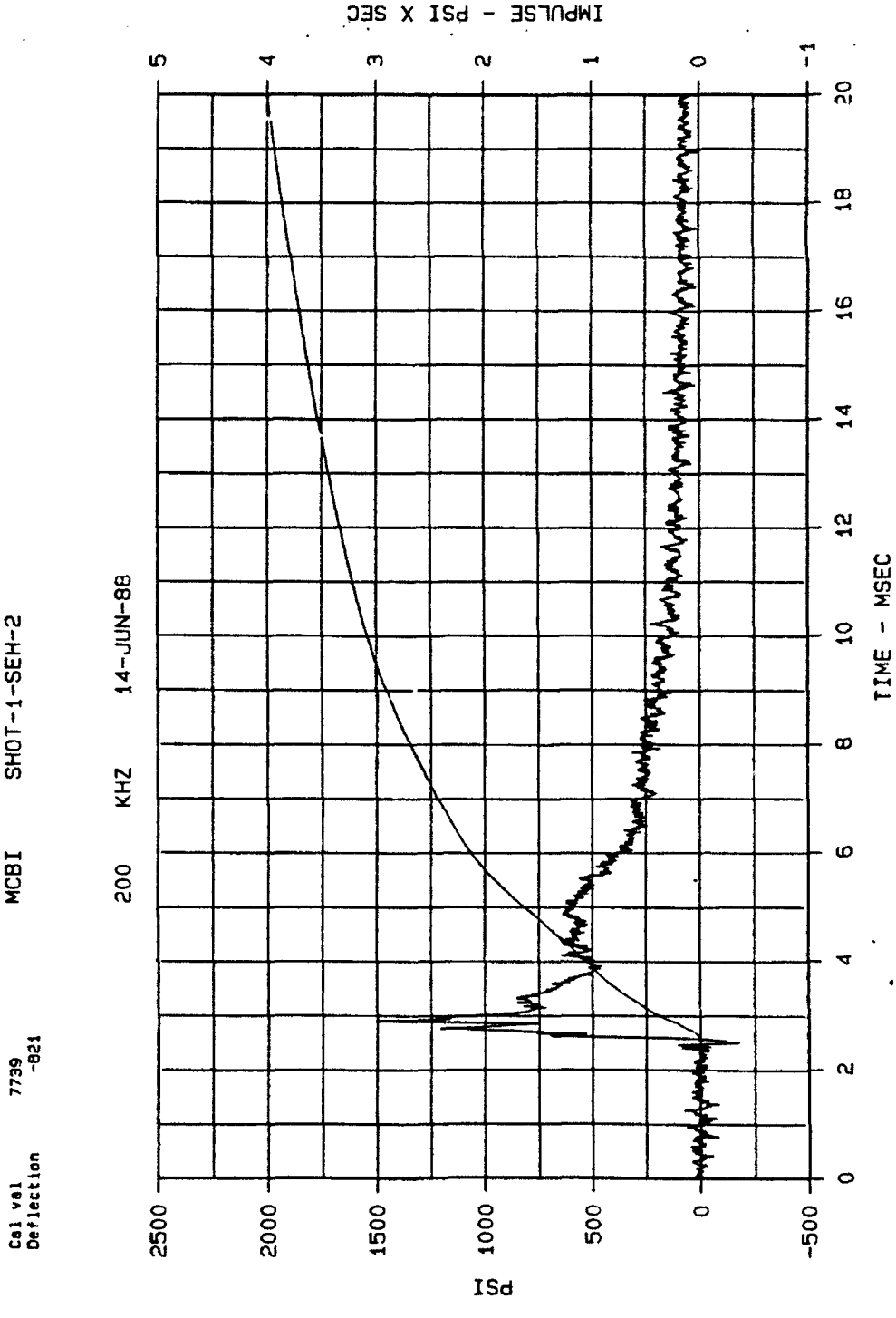

Figure 80. Soil stress wave form measured by gage SEH-2, 20 msec duration, MCBI Gage Validation Test 1

APPENDIX C

MCBI TEST 2 DATA WAVE FORMS

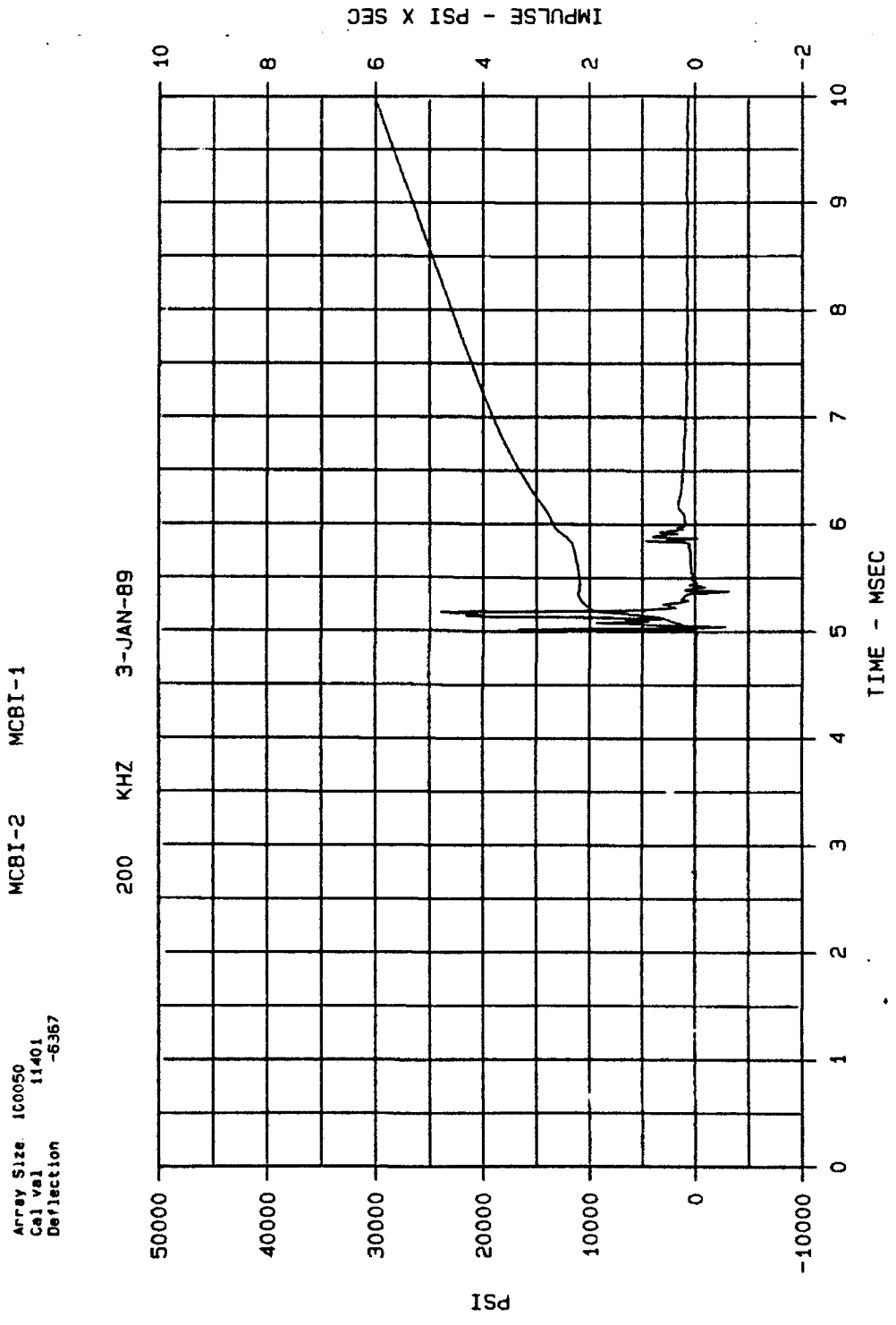

Figure 81. Interface stress wave form measured by gage MCBI-1, 10 msec duration, MCBI Gage Validation Test 2

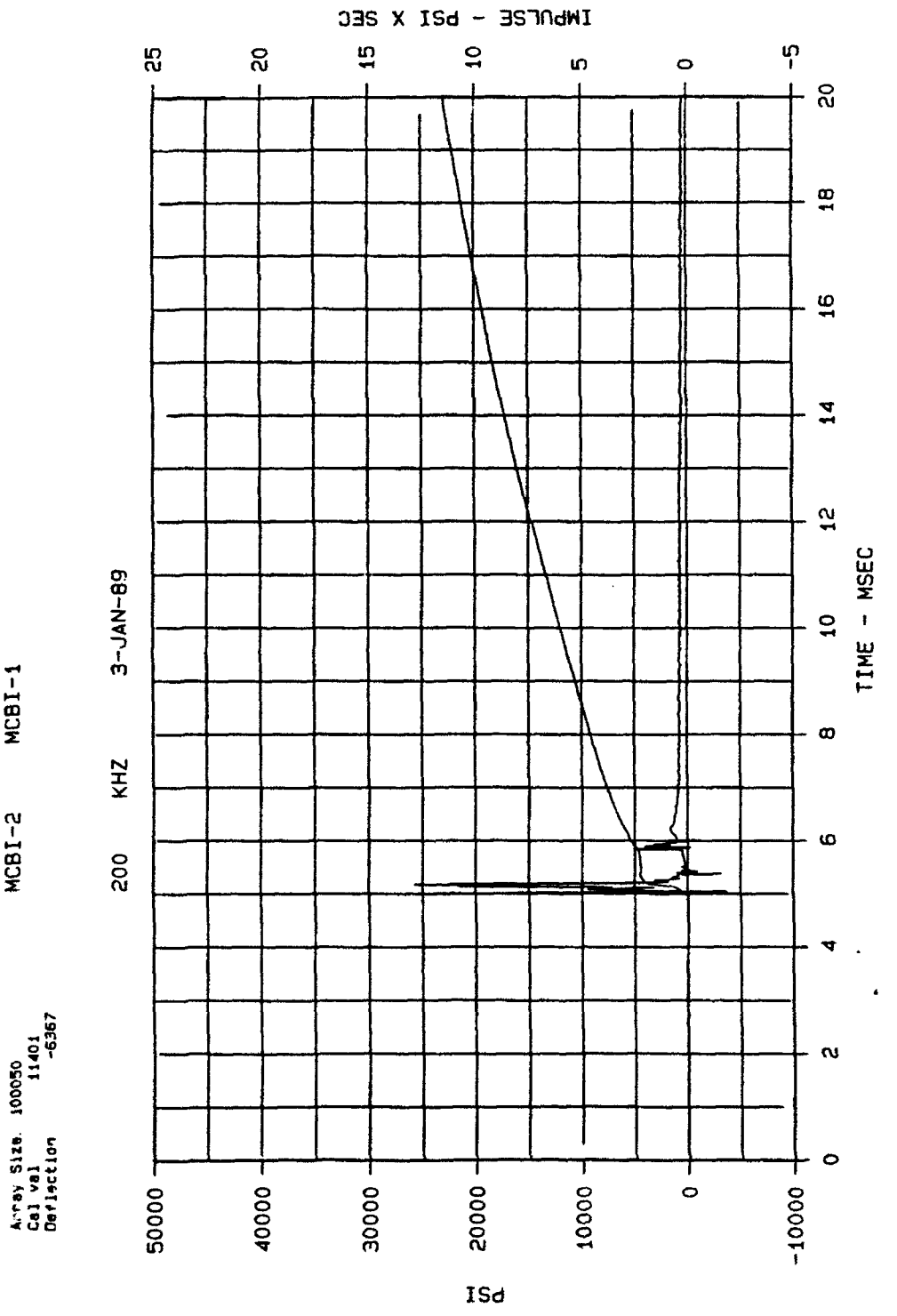

Figure 82. Interface stress wave form measured by gage MCBI-1, 20 msec duration, MCBI Gage Validation Test 2

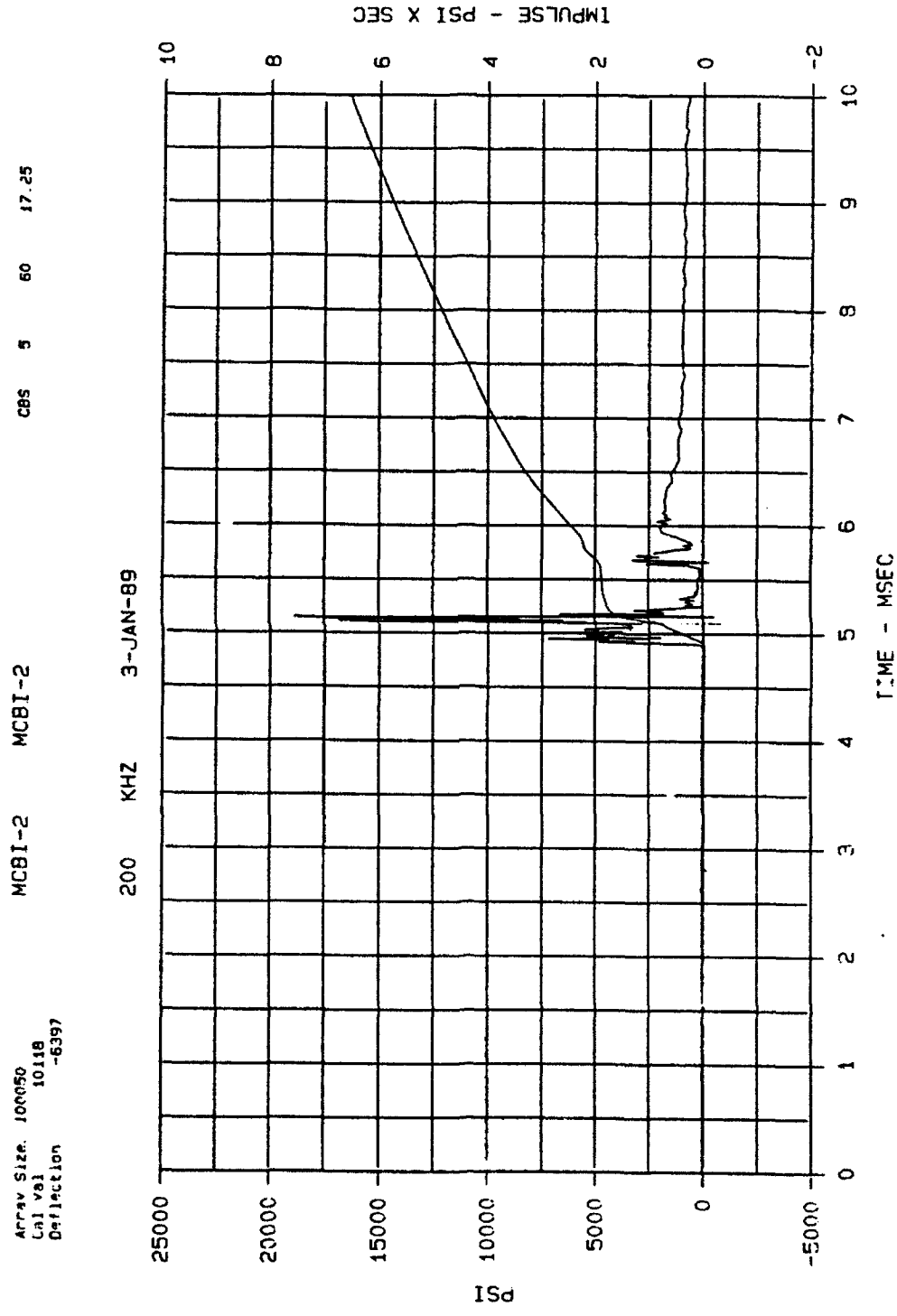

Figure 83. Interface stress wave form measured by gage MCBI-2, 10 msec duration, MCBI Gage Validation Test 2

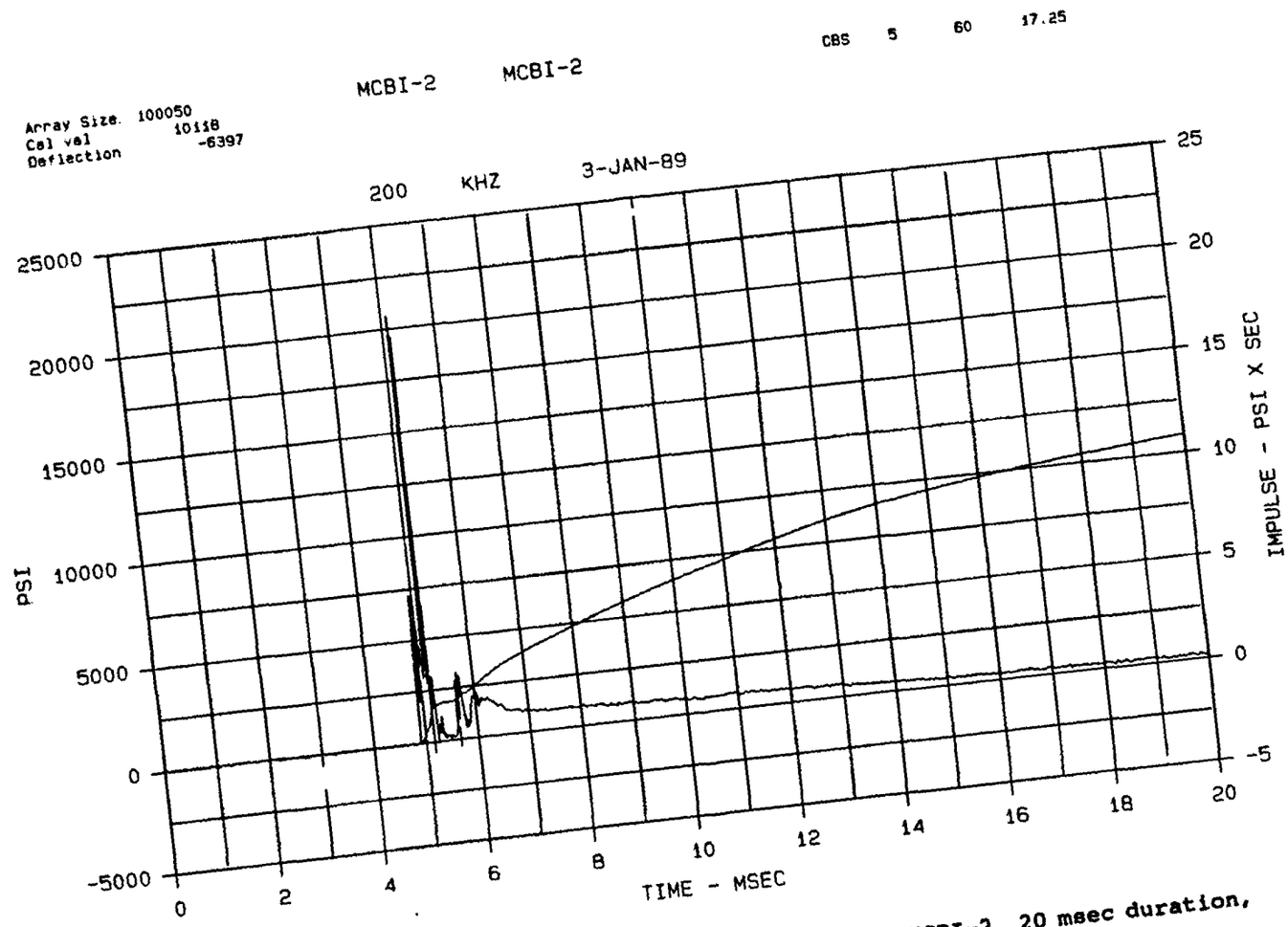

Figure 84. Interface stress wave form measured by gage MCBI-2, 20 msec duration, MCBI Gage Validation Test 2

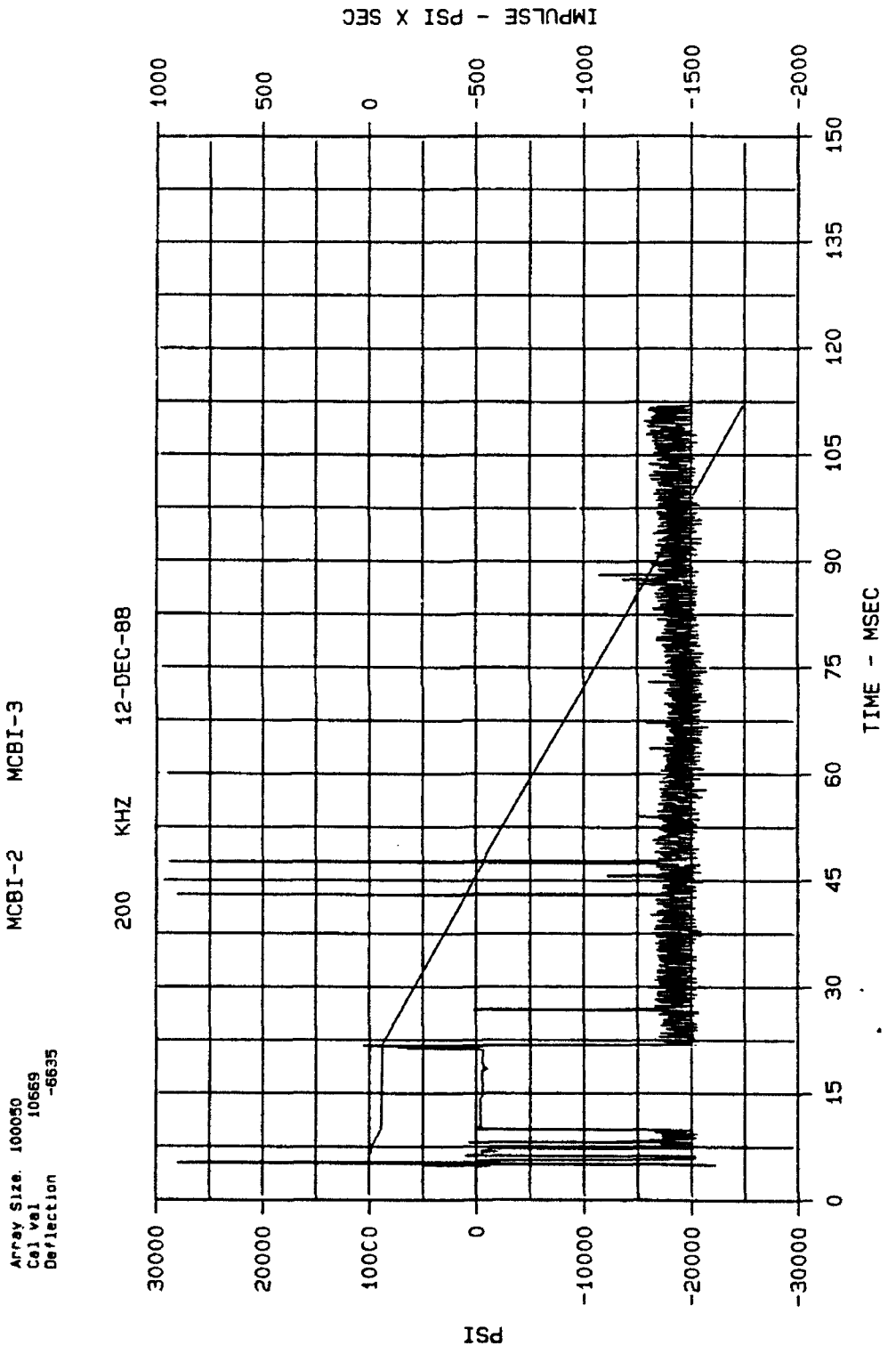

Figure 85. Interface stress wave form measured by gage MCBI-3, 150 msec duration, MCBI Gage Validation Test 2

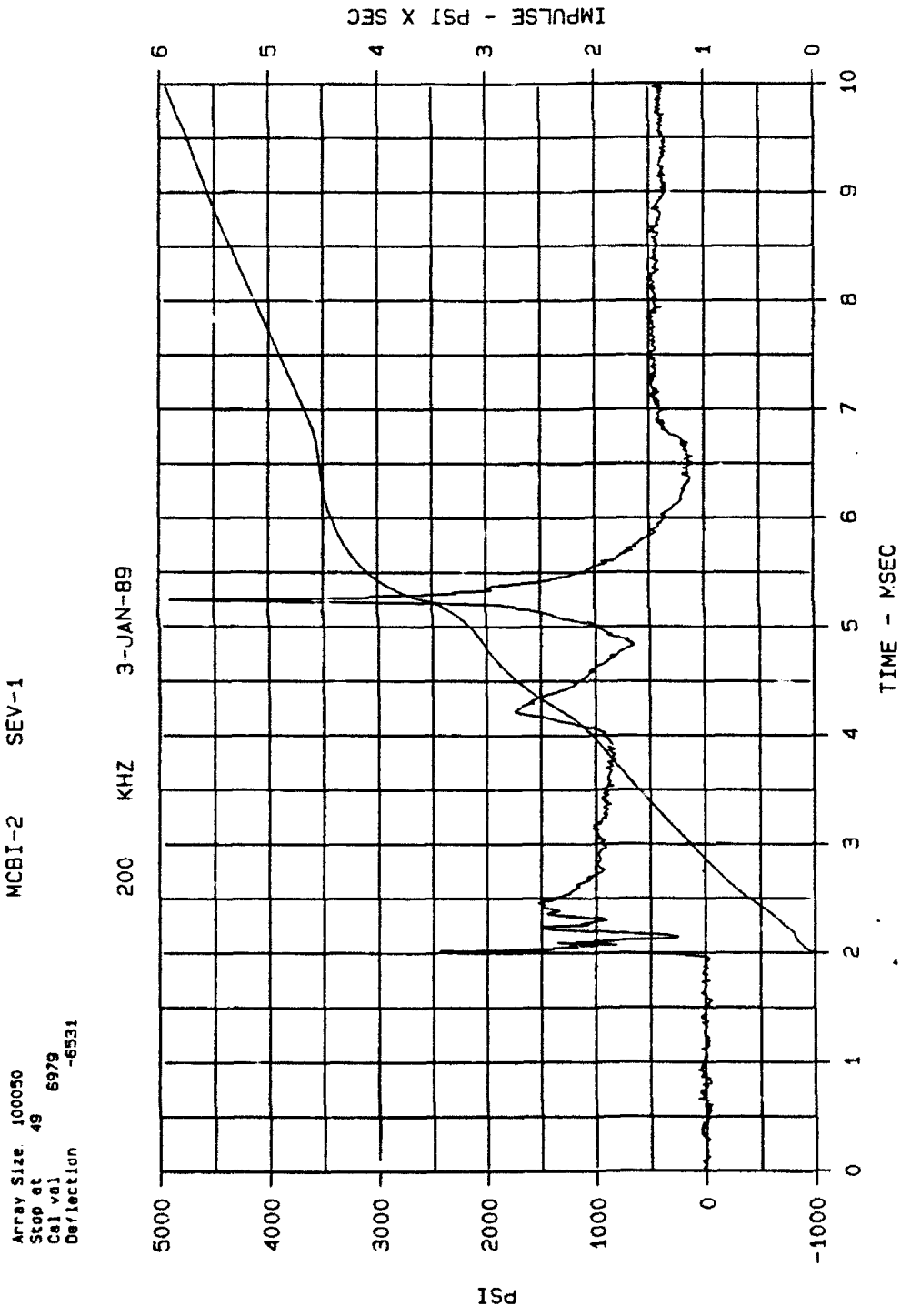

Figure 86. Soil stress wave form measured by gage SEV-1, 10 msec duration, MCBI Gage Validation Test 2

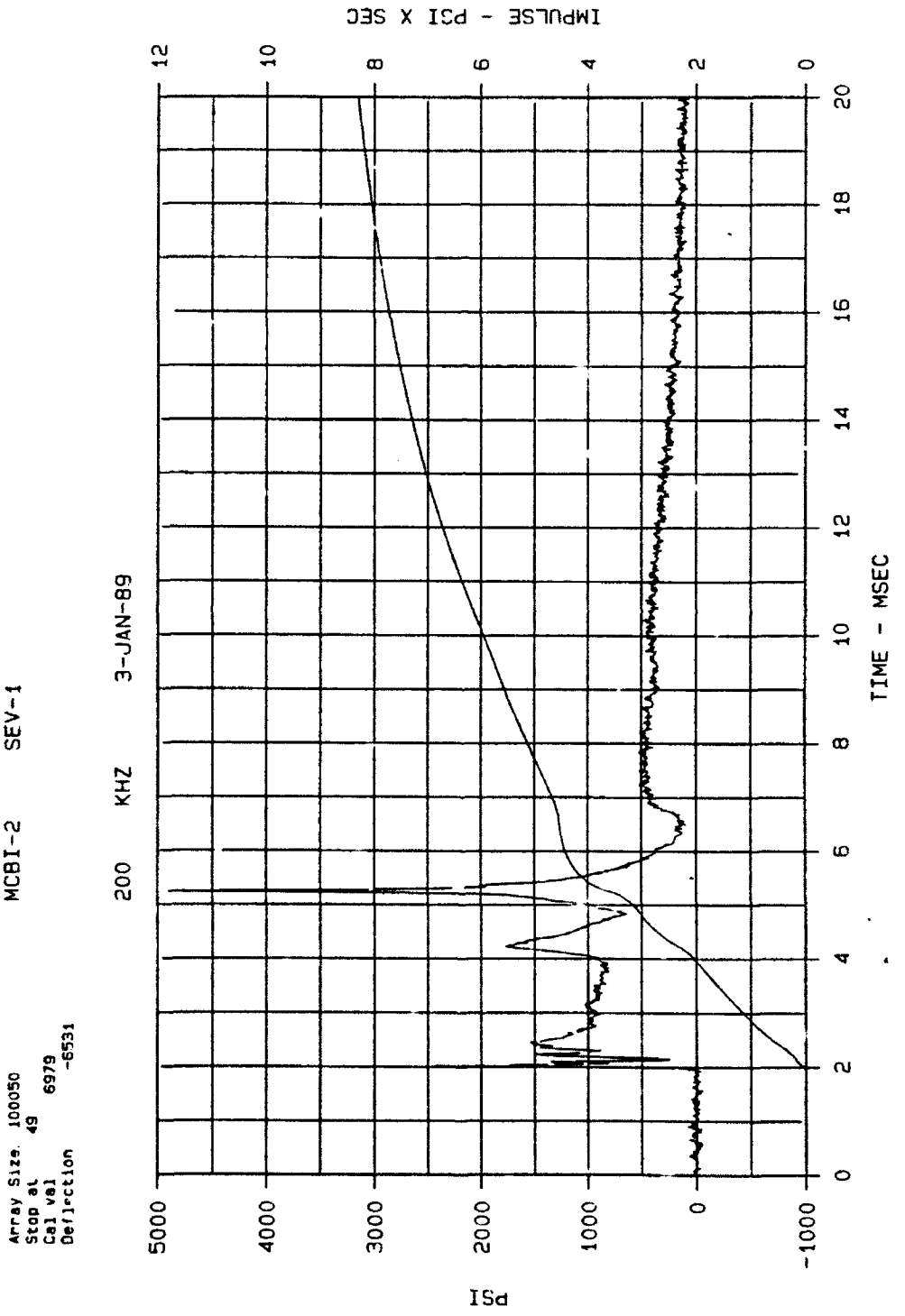

Figure 87. Soil stress wave form measured by gage SEV-1, 20 msec duration, MCBI Gage Validation Test 2

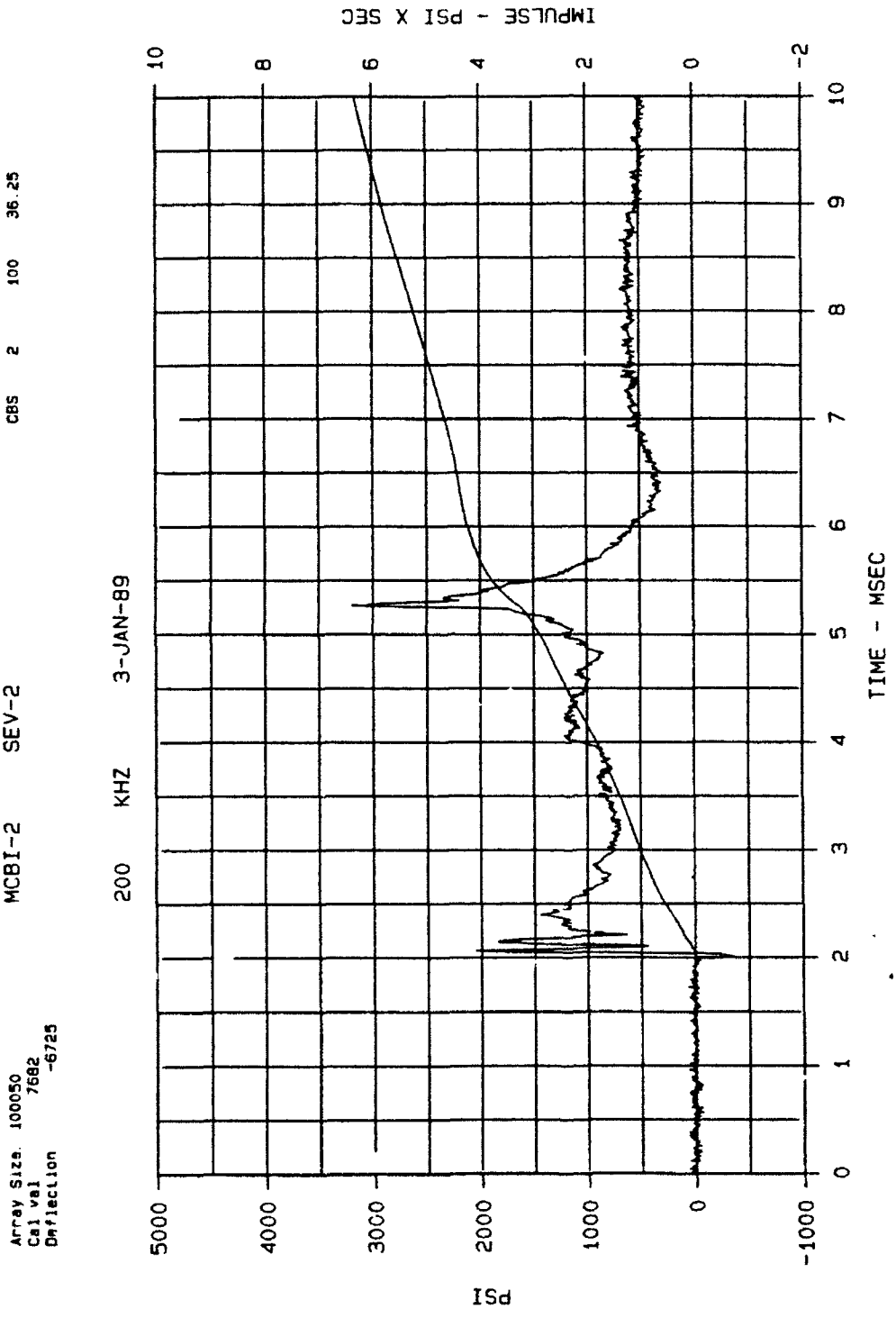

Figure 88. Soil stress wave form measured by gage SEV-2, 10 msec duration, MCBI Gage Validation Test 2

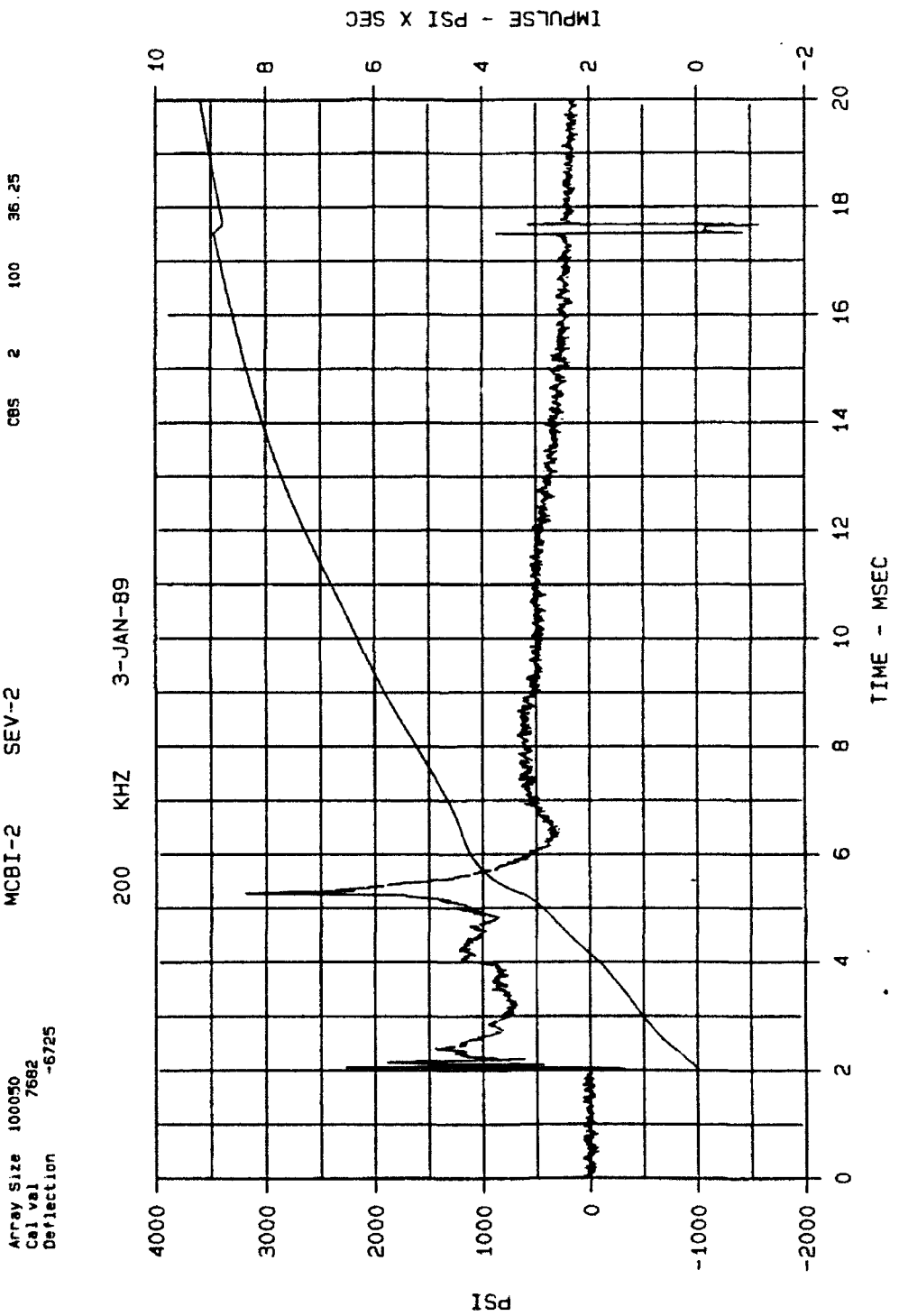

Figure 89. Soil stress wave form measured by gage SEV-2, 20 msec duration, MCBI Gage Validation Test 2

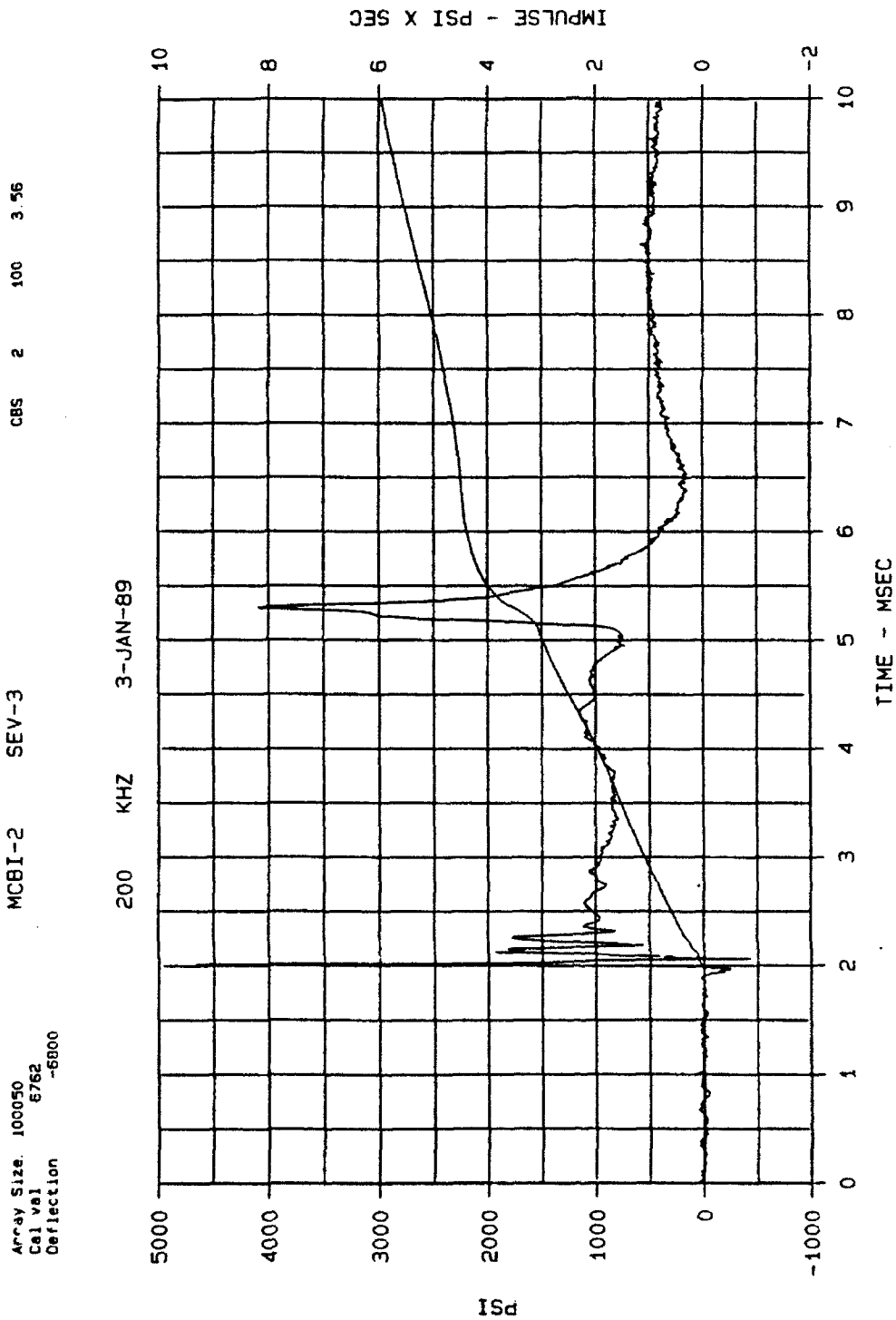

Figure 90. Soil stress wave form measured by gage SEV-3, 10 msec duration, MCBI Gage Validation Test 2

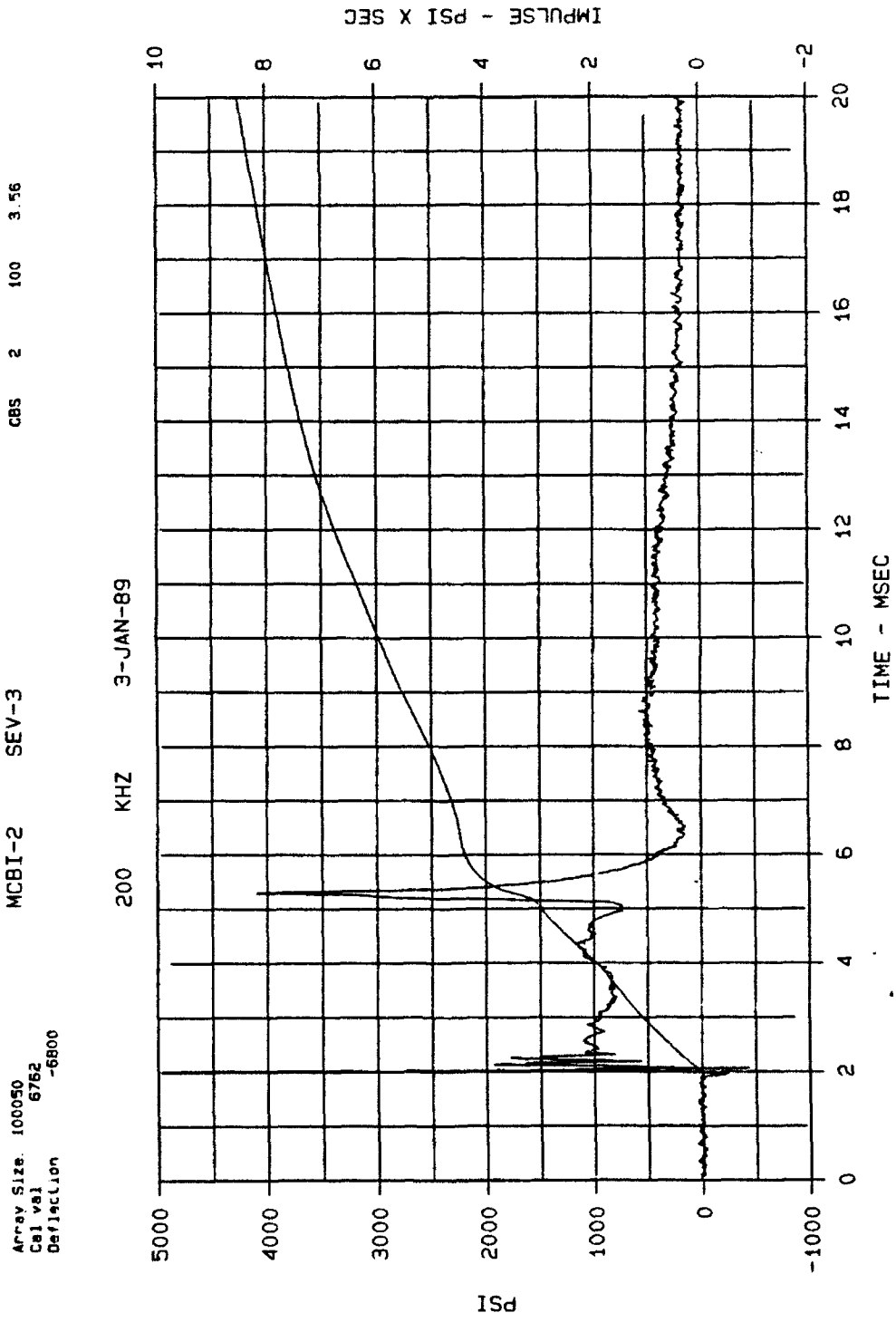

Figure 91. Soil stress wave form measured by gage SEV-3, 20 msec duration, MCBI Gage Validation Test 2

APPENDIX D

MAZE INPUT FILE FOR FINITE ELEMENT CALCULATIONS

```
7
c
c define lines
c
ld 1 lp 2 0 0 .7 0
ld 2 lp 2 0 .8 .7 .8
ld 3 lp 2 0 .954 .374 .954
ld 4 lp 2 0 1.096 .374 1.096
ld 5 lp 2 0 1.25 .7 1.25
ld 6 lp 2 0 0 0 1.25
ld 7 lp 2 .374 .8 .374 1.25
ld 8 lp 2 .294 0 .294 1.25
ld 9 lp 2 .32 0 .32 1.25
ld 10 lp 2 0 .3 .7 .3
ld 11 lp 2 .55 0 .55 .7
ld 12 lp 2 .7 0 .7 1.25
ld 13 lp 2 .474 .3 .474 .7
ld 14 lp 2 .474 .7 .7 .7
ld 15 lp 2 .374 .8 .474 .7
ld 16 lp 2 .5 .8 .5 1.25
ld 17 lp 2 .5 .8 .55 .7
c
c column parts
c
part 1 8 10 6 1 8 6 yes
part 1 11 10 9 1 6 6 yes
part 1 9 10 8 1 1 6 yes
part 10 8 2 6 1 8 10 yes
part 10 9 2 8 1 1 10 yes
part 2 8 3 6 1 8 4 yes
part 2 9 3 8 1 1 4 yes
part 3 8 4 6 1 8 3 yes
part 4 8 5 6 1 8 4 yes
part 4 9 5 8 1 1 4 yes
part 2 7 3 9 1 2 4 yes
part 4 7 5 9 1 2 4 yes
c
c housing parts
c
part 1 12 10 11 1 3 6 yes
part 10 11 14 13 1 2 6 yes
part 10 12 14 11 1 3 6 yes
```

```
part 14 17 2 15 1 2 2 yes
part 14 12 2 17 1 3 2 yes
part 2 16 5 7 1 2 12 yes
part 2 12 5 16 1 3 12 yes
c
tty
assm
c
c merge parts
maztol .01
c
mg 1 3
mg 1 2
mg 1 4
mg 1 5
mg 1 6
mg 1 7
mg 1 8
mg 1 9
mg 1 10
mg 1 11
mg 1 12
mg 13 15
mg 13 14
mg 13 16
mg 13 17
mg 13 18
mg 13 19
m 1 13
tty
c
c constrain lines r=0 and z=0
c
rcon 0
zcon 0
c
c define load curve
c
lcd 1 3 0 0 .00001 -1.0e4 .001 -1.0e4
p 1 b
tty
pbcs 11 1 1 1
```

```
p 13 b
tty
pbcs 3 1 1 1
tty
c
title
DYNA2D Analysis of MCBI Gage Response
term .001
plti .000002
prti 1
c
tty
wbcd dyna2d
c
c define steel properties
c
mat 1 1
e 30.e6
ro .7642e-3
pr 0.3
endmat
c
t
```

DISTRIBUTION LIST

DEPARTMENT OF DEFENSE

DEFENSE NUCLEAR AGENCY
ATTN: ADDST(T)
ATTN: TDTR (Mr. Kennedy, MAJ Holm,
5 CYS Mr. Flohr

DEFENSE NUCLEAR AGENCY
ATTN: FCX (Dr. Leech)
FCTP (LTC Leners, Mr. Martinez, Dr. Rinehart, Dr. Randles)

DEPARTMENT OF THE AIR FORCE

AIR FORCE TECHNICAL APPLICATIONS CENTER
ATTN: TXOS (CPT Anderson)

DEPARTMENT OF THE ARMY

BELVOIR RESEARCH & DEVELOPMENT CENTER
ATTN: STRBE-EMP (Mr. Ess)

CHEMICAL RESEARCH AND DEVELOPMENT CENTER
ATTN: SMCCR-PPP (Mr. Schumchyk)
ATTN: SMCCR-RSP-P (Mr. Birenzevige)

HARRY DIAMOND LABORATORIES
ATTN: SLCHD-NW-RA (Mr. Lingebach, Mr. Belliveau)

U.S. ARMY NATICK RESEARCH AND DEVELOPMENT CENTER
ATTN: Engineering Technology Division, Aero Mechanical Engineering Lab
ATTN: STRNC-UE (Mr. Fanucci)
ATTN: STRNC-ICCC (Mr. Wajda)
ATTN: STRNC-UST (Mr. Nykvist, Mr. Godfrey)

U.S. ARMY ENGINEER WATERWAYS EXPERIMENT STATION
ATTN: CEWES-SE (Mr. L. K. Davis, Mr. J. Ingram, Mr. J. Stout, Mr. C. Welch, Mr. H. White, Mr. B. Fuller)
ATTN: CEWES-SS (Mr. F. Dallriva, Mr. J. Davis, Mr. P. Graham, Mr. R. Holmes)
ATTN: CEWES-SD (Dr. J. Zelasko, Dr. J. Windham, Mr. B. Phillips
ATTN: CEWES-JS (Mr. F. Leake, Mr. J. Johnson, Mr. B. Barker)

U.S. ARMY BALLISTIC RESEARCH LAB
ATTN: SLCBR-TB-B (Dr. Mark, Dr. Polk, Mr. Sullivan)

NAVY

NAVAL RESEARCH LABORATORY
ATTN: Code 4040 (Dr. Book)

NAVAL RESEARCH LABORATORY
ATTN: Code 6303 (Mr. Simpson)

NAVAL WEAPONS CENTER
ATTN: Code 326 B

OTHER AGENCIES

CALIFORNIA RESEARCH AND TECHNOLOGY, INC.
ATTN: Mr. J. Thomsen

CALIFORNIA RESEARCH AND TECHNOLOGY, INC.
ATTN: Mr. Rocco

KARAGOZIAN AND CASE
ATTN: Mr. Wesevich, Mr. Bogosian

LOS ALAMOS TECHNICAL ASSOCIATES
ATTN: Mr. McKee

RESEARCH & DEVELOPMENT ASSOCIATES
ATTN: Dr. Ganong

WEIDLINGER ASSOCIATES
ATTN: Dr. Levine

REPORT DOCUMENTATION PAGE

Form Approved
OMB No. 0704-0188

1. AGENCY USE ONLY (Leave blank)	2. REPORT DATE	3. REPORT TYPE AND DATES COVERED
	April 1993	Final Report

4. TITLE AND SUBTITLE
Design and Development of a Miniature, Column-based Interface (MCBI) Stress Gage

5. FUNDING NUMBERS
DNA-MIPR-88-503

6. AUTHOR(S)
Denis D. Rickman

7. PERFORMING ORGANIZATION NAME(S) AND ADDRESS(ES)
USAE Waterways Experiment Station
Structures Laboratory
3909 Halls Ferry Road
Vicksburg, Mississippi 39180-6199

8. PERFORMING ORGANIZATION REPORT NUMBER
Technical Report
SL-93-3

9. SPONSORING/MONITORING AGENCY NAME(S) AND ADDRESS(ES)
Defense Nuclear Agency
Washington, DC 20305-1000

10. SPONSORING/MONITORING AGENCY REPORT NUMBER

11. SUPPLEMENTARY NOTES

12a. DISTRIBUTION/AVAILABILITY STATEMENT
Approved for public release, distribution unlimited

12b. DISTRIBUTION CODE

13. ABSTRACT *(Maximum 200 words)*

Tests are routinely conducted to evaluate the survivability, under simulated battlefield conditions, of buried military structures subjected to high-explosive loadings. The survivability assessments require the measurement of dynamic normal stresses induced at soil/structure interfaces. Stresses in excess of 10,000 psi and accelerations greater than 100,000 g's may be applied at interface locations. Normal-incidence interface stress gages currently used in such tests are incapable of accurately measuring stresses above 5,000 psi, and are sensitive to lateral accelerations and structure-transmitted stresses which distort the measurement.

This study explores the design, development, and testing of a miniature, column-based, interface (MCBI) stress gage. The MCBI gage is designed to measure normal stresses up to 35,000 psi. Laboratory tests indicate that the gage produces a linear output due to applied pressure and is virtually insensitive to lateral stresses. Explosive tests have shown the MCBI gage compares favorably to commonly-used interface stress gages at stresses up to 3,000 psi, and is survivable at stresses up to 25,000 psi.

14. SUBJECT TERMS
Interface stress, Lateral sensitivity

15. NUMBER OF PAGES
144

16. PRICE CODE

17. SECURITY CLASSIFICATION OF REPORT	18. SECURITY CLASSIFICATION OF THIS PAGE	19. SECURITY CLASSIFICATION OF ABSTRACT	20. LIMITATION OF ABSTRACT
UNCLASSIFIED	UNCLASSIFIED		